Universidade de Brasília

Instituto de Ciências Biológicas

Programa de Pós-Graduação em Nanociência e Nanobiotecnologia

NOVOS POTENCIAIS AGENTES FOTOSSENSIBILIZANTES PARA USO EM TERAPIA FOTODINÂMICA ANTICÂNCER: SÍNTESE, NANOESTRUTURAÇÃO E AVALIAÇÃO DE SUA ATIVIDADE FOTODINÂMICA *IN VITRO*

BRASÍLIA
2018

JUAN ZHANG

NOVOS POTENCIAIS AGENTES FOTOSSENSIBILIZANTES PARA USO EM TERAPIA FOTODINÂMICA ANTICÂNCER: SÍNTESE, NANOESTRUTURAÇÃO E AVALIAÇÃO DE SUA ATIVIDADE FOTODINÂMICA *IN VITRO*

Dissertação apresentada ao programa de Pós-Graduação em Nanociência e Nanobiotecnologia, do Instituto de Ciências Biológicas da Universidade de Brasília, como parte integrante dos requisitos para a obtenção do Título de Doutor em Nanociência e Nanobiotecnologia.

Orientador: Prof. Dr. Luis Alexandre Muehlmann

BRASÍLIA
2018

SUMÁRIO

Resumo

A terapia fotodinâmica (TFD) é baseada na geração de espécies oxidantes que se segue à fotoativação de fotossensibilizantes (FS) em um tecido ou célula alvo. A TFD tem atraído muita atenção na área de tratamentos anticâncer principalmente por sua segurança superior em comparação à quimioterapia convencional. No entanto, mesmo levando-se em conta os resultados positivos obtidos com a TFD tanto nos níveis experimental e da prática clínica, um FS ideal ainda não foi desenvolvido. Enquanto alguns FS se acumulam em tecidos sadios superficiais, tais como a pele, levando à fotossensibilização de tecidos não alvo, outros FS não possuem propriedades fotofísicas e fotoquímicas satisfatórias. Assim, muitas pesquisas têm buscados desenvolver novas moléculas FS. No mesmo sentido, o desenvolvimento de nanocarreadores de FS tem se mostrado uma estratégia adequada para melhorar os resultados obtidos em TFD. Assim, este trabalho objetivou desenvolver e testar novos FS, de acordo com o artigo e manuscritos anexados ao presente documento. No anexo II é apresentada uma revisão sistemática realizada antes do início das pesquisas deste doutorado, abrangendo os FS clássicos e especialmente focada nos avanços mais recentes no desenvolvimento de FS para aplicação em TFD anticâncer. O primeiro FS testado foi o DHX-1 um derivado xanteno-indólico que absorve luz no vermelho e infravermelho próximo. Apesar de este composto já ter sido investigado para aplicação em imageamento por fluorescência, sua atividade como FS ainda não havia sido estudada. Assim, o manuscrito apresentado no anexo II descreve os testes *in vitro* acerca da atividade fotodinâmica do FS DHX-1. O DHX-1 também foi escolhido como um FS modelo para ser incorporado a um CLN. Os resultados mostram que o DHX-1, tanto na forma livre quanto associado ao CLN, apresenta uma banda larga de absorção de luz na janela óptica de tecidos biológicos (600-800 nm), gera espécies reativas de oxigênio quando fotoativado, e é fototóxico contra células de adenocarcinoma mamário murino 4T1 e contra fibroblastos murinos NIH-3T3 *in vitro*. Vale ressaltar que o DHX-1 associado ao CLN, em relação à mesma molécula livre, apresentou maior atividade fotodinâmica em meio aquoso e ainda foi menos fototóxico contra a linhagem de células normais. Apesar de os resultados com o DHX-1 terem mostrado que esta molécula é um FS com potencial para ser usado na clínica oncológica, a sua atividade foi baixa frente a FS clássicos, como as ftalocianinas. Assim, além do DHX-1, foram

desenvolvidos outros cinco derivados de benzo[a]fenoxazínio (PS1 ao PS5) que demonstraram atividade fotodinâmica contra células de adenocarcinoma mamário murino 4T1, mas com intensidades de efeito fotodinâmico diferentes, conforme descrito no manuscrito que consta no anexo III. Destes compostos, o PS4 exibiu o maior rendimento quântico para geração de espécies reativas de oxigênio. Em ensaios in vitro com células, os compostos PS1 e PS4 não foram significativamente tóxicos no escuro, mas exibiram alta atividade contra ambas as linhagens celulares, fibroblastos murinos NIH-3T3 e 4T1, quando fotoativados. Ainda, o composto PS5 foi particularmente seletivo às células cancerosas 4T1, sendo altamente fototóxico contra estas células, e praticamente não fototóxico contra células NIH-3T3.

Palavras-chaves: carreador lipídico nanoestruturado, benzo[a]fenoxazínio, DHX-1, adenocarcinoma mamário, nanotecnologia, fototoxicidade

Abstract

Photodynamic therapy (PDT) is based on the oxidative burst generated by the photoactivation of photosensitizers (PS) in a target tissue or cell. It has drawn much attention in the field of anticancer treatments mainly for its superior safety in comparison to conventional chemotherapy. Although many positive results have been reached with PDT, both at experimental and at clinical practice levels, an ideal PS does not exist. Some PS accumulate in superficial healthy tissues, such as the skin, leading to prolonged photosensitization of non target tissues, while others do not present good photophysical and photochemical properties. Thus, many researches have been focused on the development of new PS molecules. In the same direction, the development of PS nanocarriers has proven to be a good approach to improve the outcomes with PS in PDT.

The present work thus aimed at summarizing the development of new PS for anticancer PDT and developing and testing new photosensitizers, according to the article and manuscripts attached to the present document.

In chapter 1, it presented an overview on the classical PS and specially focused on the most significant recent advances in the development of PS with regard to their potential application in oncology. In addition, the methods for the rational design of novel PS with desirable properties were highlighted. Based our experience in preparing the PS review paper, we begin to design and synthesize new PS and test their potential as PS in anticancer PDT study.

First, I found the a novel NIR fluorescent sensors with xanthene-indolium framework which showed suitable light absorption window in red light zone. Lots of studies were conducted to investigate its imaging application function, however its potential PS activity has not been explored. Thus in chapter 2, DHX-1 as xanthene derivative was selected as one of the candidate PS molecules, which was also associated with a nanostructured lipid carrier (NLC). The results show that the DHX-1, both free and associated to NLC, presents a broad band of light absorption within the optical window of biological tissues (600-800 nm), generates reactive oxygen species when photoactivated, and is phototoxic against murine breast adenocarcinoma 4T1 cells and murine fibroblast NIH-3T3 *in vitro*. Noteworthy, the association of DHX-1 to the NLC enhanced its activity in aqueous media and strongly reduced its phototoxicity against the normal cell line.

Although DHX-1 showed interesting PDT activity, its potency of cytotoxicity

in PDT condition is still weak. So in the next step, we tried to design new PS with stronger anticancer PDT activity. During the literature survey, a group of benzo[a]phenoxazinium dyes came to our attention due to their good photostability, high molar absorption, long-wavelength absorption, and especially relatively low fluorescence quantum yield. Some benzo[a]phenoxazinium derivatives were reported to function as PS in antimicrobial PDT. However, the potential anticancer PDT of benzo[a]phenoxazinium dyes has been little investigated. Thus, based on ligand-mediated targeting strategy five benzo[a]phenoxazinium derivatives, PS1-PS5, were developed and evaluated for their *in vitro* anticancer photodynamic activities. Of these compounds, PS4 exhibited a higher quantum yield for ROS generation. The assays with cells in vitro showed that PS1 and PS4 were not significantly toxic in the dark, but robustly reduced the viability of the tested cells under photoactivation. Interestingly, PS5 was particularly selective to 4T1 cells, being strongly phototoxic against these cells and nearly non-phototoxic to NIH3T3.

Keywords: nanostructured lipid carrier, xanthene-indolium derivative, breast adenocarcinoma, nanotechnology, phototoxicity, benzo[a]phenoxazinium derivatives

Introdução

O câncer figura entre as principais causas de morte e de morbidade no mundo. Os tratamentos clínicos mais utilizados contra esta doença incluem cirurgia, radioterapia, quimioterapia e, mais recentemente, imunoterapia (Lucky et al. 2015). Entretanto, essas terapias apresentam alguns inconvenientes importantes. Por exemplo, a quimioterapia convencional é muitas vezes associada com efeitos adversos sistêmicos severos, tais como mielossupressão, mucosites, alopecia, e outros (Lucky et al. 2015). Ainda, a ressecção cirúrgica de tumores é ineficaz em evitar a recorrência de certos tumores (Uramoto and Tanaka 2014), enquanto a radioterapia possui limitações de dose aplicável que reduzem a sua eficácia (Liu et al. 2016). Assim, além do aprimoramento das terapias convencionais, devem ser desenvolvidas novas alternativas para o tratamento do câncer que sejam, idealmente, seguras, eficazes e com baixa relação custo/benefício.

Neste sentido, a terapia fotodinâmica (TFD) tem sido apontada na literatura como uma modalidade eficaz e segura de terapia do câncer (Kennedy et al. 1990). Apesar de ter sido descrita há mais de um século, seu uso clínico não tem sido extensivo. A TFD é baseada na fotoativação focal de fotossensibilizantes (FS) diretamente no tecido alvo, gerando reações fotoquímicas que produzem estresse oxidativo (Zhang et al. 2017). As principais consequências destes eventos são citotoxicidade direta, colapso da microvasculatura tumoral, a/ou ativação de resposta imunitária contra antígenos tumorais(Dougherty et al. 1998). Um ponto positivo importante da TFD enquanto terapia anticâncer é a possibilidade de restringir seus efeitos ao sítio irradiado, poupando tecidos sadios. Apesar de a TFD ter sido aplicada com sucesso no tratamento de diferentes cânceres, ainda há a necessidade de se aperfeiçoar as moléculas FS e os sistemas de entrega destas moléculas. A maioria das moléculas FS disponíveis para uso clínico apresentam baixa solubilidade em água, baixa absorção na região do infravermelho próximo, meia-vida inadequadamente longa, e intensa acumulação na pele(Yano et al. 2011). Muitos compostos têm sido propostos como novos candidatos a FS[2]. O derivado de xanteno rosa bengala, por exemplo, é um corante fluorescente fotoativo testado

como agente FS antimicrobiano (Costa et al. 2012) e anticâncer (Panzarini et al. 2014).

Idealmente, um FS deve apresentar (Sharman et al. 1999; DeRosa and Crutchley 2002; Detty et al. 2004; Yano et al. 2011; Zhang et al. 2017): 1) alto coeficiente de extinção molar na região espectral entre vermelho e infravermelho próximo, 2) energia suficiente no seu estado triplete excitado para promover a conversão do oxigênio molecular de triplete a singlete ($E_T \geq 21{,}5$ kcal.mol^{-1}), 3) alto rendimento quântico de produção de seu estado triplete ($\Phi_T > 0{,}4$), 4) estado triplete excitado com vida média longa ($\tau_T \geq 1$ µs), 5) fotoestabilidade que permita manter sua atividade durante todo o tempo de irradiação, 6) acúmulo seletivo no sítio alvo (e.g., câncer), 7) inocuidade no escuro, 8) rápida depuração no organismo após a aplicação da TFD, 9) não fotossensibilizar tecidos não alvo, como a pele, 10) alta atividade fotodinâmica em meios aquosos, e 11) pureza química.

Nos últimos anos, nosso grupo de pesquisa tem continuamente buscado novas moléculas FS e novos sistemas de veiculação de FS (Muehlmann et al. 2014, 2015; Rodrigues 2015; Monge-Fuentes et al. 2017). Recentemente, diferentes moléculas desenvolvidas em colaboração com a Universidade de Jinan, China, dentre elas certos corantes do tipo benzo[a]fenoxazínio, foram incluídas em trabalhos de pesquisa de novas moléculas FS devido a sua alta fotoestabilidade, alto coeficiente de absortividade molar, e absorção em comprimentos de onda dentro do vermelho e do infravermelho próximo (Frade et al. 2007; Yuan et al. 2013; Leitão et al. 2016). Neste trabalho, portanto, são descritos as sínteses e os testes *in vitro* realizados para verificar o potencial fotossensibilizante de novas moléculas. No anexo I é apresentada uma revisão publicada na revista Acta Pharmaceutica Sinica B, detalhando características estruturais de FS clássicos bem como o estado da arte de desenvolvimento de novos FS. Durante o estudo da literatura chamou a atenção um fluoróforo derivado xantênico, DHX-1, que absorve luz na melhor janela biológica da TFD, ou seja, no vermelho e no infravermelho próximo, mas que ainda não havia sido testado como FS. Assim, os detalhes dos experimentos realizados com esta molécula afim de testar a sua atividade fotodinâmica *in vitro* podem ser encontrados no anexo II. O DHX-1 livre não apresentou atividade fotodinâmica *in vitro* comparável com FS clássicos, como as ftalocianinas, contra

células de adenocarcinoma mamário murino 4T1. Este mesmo FS foi encapsulado em nanopartículas lipídicas, apresentando, nesta forma, maior atividade contra células 4T1 em relação às células normais NIH-3T3. Como a atividade fotodinâmica do DHX-1 foi insatisfatória, outros cinco FS (PS1-PS5) foram desenvolvidos. Estes derivados benzo[a]fenoxazínicos apresentaram maior atividade fotodinâmica *in vitro* contra células 4T1, como descrito no manuscrito do anexo III, sendo assim considerados como potenciais FS para uso em TFD anticâncer.

Objetivos

O objetivo deste estudo foi testar a atividade fotodinâmica *in vitro* de moléculas potencialmente fotossensibilizantes, tanto novas quanto já descritas na literatura.

As metas traçadas para atingir este objetivo foram:

- sintetizar compostos benzo[a]fenoxazínicos e derivados de xanteno;
- verificar o espectro de absorção de luz e de fluorescência destes compostos;
- testar a capacidade destes compostos em produzirem espécies reativas de oxigênio quando irradiados com luz vermelha (λ 660 nm);
- associar um destes compostos a carreadores lipídicos nanoestruturados.
- testar a capacidade destes compostos, livres ou nanoestruturados, em reduzir a viabilidade de células cancerosas (4T1) e não cancerosas (NIH-3T3) *in vitro* quando fotoativados

ANEXO I

Acta Pharmaceutica Sinica B ▮▮▮▮;▮(▮):▮▮▮–▮▮▮

Chinese Pharmaceutical Association
Institute of Materia Medica, Chinese Academy of Medical Sciences

Acta Pharmaceutica Sinica B

www.elsevier.com/locate/apsb
www.sciencedirect.com

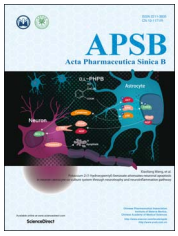

REVIEW

An updated overview on the development of new photosensitizers for anticancer photodynamic therapy

Juan Zhang[a,b,1], Chengshi Jiang[a,1], João Paulo Figueiró Longo[b], Ricardo Bentes Azevedo[b], Hua Zhang[a,*], Luis Alexandre Muehlmann[b,c,]**

[a]*School of Biological Science and Technology, University of Jinan, Jinan 250022, China*
[b]*Institute of Biological Sciences, University of Brasilia, Brasilia 70910-900, Brazil*
[c]*Faculty of Ceilandia, University of Brasilia, Brasilia 72220-900, Brazil*

Received 31 May 2017; revised 6 July 2017; accepted 6 September 2017

KEY WORDS

Anti-cancer;
Photosensitizers;
Photodynamic therapy;
Photochemical reactions

Abstract Photodynamic therapy (PDT), based on the photoactivation of photosensitizers (PSs), has become a well-studied therapy for cancer. Photofrin®, belonging to the first generation of PS, is still widely used for the treatment of different kinds of cancers; however, it has several drawbacks that significantly limit its general clinical use. Consequently, there has been extensive research on the design of PS molecules with optimized pharmaceutical properties, with aiming of overcoming the disadvantages of traditional PS, such as poor chemical purity, long half-life, excessive accumulation into the skin, and low attenuation coefficients. The rational design of novel PS with desirable properties has attracted considerable research in the pharmaceutical field. This review presents an overview on the classical photosensitizers and the most significant recent advances in the development of PS with regard to their potential application in oncology.

*Corresponding author.
**Corresponding author at: School of Biological Science and Technology, University of Jinan, Jinan 250022, China.
E-mail addresses: bio_zhangh@ujn.edu.cn (Hua Zhang), luismuehlmann88@gmail.com (LuisAlexandre Muehlmann).

[1]These authors made equal contribution to this work.

Peer review under responsibility of Institute of Materia Medica, Chinese Academy of Medical Sciences and Chinese Pharmaceutical Association.

http://dx.doi.org/10.1016/j.apsb.2017.09.003

Please cite this article as: Zhang Juan, et al. An updated overview on the development of new photosensitizers for anticancer photodynamic therapy. *Acta Pharmaceutica Sinica B* (2017), http://dx.doi.org/10.1016/j.apsb.2017.09.003

1. Introduction

Cancer is among the leading causes of morbidity and mortality worldwide. In 2012, approximately 14 million cancer cases were newly diagnosed, and the number of cancer-related deaths was 8.2 million, which is projected to rise by about 70% over the next two decades.[1] Currently, clinical treatments for cancer include surgery, radiation therapy, chemotherapy and, more recently, immunotherapy and other small-molecule targeted therapies, along with a combination of these strategies.[2] However, these treatments present some important drawbacks. For instance, traditional chemotherapy, as it interferes in cell division, is often associated with severe systemic adverse effects, such as myelosuppression, mucositis, alopecia, and others.[3] Also, surgical resection of certain tumors cannot avoid a high recurrence rate,[4] while the cumulative radiation dose extremely limits the radiotherapy.[5] Thus, although refinement of the conventional anticancer therapy is important, development of new treatment approaches that are safe, potent, and cost-effective seems especially urgent.

2. Photodynamic therapy

2.1. An accidental finding for cancer treatment

In the 1890s, Raab[6] accidentally found that the irradiation with visible light was lethal to paramecia previously exposed to acridine, and postulated that the transfer of light energy to the acridine red was the crucial event behind the cytotoxicity observed in paramecia and that this effect was related to the fluorescence of the dye.[7] Then the first clinical observation of PDT with oral eosin to treat epilepsy was reported by the neurologist Jean Prime in 1900.[8] Later, von Tappeiner and Jesionek[9] proposed the use of topical eosin with light exposure to treat skin tumors. This was the first published report on the use of PDT to treat tumors in human patients. Subsequently, von Tappeiner[10] observed that O_2 was an important component of the events found by Raab, and coined the term "photodynamic action".

The study of the anticancer potential of PDT was conducted by few researchers up to the 1950s when the interest in this field began to increase. The publication of some seminal reports on the use of porphyrins as both PSs and fluorescence diagnostic tools[11] in the 1950s and 1960s was followed by a series of works on the anticancer activity of PDT against different tumors.[12] Mainly over the last three decades, several types of PSs have been developed and applied in preclinical and clinical trials; some of these molecules reached the market and have shown to be effective against different kinds of cancers.[13–15] The main advantage of PDT over conventional anticancer therapies is the ability to limit toxic effects to the biological tissues exposed to both the PS and light, thus protecting normal tissues.

In addition, PDT has also been used successfully against non-malignant disorders in diverse fields, such as urology,[16] immunology,[17] ophthalmology,[18] dentistry,[19] dermatology,[20] and others.

2.2. Photodynamic therapy mechanisms

PDT is based on the excitation of PS with light at specific wavelengths, culminating in type I and type II photochemical reactions.[21] As shown in Fig. 1, a PS can be activated from its ground state to a short-lived excited singlet state (PS_{Es}) by light. Then, either the excited PS may decay back to the ground state by emitting fluorescence, or it can undergo intersystem crossing whereby the spin of its excited electron inverts to form a relatively long-lived triplet state (PS_{Et}). The triplet excited PS can also decay back to the ground state by emitting phosphorescence, but most importantly it can directly interact with surrounding substrates (*e.g.*, cell membrane or other biomolecules) to form radicals, which then react with O_2 to produce reactive oxygen species (ROS), such as superoxide anion radicals ($O_2^{\cdot-}$), hydroxyl radicals (.OH), and hydrogen peroxides (H_2O_2, type I reaction). Alternatively, the energy of the excited PS can be directly transferred to $^3O_2$ (itself a triplet in the ground state) to form $^1O_2$ (type II reaction). It is worth noting that both type I and type II reactions can occur simultaneously, and the ratio between these processes is affected by the nature of the PS, as well as by the concentrations of $^3O_2$ and other substrates. However, most of the experimental studies indicate that the photoactivated production of $^1O_2$, namely type II reaction, plays a dominant role in *in vivo* PDT.

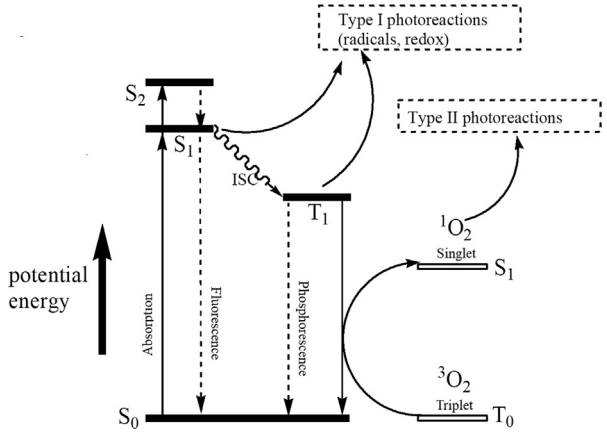

Figure 1 Jablonski diagram showing the main events leading to type I and type II photochemical reactions, which eventually may result in oxidative cell damage. S_0, ground state of the photosensitizer (PS); S_1, first excited singlet state of PS; S_2, second excited singlet state of PS; T_1, first excited triplet state of PS; ISC, intersystem crossing; $^3O_2$, triplet oxygen; $^1O_2$, singlet oxygen.

In a biological medium the reactive species generated by the photodynamic process can react with a large number of biomolecules, mainly proteins, nucleic acids, and lipids. The damage to biomolecules may (i) irreversibly damage tumor cells resulting in necrosis, apoptosis, or autophagy, (ii) cause tumor ischemia following PDT-induced vascular injury, and (iii) activate the immune response against tumor antigens.[22–25] Therefore, the main downstream targets of PDT include tumor cells, as well as tumor-associated microvasculature, and, indirectly, the host immune system.[26] Moreover, the combination of PDT with other chemotherapeutic drugs may help to achieve a long-term tumor control, due to their possible synergistic effects resulting from the combination of downstream responses in PDT and the mechanisms of chemotherapeutic drugs.[27]

3. The photosensitizers for anticancer PDT

3.1. First generation PSs

Hematoporphyrin (Hp), a complex mixture of porphyrinic compounds,[28] was the first porphyrin used as PS. The purification and chemical modification of Hp led to the discovery of a

Please cite this article as: Zhang Juan, et al. An updated overview on the development of new photosensitizers for anticancer photodynamic therapy. *Acta Pharmaceutica Sinica B* (2017), http://dx.doi.org/10.1016/j.apsb.2017.09.003

hematoporphyrin derivative (HpD), which was shown to be more selective for tumor tissues, inducing a less intense skin photosensitization in comparison to Hp.[29] Later, a mixture of porphyrin dimers and oligomers isolated from HpD was marketed as Photofrin.[30] Despite Photofrin® was widely used for treating different cancers, the clinical use was limited by its intrinsic drawbacks, including I) poor chemical purity with a mixture of more than 60 molecules; II) its long half-life and intense accumulation in the skin, responsible for the induction of a prolonged skin photosensitization, which sometimes persists for 2 or even 3 months after Photofrin® administration; III) its low molar attenuation coefficient (1.17×10^3 mol/L cm); and IV) its activation wavelengths being too short for a good tissue penetration.[30–32]

3.2. *Second generation PSs*

The disadvantages associated with first generation PSs have led to extensive investigation aimed at improving the efficacy of PS molecules *via* alteration of the peripheral functionality of the porphyrin,[33] or direct modification of the porphyrin core.[34] The following the seminal works on the first generation PS have resulted in the production of several new non-porphyrinoid PS molecules (Fig. 2). These have been developed over the decades, including metalloporphyrins (Lutrin® and Lutex®),[35,36] porphycenes,[37,38] pheophorbides (Tookad®),[39,40] purpurins (Purlytin®),[41] phthalocyanines,[42–46] chlorins (Foscan®),[47] protoporphyrin IX precursors (Hexvix®, Metvix® and Levulan®),[48,49] phenothiazines (methylene blue, and toluidine blue),[50–55] cyanines (merocyanine 540),[56,57] dipyrromethenes,[58,59] hypericin,[60–62] and xanthenes (Rose Bengal).[63]

3.3. *Strategies for designing new generation PSs*

Despite the extensive research performed to develop new and improved PS, only a few second generation PSs, such as Levulan®, MetVix®, Photochlor®[64] and NPe6,[65] have been approved for the clinical treatment of cancer.[66] The rational design of novel PS with desirable properties remains a big challenge for the pharmaceutical industry. The latest review article related to the design of PSs for photodynamic therapy, authored by Garland et al.[67], dates back to 2009. As stated before, the overall success of PDT mainly depends on the $^1O_2$ yield, molecule stability, the penetration depth of absorbed light and distribution of PSs, so that:

1) The $^1O_2$ generated in type II photoreaction is a key factor for PDT, since it is considered as the major cytotoxic species in PDT.[68] Generally, the introduction of heavy atoms (such as Br, and I) into the PS molecule or inhibition of the interaction between triplet excited PS and native free radicals can increase the $^1O_2$ production;
2) A disadvantage of many of the current PSs is their tendency to aggregate, resulting in short triplet state lifetimes and decreased $^1O_2$ yields. Therefore, a structural modification that can suppress the aggregation tendency of a PS should be considered carefully to improve the property of PS. Usually, the presence of a central metal ion and the number of charges in the molecule will have an important role for the stability of PSs;
3) The increased energy of light of longer wavelength is also a major motivation for the development of new PSs. Generally, expanding the molecular conjugate system by introducing an electron-rich donor can improve the PS absorption efficiency of red light, and enhance the penetration of light into human tissue;
4) Improving the target distribution of PS is also very important to increase its efficacy and reduce adverse effects. The ligand-mediated targeting strategy in PDT has been explored. Herein, the targeted ligands, such as biotin, folate, peptide, etc., were frequently used for delivery of PS to cancer tissues;
5) In addition, the positions and types of the substituent groups on the molecule can influence the lipophilicity of the molecule, which further influences the tissue location of PS.

4. Recent development in anticancer PSs

A literature survey indicates that there are quite a lot of review articles about PSs and PDT,[2,69–71] but few of them specifically focus on the discovery and development of new PSs as anticancer agents. With the rapid development in PS research area, a number of new, more potent and tumor-specific PSs showing promising clinic potential have been investigated. Herein, this section summarizes the recently reported PSs mainly focusing on porphyrin, chlorin, phthalocyanine and BODIPY derivatives, aiming to provide a better understanding of the factors affecting the efficacy of PS molecules.

4.1. *Porphyrin-type PSs*

The porphyrin macrocyles were mainly developed and clinically used in the last few decades. Side-chains containing functional

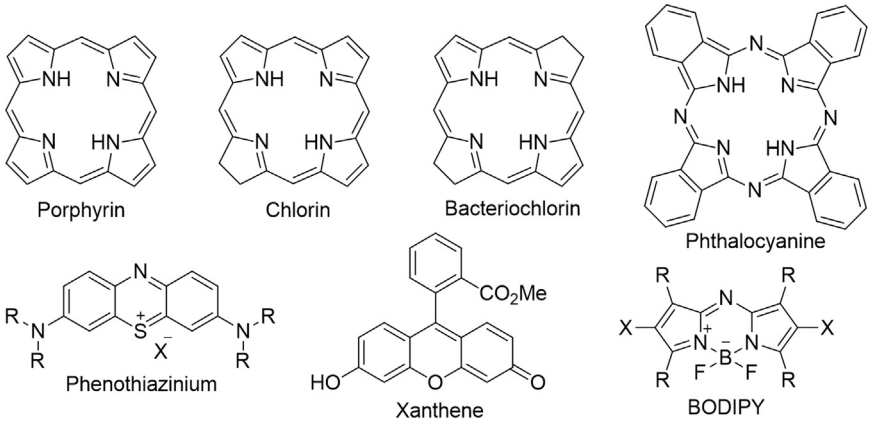

Figure 2 Structural skeletons of several anticancer PSs.

Please cite this article as: Zhang Juan, et al. An updated overview on the development of new photosensitizers for anticancer photodynamic therapy. *Acta Pharmaceutica Sinica B* (2017), http://dx.doi.org/10.1016/j.apsb.2017.09.003

groups, such as nitrogen atoms,[72,73] carboxylic acid[74] and sugar,[75] are frequently incorporated into the porphyrin skeleton. For example, a novel porphyrin-based PS (5,10,15,20-tetrakis[(5-diethylamino)pentyl] porphyrin, TDPP, **1**) with four diethylaminopentyl side-chains recently reported by Li et al.[72] showed a high $^1O_2$ yield with the ability to kill human esophageal cancer cell lines (Eca-109) and significantly reduce the growth of Eca-109 xenograft tumors in BABL/c nude mice. Among a series of *β*-alkylaminoprophyrins reported later by Chen's group,[73] derivative **2** showed higher phototoxicity than Hp monomethyl ether and the lowest toxicity in the dark. Another new porphyrin derivative **3** bearing ethylenediaminetetraacetic acid showed intense *in vitro* phototoxicity on HepG2 and BGC823 cell lines, and further inhibited the growth of BGC823 tumors in nude mice.[74] Mechanism studies indicated that **3** can induce cell death *via* the mitochondrial apoptotic pathway mainly triggered by lysosomal photodamage. Costa et al.[76] recently reported a hydrophobic porphyrin derivative **4** bearing four isoquinoline moieties, which showed a high quantum yield of $^1O_2$ generation, the absence of toxicity in the dark, and significant *in vitro* phototoxicity against HT29 cells with an IC_{50} in the micromolar range.

Horiuchi and co-workers[77] studied the effect of a silyl group on the photodynamic properties of tetraphenylporphyrin derivatives **5**. The results indicated that silylation could lead to an improvement in the quantum yield of $^1O_2$ sensitization for derivatives. In addition, there has been recent growth in interest in the preparation of metal-porphyrin conjugates as potential photocytotoxic agents. The porphyrins functionalized with Pt^{II} were the first metal-porphyrin derivatives developed for biomedical application.[78] Later, examples related to other metal-porphyrin conjugates have been described. For example, the glucopyranoside-conjugated porphyrin **6** bearing In^{+3} synthesized by Nakai et al.[75] exhibited strong phototoxicity, correlating with its high abilities of $^1O_2$ yield and cell permeability. Another Re-porphyrin conjugate **7**, bearing four [1,4,7]-triazacyclononane units prepared by Mion et al.[79], showed remarkable phototoxicity on Hela cells with non-toxicity in the dark (Fig. 3).

4.2. *Chlorin-type PSs*

Compared with porphyrins, chlorin-type PSs attracted considerable attention due to their intense absorption in relatively harmless NIR region, which can penetrate deeply into biological tissues. However, the development of chlorin derivatives was significantly limited by their poor water solubility. Therefore, chlorin-type PSs have been modified by conjugation with amino acids, peptides, and sugars to improve their solubility for PDT investigations. For example, Meng et al.[80] prepared a series of chlorin P_6-based water-soluble amino acid conjugates. Among these synthetic derivatives, compound **8** showed strong absorption in the phototherapeutic window, relatively high $^1O_2$ quantum yield, and high phototoxicity against melanoma cells with low toxicity in the dark. Also, compound **8** exhibited better *in vivo* PDT antitumor efficacy than verteporfin on mice bearing B16F10 tumors. Another photocytotoxic chlorin e_6 bis(amino acid) conjugate **9** bearing two different amino acids, lysine at 13 and aspartate at 15 was regioselectively synthesized by Smith and co-workers.[81] A water-soluble chlorin

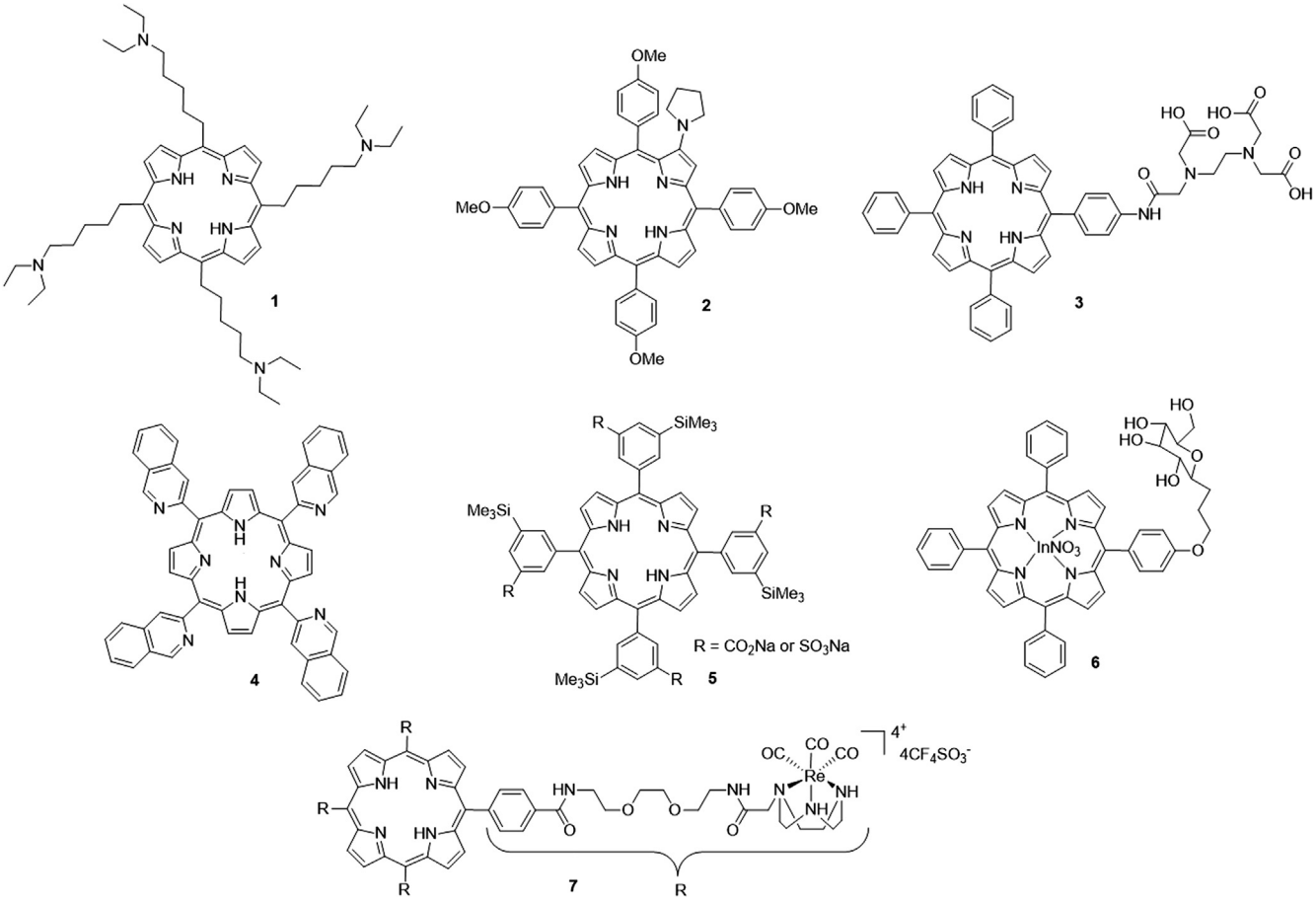

Figure 3 Chemical structures of porphyrin-type PSs **1**–**7**.

Please cite this article as: Zhang Juan, et al. An updated overview on the development of new photosensitizers for anticancer photodynamic therapy. *Acta Pharmaceutica Sinica B* (2017), http://dx.doi.org/10.1016/j.apsb.2017.09.003

derivative **10**, which was surrounded by four perfluorinated aromatic rings and conjugated with maltotriose (MaI_3) molecules, showed excellent biocompatibility, strong photoabsorption in the longer wavelength regions and high photocytotoxicity.[82]

The use of boron-containing substances in the treatment of cancer has received a great deal of attention due to their high probability of producing particles and lithium-7 nuclei.[83] Boron-containing chlorin derivatives have also been explored in PDT applications.[84] Recently, a new chlorin derivative **11** containing phenylboronic acid moieties was synthesized by Tai and co-workers.[84] This compound could significantly inhibit tumor growth *in vivo* and showed rapid clearance from normal tissues. To improve the cell permeability of chlorin-type PSs, Gushchina et al.[85] introduced hydrophobic carbon chains into chlorin e_6 to yield a series of new amide derivatives **12**, which exhibited good photoactivity and low toxicity in the dark against P388 and K562 cancer cells. Chlorin and bacteriochlorin derivatives **13**[86] bearing chloro-5-sulfophenyl fragments showed promising photo-therapeutic properties, such as high water solubility, high photo-stability, high $^1O_2$ quantum yields and negligible dark cytotoxicity. Patel et al.[87] recently reported an NIR bacteriochlorin analogue **14** to be a promising dual-function agent for fluorescence-guided surgery with an option for treating cancer in PDT. This compound exhibited higher tumor uptake and long-term cure in BALB/c mice bearing Colon 26 tumors. Most of all, it showed low skin phototoxicity, which provides a significant advantage over the clinically approved HD as well as other porphyrin-based PSs (Fig. 4).

4.3. *Phthalocyanine-type PSs*

Phthalocyanine derivatives were shown to be most promising PSs. However, the low solubility and π–π stacking in these molecules limited their further clinical application. Strategies to overcome these disadvantages can involve incorporations of cationic[88] or anionic groups,[89] peptides,[90] β-cyclodextrins,[91] crown ethers,[92] glycerinum[93] and so on. Recently, 2-(morpholin-4-yl)ethoxy-substituted phthalocyanine **15** was synthesized by Kucinska et al.[94]. Biological test results indicated that **15** showed potent cytotoxicity against PC3 and A375 under irradiation, while its cytotoxicity in the dark was very low. Another novel Mg(II)-phthalocyanine **16**, bearing (2-methyl-5-nitro-1*H*-imidazol-1-yl)ethoxy substituent at a non-peripheral position, was found to show strong photocytotoxicity at 1 mol/L with 100% photokilling of the human oral squamous cell carcinoma cell lines, HSC-3.[95]

The development of multifunctional molecules has also been considered for overcoming drug resistance and low therapeutic efficacy. For example, Zhou et al.[96] reported a derivative **17** bearing a cytostatic coumarin moiety, zinc(II) phthalocyanine and a tri(ethyleneglycol) linkage showed dual photodynamic and chemotherapeutic activities. These conjugates exhibit high photocytotoxicity against HepG2 cells ($IC_{50} \approx 14$–44 nmol/L), low aggregation tendency and high cellular uptake. Other similar examples are the phthalocyanine-8-hydroxyquinoline conjugates **18**.[97] Ranyuk et al.[98] reported a series of water-soluble zinc phthalocyanine-peptide conjugates **19**, which targeted the gastrin-releasing peptide receptor. Novel far-red-absorbing Zn(II) phthalocyanine derivative **20** bearing [(triethylammonio)ethyl]sulfanyl substituents in the peripheral or nonperipheral positions were synthesized by Machacek et al.[99]. The bioassay results indicated that the Zn complex exhibited photocytotoxicity against 3T3, Hela, SK-MEL-28, and HCT116 cancer cell with IC_{50} values in a submicromolar range, and low toxicity in the dark ($TC_{50} \approx 1500$ mol/L). Shen et al.[100] reported a series of first silicon(IV) phthalocyanine nucleoside (uridine, 5-methyluridine, cytidine, and 5-*N*-cytidine) conjugates. Among them, the uridine-containing complex **21** exhibited the highest photocytotoxicity against HepG2

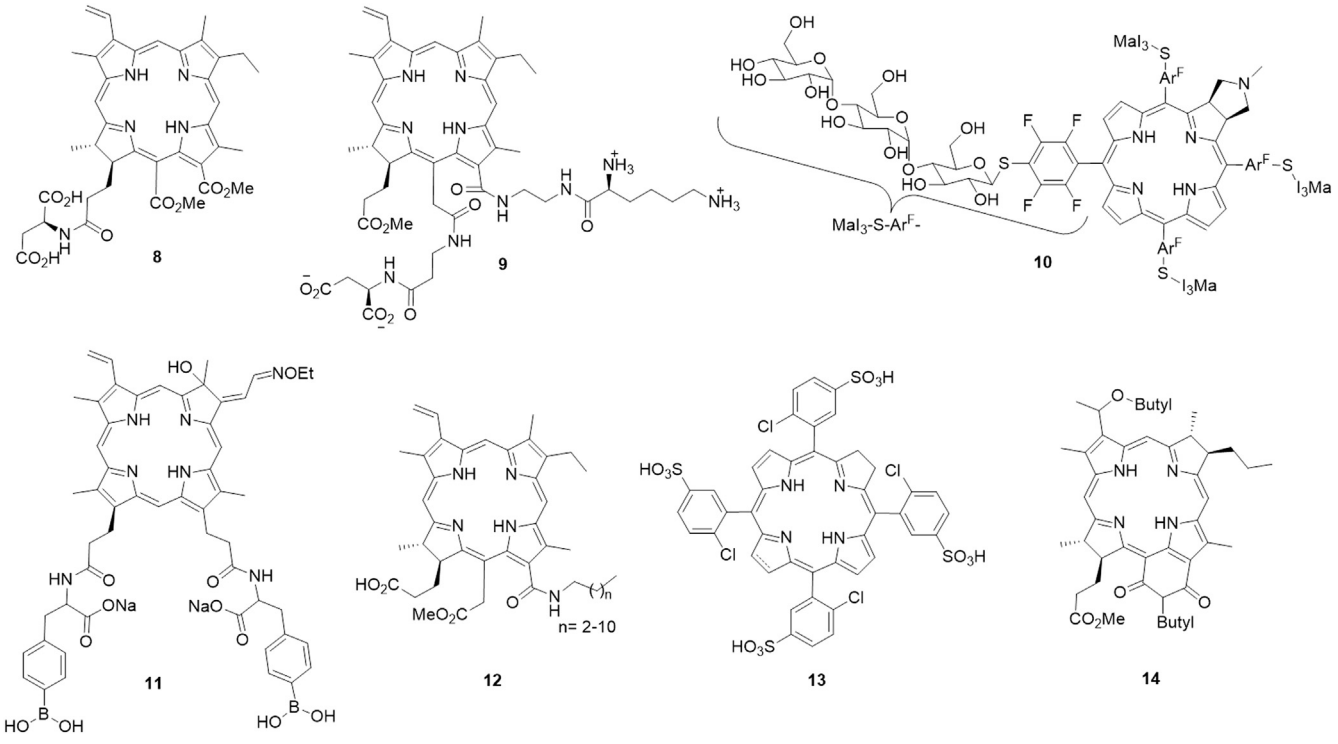

Figure 4 Chemical structures of chlorin-type PSs **8**–**14**.

Please cite this article as: Zhang Juan, et al. An updated overview on the development of new photosensitizers for anticancer photodynamic therapy. *Acta Pharmaceutica Sinica B* (2017), http://dx.doi.org/10.1016/j.apsb.2017.09.003

cells (IC_{50} = 6 nmol/L), with high cellular uptake and non-aggregated nature in the biological media. Bio et al.[101] developed a multifunctional prodrug **22** composed with Si phthalocyanine, a SO-labile aminoacrylate linker and the cytotoxic drug combretastatin A-4 (CA4). Once illuminated, **22** showed improved toxicity, but reduced toxicity in the dark compared with CA4 (Fig. 5).

4.4. *BODIPY-type PSs*

Another promising class of PS suitable for PDT is the distyryl boron dipyrromethene (BODIPY) dyes, which have proven to be a valuable family of compounds with diverse applications rivaling that of porphyrin. The BODIPY PSs are equipped with heavy halogen atoms, such as Br and I, in the organic chromophore to make compounds reach the triplet excited state by quenching the fluorescence and facilitating intersystem crossing.

Erbas-Cakmak et al.[102] designed a water-soluble pH and GSH responsive distyryl-BODIPY PS **23**, which could be activated by protonation at neutral pH and reductive cleavage of the disulfide linker at elevated GSH concentration. Recently, Lo and coworkers[103] reported another new class of pH/thiol responsive BODPY PSs that contained either the ketal or disulfide linker. Noteworthy, the unsymmetrical complex **24** exhibited the greatest enhancement in the $^1O_2$ generation and fluorescence intensity upon activation, which was considered to be a promising theranostic agent for targeted imaging and PDT of cancer. Platinum (II) complex **25** synthesized by Mitra et al.[104] could achieve mitochondria-targeted photocytotoxicity *via* disruption of the mitochondrial membrane potential and apoptosis. This complex generated excellent photocytotoxicity against HaCaT cells but remained non-toxic in the dark (IC_{50} > 100 mol/L). A novel photoactivatable bichromophoric conjugate **26** was developed by Fraix and coworkers.[105] This compound combined BODIPY and aniline derivative as nitric oxide photodonor, which had an amplified photomortality on melanoma cancer cells. Lincoln et al.[106] prepared two small meso-acetoxymethyl BODIPY dyes **27**, which showed improved photostability against singlet oxygen compared to the BODIPY PSs lacking the acetoxymethyl group. Compounds **27** can readily embed in the lipid membranes of Hela cells and efficiently induced light-dependent apoptosis at nanomolar concentration. An orthogonal BODIPY trimer **28** without halogen atom substituent was shown to have strong absorption in the visible region and high $^1O_2$ generation capability[107] (Fig. 6).

5. Conclusions

The discovery of novel PS molecules with desired pharmaceutical properties and the application of novel PS in clinical trials are challenging tasks. During the last several years, most research work is based on the modification and optimization of old-style PSs. Therefore, molecules considered as the second generation PS mainly have been derived from porphyrin and porphyrin-related structures. The most recent activity in the PS field for PDT of cancer has been considerable, and the design of non-porphyrin PSs, which possess shorter periods of photosensitization, longer activation wavelengths and higher singlet oxygen yield, still attracts more attention in the field of anticancer PDT.

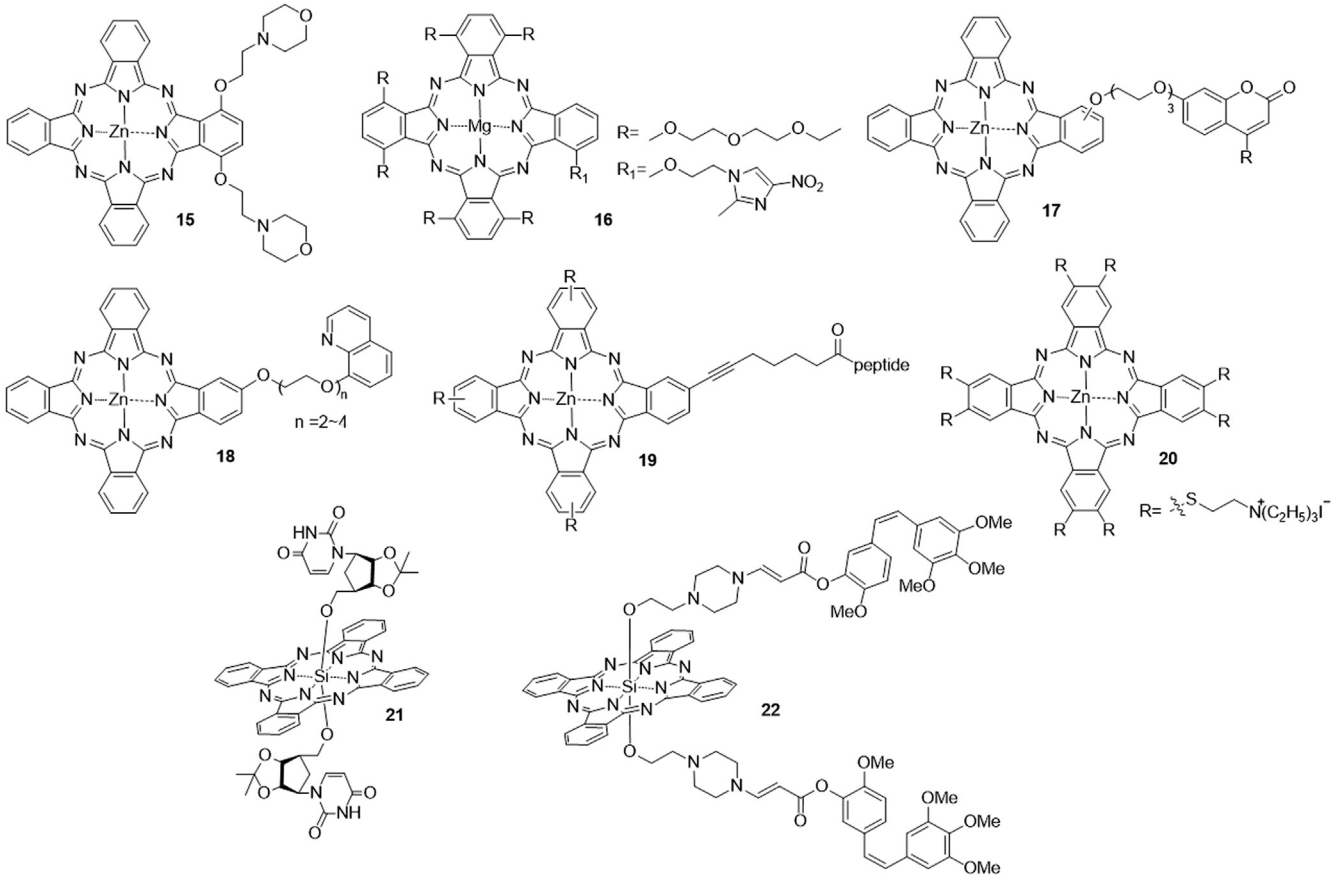

Figure 5 Chemical structures of phthalocyanine-type PSs **15**–**22**.

Please cite this article as: Zhang Juan, et al. An updated overview on the development of new photosensitizers for anticancer photodynamic therapy. *Acta Pharmaceutica Sinica B* (2017), http://dx.doi.org/10.1016/j.apsb.2017.09.003

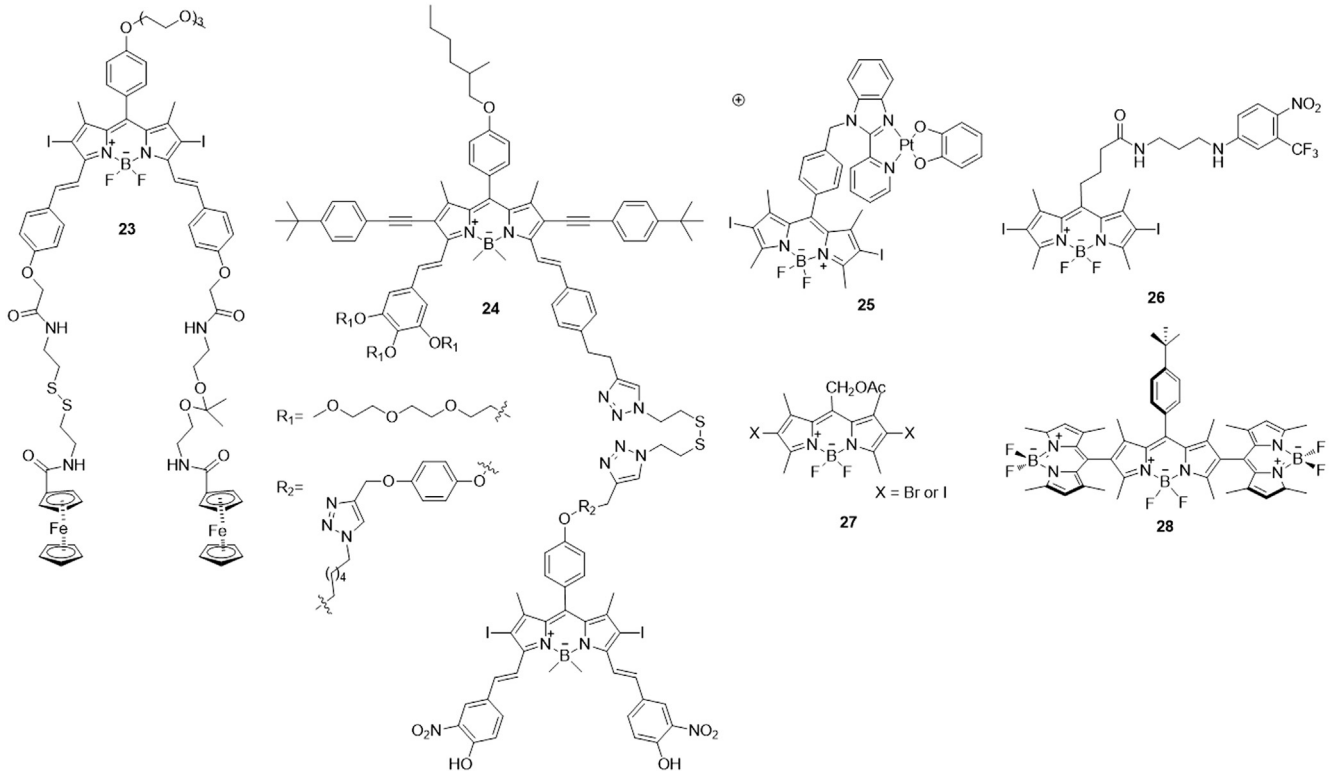

Figure 6 Chemical structures of BODIPY-type PSs **23–28**.

Additional to the synthesis of new types of PS molecules, the association of classical PSs to different carriers has also been explored to improve their photophysical properties and/or their targeting to tumors. On one hand, antibodies, receptor ligands, and other targeting molecules have been used to actively increase the accumulation of PSs in tumors. On the other hand, different nanostructures have been used to enhance or to maintain the activity of PSs in aqueous media, and to actively and/or passively deliver these molecules to tumors. Both of these systems, and even combinations of them, have been referred to as the third generation PS, and some encouraging results have been reported in the literature regarding the use of this strategy in anticancer PDT. With the significant successes on the developments of new PSs for PDT, it is expected that PDT will gain more widespread use in clinical practice.

Acknowledgments

This work was financially supported by the National Natural Science Foundation of China (No. 21672082), Shandong Key Development Project (No. 2016GSF201209), Young Taishan Scholars Program (No. tsqn20161037), Shandong Talents Team Cultivation Plan of University Preponderant Discipline (No. 10027), Shandong Natural Science Foundation for Distinguished Young Scholars (JQ201721), and by the Brazilian Government Agencies FAP/DF (0193.001020/2015) and CNPq (447.628/2014-3).

References

1. World Health Organization. Cancer. [Cited 30 March 2017]. Available from: ⟨http://www.who.int/mediacentre/factsheets/fs297/en/⟩.
2. Lucky SS, Soo KC, Zhang Y. Nanoparticles in photodynamic therapy. *Chem Rev* 2015;**115**:1990–2042.
3. De Angelis C. Side effects related to systemic cancer treatment: are we changing the Promethean experience with molecularly targeted therapies?. *Curr Oncol* 2008;**15**:198–9.
4. Uramoto H, Tanaka F. Recurrence after surgery in patients with NSCLC. *Transl Lung Cancer Res* 2014;**3**:242–9.
5. Liu G, Zhang S, Ma Y, Wang Q, Chen X, Zhang L, et al. Effects of error on dose of target region and organs at risk in treating nasopharynx cancer with intensity modulated radiation therapy. *Pak J Med Sci* 2016;**32**:95–100.
6. Raab O. Uber die Wirkung fluoreszierender Stoffe auf Infusorien. *Z Biol* 1900;**39**:524–46.
7. Ackroyd R, Kelty C, Brown N, Reed M. The history of photodetection and photodynamic therapy. *Photochem Photobiol* 2001;**74**:656–69.
8. Prime J. In: *Des Accidents Toxiques Produlit par l'Eosinate se Sodium*. 2nd ed. Paris: Jouve et Boyer; 1900.
9. Von Tappeiner H, Jesionek A. Therapeutische Versuche mit fluoreszierenden Stoffen. *Muench Med Wochenschr* 1903;**47**:2042–4.
10. Tappeiner H, Jodlbauer A. Über die Wirkung der photodynamischen (fluoreszierenden) Stoffe auf Infusorien. *Dtsch Arch Klin Med* 1904;**80**:427–87.
11. Lipson RL, Baldes EJ, Olsen AM. The use of a derivative of hematoporphyrin in tumor detection. *J Natl Cancer Inst* 1961;**26**:1–11.
12. Dougherty TJ, Kaufman JE, Goldfarb A, Weishaupt KR, Boyle D, Mittleman A. Photoradiation therapy for the treatment of malignant tumors. *Cancer Res* 1978;**38**:2628–35.
13. Lovell JF, Liu TWB, Chen J, Zheng G. Activatable photosensitizers for imaging and therapy. *Chem Rev* 2010;**110**:2839–57.
14. Cerman E, Çekiç O. Clinical use of photodynamic therapy in ocular tumors. *Surv Ophthalmol* 2015;**60**:557–74.
15. Benov L. Photodynamic therapy: current status and future directions. *Med Princ Pract* 2015;**24**:14–28.
16. Bozzini G, Colin P, Betrouni N, Nevoux P, Ouzzane A, Puech P, et al. Photodynamic therapy in urology: what can we do now and where are we heading?. *Photodiagn Photodyn Ther* 2012;**9**:261–73.

Please cite this article as: Zhang Juan, et al. An updated overview on the development of new photosensitizers for anticancer photodynamic therapy. *Acta Pharmaceutica Sinica B* (2017), http://dx.doi.org/10.1016/j.apsb.2017.09.003

17. Cotter TG. Apoptosis and cancer: the genesis of a research field. *Nat Rev Cancer* 2009;**9**:501–7.
18. Silva JN, Filipe P, Morlière P, Mazière JC, Freitas JP, Gomes MM, et al. Photodynamic therapy: dermatology and ophthalmology as main fields of current applications in clinic. *Biomed Mater Eng* 2008;**18**:319–27.
19. Konopka K, Goslinski T. Photodynamic therapy in dentistry. *J Dent Res* 2007;**86**:694–707.
20. Babilas P, Schreml S, Landthaler M, Szeimies RM. Photodynamic therapy in dermatology: state-of-the-art. *Photodermatol Photoimmunol Photomed* 2010;**26**:118–32.
21. Ding HY, Yu HJ, Dong Y, Tian RH, Huang G, Boothman DA, et al. Photoactivation switch from type II to type I reactions by electron-rich micelles for improved photodynamic therapy of cancer cells under hypoxia. *J Control Release* 2011;**156**:276–80.
22. Shah J, Park S, Aglyamov S, Larson T, Ma L, Sokolov K, et al. Photoacoustic imaging and temperature measurement for photothermal cancer therapy. *J Biomed Opt* 2008;**13**:034024.
23. Dougherty TJ, Gomer CJ, Henderson BW, Jori G, Kessel D, Korbelik M, et al. Photodynamic therapy. *J Natl Cancer Inst* 1998;**90**:889–905.
24. Solban N, Rizvi I, Hasan T. Targeted photodynamic therapy. *Lasers Surg Med* 2006;**38**:522–31.
25. Dolmans DE, Fukumura D, Jain RK. Photodynamic therapy for cancer. *Nat Rev Cancer* 2003;**3**:380–7.
26. Longo JPF, Muehlmann LA, Miranda-Vilela AL, Portilho FA, De Souza LR, Silva JR, et al. Prevention of distant lung metastasis after photodynamic therapy application in a breast cancer tumor model. *J Biomed Nanotechnol* 2016;**12**:689–99.
27. Castano AP, Mroz P, Wu MX, Hamblin MR. Photodynamic therapy plus low-dose cyclophosphamide generates antitumor immunity in a mouse model. *Proc Natl Acad Sci USA* 2008;**105**:5495–500.
28. Dougherty TJ, Grindey GB, Fiel R, Weishaupt KR, Boyle DG. Photoradiation therapy. II. Cure of animal tumors with hematoporphyrin and light. *J Natl Cancer Inst* 1975;**55**:115–21.
29. Juzeniene A, Peng Q, Moan J. Milestones in the development of photodynamic therapy and fluorescence diagnosis. *Photochem Photobiol Sci* 2007;**6**:1234–45.
30. Triesscheijn M, Baas P, Schellens JHM, Stewart FA. Photodynamic therapy in oncology. *Oncologist* 2006;**11**:1034–44.
31. Bellnier DA, Greco WR, Loewen GM, Nava H, Oseroff AB, Dougherty TJ. Clinical pharmacokinetics of the PDT photosensitizers porfimer sodium (photofrin), 2-[1-hexyloxyethyl]-2-devinyl pyropheophorbide-a (photochlor) and 5-ALA-induced protoporphyrin IX. *Lasers Surg Med* 2006;**38**:439–44.
32. Sharman WM, Allen CM, Van Lier JE. Photodynamic therapeutics: basic principles and clinical applications. *Drug Discov Today* 1999;**4**:507–17.
33. Josefsen LB, Boyle RW. Photodynamic therapy: novel third-generation photosensitizers one step closer?. *Br J Pharmacol* 2008;**154**:1–3.
34. Wall Jr MH, Basu P, Buranda T, Wicks BS, Findsen EW, Ondrias M, et al. Photoinduced electron transfer in covalently linked oxomolybdenum(V) porphyrin systems. *Inorg Chem* 1997;**36**:5676–7.
35. Magda D, Miller RA. Motexafin gadolinium: a novel redox active drug for cancer therapy. *Semin Cancer Biol* 2006;**16**:466–76.
36. Young SW, Woodburn KW, Wright M, Mody TD, Fan Q, Sessler JL, et al. Lutetium texaphyrin (PCI-0123): a near-infrared, water-soluble photosensitizer. *Photochem Photobiol* 1996;**63**:892–7.
37. Vogel E, Köcher M, Schmickler H, Lex J. Porphycene-α novel porphin isomer. *Angew Chem Int Ed* 1986;**25**:257–9.
38. Guardiano M, Biolo R, Jori G, Schaffner K. Tetra-n-propylporphycene as a tumour localizer: pharmacokinetic and phototherapeutic studies in mice. *Cancer Lett* 1989;**44**:1–6.
39. Trachtenberg J, Weersink RA, Davidson SRH, Haider MA, Bogaards A, Gertner MR, et al. Vascular-targeted photodynamic therapy (padoporfin, WST09) for recurrent prostate cancer after failure of external beam radiotherapy: a study of escalating light doses. *BJU Int* 2008;**102**:556–62.
40. Taneja SS, Bennett J, Coleman J, Grubb R, Andriole G, Reiter RE, et al. Final results of a phase I/II multicenter trial of WST11 vascular targeted photodynamic therapy for hemi-ablation of the prostate in men with unilateral low risk prostate cancer performed in the United States. *J Urol* 2016;**196**:1096–104.
41. Forsyth TP, Nurco DJ, Pandey RK, Smith KM. Synthesis and structure of a 5,15-bis(4-pyridyl)purpurin. *Tetrahedron Lett* 1995;**36**:9093–6.
42. De Moraes M, De Vasconcelos RC, Longo JPF, Muehlmann LA, De Azevedo RB, Lemos TM, et al. Effects of photodynamic therapy mediated by nanoemulsion containing chloro-aluminum phthalocyanine: a histologic and immunohistochemical study in human gingiva. *Photodiagn Photodyn Ther* 2015;**12**:592–7.
43. Muehlmann LA, Rodrigues MC, Longo JPF, Garcia MP, Py-Daniel KR, Veloso AB, et al. Aluminium-phthalocyanine chloride nanoemulsions for anticancer photodynamic therapy: development and in vitro activity against monolayers and spheroids of human mammary adenocarcinoma MCF-7 cells. *J Nanobiotechnol* 2015;**13**:36.
44. Miller JD, Baron ED, Scull H, Hsia A, Berlin JC, McCormick T, et al. Photodynamic therapy with the phthalocyanine photosensitize Pc 4: the case experience with preclinical mechanistic and early clinical-translational studies. *Toxicol Appl Pharmacol* 2007;**224**:290–9.
45. Borgatti-Jeffreys A, Hooser SB, Miller MA, Thomas RM, De Gortari A, Lucroy MD. Preclinical evaluation of zinc phthalocyanine tetrasulfonate-based PDT. *Proc SPIE* 2005;**5686**:624–30.
46. Wainwright M. Photodynamic therapy: the development of new photosensitisers. *Anti-Cancer Agents Med Chem* 2008;**8**:280–91.
47. Biel MA. Photodynamic therapy of head and neck cancers. In: Gomer C, editor. *Photodynamic Therapy. Methods in Molecular Biology*. Totowa, NJ: Humana Press; 2010.
48. Kennedy JC, Pottier RH, Pross DC. Photodynamic therapy with endogenous protoporphyrin. IX: basic principles and present clinical experience. *J Photochem Photobiol B Biol* 1990;**6**:143–8.
49. Ormond AB, Freeman AB. Dye sensitizers for photodynamic therapy. *Materials* 2013;**6**:817–40.
50. Tardivo JP, Del Giglio A, De Oliveira CS, Gabrielli DS, Junqueira HC, Tada DB, et al. Methylene blue in photodynamic therapy: from basic mechanisms to clinical applications. *Photodiagn Photodyn Ther* 2005;**2**:175–91.
51. Graciano TB, Coutinho TS, Cressoni CB, de Paula Freitas C, Pierre MBR, De Lima Pereira SA, et al. Using chitosan gels as a toluidine blue O delivery system for photodynamic therapy of buccal cancer: in vitro and in vivo studies. *Photodiagn Photodyn Ther* 2015;**12**:98–107.
52. Harris F, Chatfield LK, Phoenix DA. Phenothiazinium based photosensitisers-photodynamic agents with a multiplicity of cellular targets and clinical applications. *Curr Drug Targets* 2005;**6**:615–27.
53. Harris F, Sayed Z, Hussain S, Phoenix DA. An investigation into the potential of phenothiazinium-based photo-sensitisers to act as PDT agents. *Photodiagn Photodyn Ther* 2004;**1**:231–9.
54. Cincotta L, Foley JW, Cincotta AH. Phototoxicity, redox behavior, and pharmacokinetics of benzophenoxazine analogues in EMT-6 murine sarcoma cells. *Cancer Res* 1993;**53**:2571–80.
55. Cincotta L, Foley JW, MacEachern T, Lampros E, Cincotta AH. Novel photodynamic effects of a benzophenothiazine on two different murine sarcomas. *Cancer Res* 1994;**54**:1249–58.
56. Delaey E, Van Laar F, De Vos D, Kamuhabwa A, Jacobs P, De Witte P. A comparative study of the photosensitizing characteristics of some cyanine dyes. *J Photochem Photobiol B Biol* 2000;**55**:27–36.
57. Atzpodien J, Gulati SC, Clarkson BD. Comparison of the cytotoxic effects of merocyanine-540 on leukemic cells and normal human bone marrow. *Cancer Res* 1986;**46**:4892–5.
58. Awuah SG, You Y. Boron dipyrromethene (BODIPY)-based photosensitizers for photodynamic therapy. *RSC Adv* 2012;**2**:11169–83.
59. Lim SH, Thivierge C, Nowak-Sliwinska P, Han JY, Van Den Bergh H, Wagnières G, et al. In vitro and in vivo photocytotoxicity of boron dipyrromethene derivatives for photodynamic therapy. *J Med Chem* 2010;**53**:2865–74.

Please cite this article as: Zhang Juan, et al. An updated overview on the development of new photosensitizers for anticancer photodynamic therapy. *Acta Pharmaceutica Sinica B* (2017), http://dx.doi.org/10.1016/j.apsb.2017.09.003

60. Kitanov GM. Hypericin and pseudohypericin in some Hypericum species. *Biochem Syst Ecol* 2001;**29**:171–8.
61. Kubin A, Wierrani F, Burner U, Alth G, Grunberger W. Hypericin-the facts about a controversial agent. *Curr Pharm Des* 2005;**11**:233–53.
62. Garg AD, Krysko DV, Vandenabeele P, Agostinis P. Hypericin-based photodynamic therapy induces surface exposure of damage-associated molecular patterns like HSP70 and calreticulin. *Cancer Immunol Immunother* 2012;**61**:215–21.
63. Panzarini E, Inguscio V, Fimia GM, Dini L. Rose bengal acetate photodynamic therapy (RBAc-PDT) induces exposure and release of damage-associated molecular patterns (DAMPs) in human HeLa cells. *PLoS One* 2014;**9**:e105778.
64. Pandey RK, Herman CK. Shedding some light on tumours. *Chem Ind* 1998;**18**:739–43.
65. O'Connor AE, Gallagher WM, Byrne AT. Porphyrin and nonporphyrin photosensitizers in oncology: preclinical and clinical advances in photodynamic therapy. *Photochem Photobiol* 2009;**85**:1053–74.
66. Yoon I, Li JZ, Shim YK. Advance in photosensitizers and light delivery for photodynamic therapy. *Clin Endosc* 2003;**46**:7–23.
67. Garland MJ, Cassidy CM, Woolfson D, Donnelly RF. Designing photosensitizers for photodynamic therapy: strategies, challenges and promising developments. *Future Med Chem* 2009;**1**:667–91.
68. Fernandez JM, Bilgin MD, Grossweiner LI. Singlet oxygen generation by photodynamic agents. *J Photochem Photobiol B Biol* 1997;**37**:131–40.
69. Xodo LE, Cogoi S, Rapozzi V. Photosensitizers binding to nucleic acids as anticancer agents. *Future Med Chem* 2016;**8**:179–94.
70. Rajendran M. Quinones as photosensitizer for photodynamic therapy: ros generation, mechanism and detection methods. *Photodiagn Photodyn Ther* 2016;**13**:175–87.
71. Abrahamse H, Hamblin MR. New photosensitizers for photodynamic therapy. *Biochem J* 2016;**473**:347–64.
72. Li JW, Wu ZM, Magetic D, Zhang LJ, Chen ZL. Antitumor effects evaluation of a novel porphyrin derivative in photodynamic therapy. *Tumour Biol* 2015;**36**:9685–92.
73. Liao PY, Wang XR, Gao YH, Zhang XH, Zhang LJ, Song CH, et al. Synthesis, photophysical properties and biological evaluation of β-alkylaminoporphyrin for photodynamic therapy. *Bioorg Med Chem* 2016;**24**:6040–7.
74. Chen JJ, Hong G, Gao LJ, Liu TJ, Cao WJ. In vitro and in vivo antitumor activity of a novel porphyrin-based photosensitizer for photodynamic therapy. *J Cancer Res Clin Oncol* 2015;**141**:1553–61.
75. Nakai M, Maeda T, Mashima T, Yano S, Sakuma S, Otake E, et al. Syntheses and photodynamic properties of glucopyanoside-conjugated indium(III) porphyrins as a bifunctional agent. *J Porphyrins Phthalocyanies* 2013;**17**:1173–82.
76. Costa LD, Silva Jde A E, Fonseca SM, Arranja CT, Urbano AM, Sobral AJ. Photophysical characterization and in vitro phototoxicity evaluation of 5,10,15,20-tetra(quinolin-2-yl)porphyrin as a potential sensitizer for photodynamic therapy. *Molecules* 2016;**21**:439.
77. Horiuchi H, Hosaka M, Mashio H, Terata M, Ishida S, Kyushin S, et al. Silylation improves the photodynamic activity of tetraphenylporphyrin derivatives in vitro and in vivo. *Chemistry* 2014;**20**:6054–60.
78. Brunner H, Obermeier H. Platinum(II) complexes with porphyrin ligands-additive cytotoxic and photodynamic effect. *Angew Chem Int Engl* 1994;**33**:2214–5.
79. Mion G, Gianferrara T, Bergamo A, Gasser G, Pierroz V, Rubbiani R, et al. Phototoxic activity and DNA interactions of water-soluble porphyrins and their rhenium(I) conjugates. *ChemMedChem* 2015;**10**:1901–14.
80. Meng Z, Yu B, Han GY, Liu MH, Shan B, Dong GQ, et al. Chlorin P_6-based water-soluble amino acid derivatives as potent photosensitizers for photodynamic therapy. *J Med Chem* 2016;**59**:4999–5010.
81. Jinadasa RGW, Zhou ZH, Vicente MG, Smith KM. Syntheses and cellular investigations of di-aspartate and aspartate-lysine chlorin e_6 conjugates. *Org Biomol Chem* 2016;**14**:1049–64.
82. Narumi A, Tsuji T, Shinohara K, Yamazaki H, Kikuchi M, Kawaguchi S, et al. Maltotriose-conjugation to a fluorinated chlorin derivative generating a PDT photosensitizer with improved water-solubility. *Org Biomol Chem* 2016;**14**:3608–13.
83. Kahl SB, Koo M-S. Synthesis of tetrakis-carborane-carboxylate esters of 2,4-bis(α,β-dihydroxyethyl)-deuteroporphyrin IX. *J Chem Soc Chem Commun* 1990;**0**:1769–71.
84. Asano R, Nagami A, Fukumoto Y, Miura K, Yazama F, Ito H, et al. Synthesis and biological evaluation of new boron-containing chlorin derivatives as agents for both photodynamic therapy and boron neutron capture therapy of cancer. *Bioorg Med Chem Lett* 2014;**24**:1339–43.
85. Gushchina OI, Larkina EA, Nikolskaya TA, Mironov AF. Synthesis of amide derivatives of chlorin e_6 and investigation of their biological activity. *J Photochem Photobiol B* 2015;**153**:76–81.
86. Dąbrowski JM, Arnaut LG, Pereira MM, Monteiro CJ, Urba□ska K, Simões S, et al. New halogenated water-soluble chlorin and bacteriochlorin as photostable PDT sensitizers: synthesis, spectroscopy, photophysics, and in vitro photosensitizing efficacy. *ChemMedChem* 2010;**5**:1770–80.
87. Patel N, Pera P, Joshi P, Dukh M, Tabaczynski WA, Siters KE, et al. Highly effective dual-function near-infrared (NIR) photosensitizer for fluorescence imaging and photodynamic therapy (PDT) of cancer. *J Med Chem* 2016;**59**:9774–87.
88. Arslanoğlu Y, Nyokong T. Synthesis and photophysical studies of mono-carboxy phthalocyanines containing quaternizable groups. *Polyhedron* 2011;**30**:2733–9.
89. de Oliveira KT, De Assis FF, Ribeiro AO, Neri CR, Fernandes AU, Baptista MS, et al. Synthesis of phthalocyanines-ALA conjugates: water-soluble compounds with low aggregation. *J Org Chem* 2009;**74**:7962–5.
90. Bıyıklıoğlu Z, Kantekin H. Synthesis and spectroscopic properties of a series of octacationic water-soluble phthalocyanines. *Synth Met* 2011;**161**:943–8.
91. Silva AR, Simioni AR, Tedesco AC. Photophysical and complexation studies of chloro-aluminum phthalocyanine with beta-cyclodextrin and hydroxypropyl-beta-cyclodextrin. *J Nanosci Nanotechnol* 2011;**11**:4046–55.
92. Durmus M, Yaman H, Göl C, Ahsen V, Hyokong T. Water-soluble quaternized mercaptopyridine-substituted zinc-phthalocyanines: synthesis, photophysical, photochemical and bovine serum albumin binding properties. *Dyes Pigm* 2011;**91**:153–63.
93. Do Nascimento FB, manieri TM, Cerchiaro G, Ribeiro AO. Synthesis of unsymmetrical phthalocyanine derivatives and their interaction with mammary MCF7 cells. *Dyes Pigm* 2013;**99**:316–22.
94. Kucinska M, Skupin-Mrugalska P, Szczolko W, Sobotta L, Sciepura M, Tykarska E, et al. Phthalocyanine derivatives possessing 2-(morpholin-4-yl)ethoxy groups as potential agents for photodynamic therapy. *J Med Chem* 2015;**58**:2240–55.
95. Wierzchowski M, Sobotta L, Skupin-Mrugalska P, Kruk J, Jusiak W, Yee M, et al. Phthalocyanines functionalized with 2-methyl-5-nitro-1H-imidazolylethoxy and 1,4,7-trioxanonyl moieties and the effect of metronidazole substitution on photocytotoxicity. *J Inorg Biochem* 2013;**127**:62–72.
96. Zhou XQ, Meng LB, Huang Q, Li J, Zheng K, Zhang FL, et al. Synthesis and in vitro anticancer activity of zinc(II) phthalocyanines conjugated with coumarin derivatives for dual photodynamic and chemotherapy. *ChemMedChem* 2015;**10**:304–11.
97. Jia X, Yang FF, Li J, Liu JY, Xue JP. Synthesis and in vitro photodynamic activity of oligomeric ethylene glycol-quinoline substituted zinc(II) phthalocyanine derivatives. *J Med Chem* 2013;**56**:5797–805.
98. Ranyuk E, Cauchon N, Klarskov K, Guérin B, Van Lier JE. Phthalocyanine-peptide conjugates: receptor-targeting bifunctional agents for imaging and photodynamic therapy. *J Med Chem* 2013;**56**:1520–34.
99. Machacek M, Cidlina A, Novakova V, Svec J, Rudolf E, Miletin M, et al. Far-red-absorbing cationic phthalocyanine photosensitizers: synthesis and evaluation of the photodynamic anticancer activity and the mode of cell death induction. *J Med Chem* 2015;**58**:1736–49.

Please cite this article as: Zhang Juan, et al. An updated overview on the development of new photosensitizers for anticancer photodynamic therapy. *Acta Pharmaceutica Sinica B* (2017), http://dx.doi.org/10.1016/j.apsb.2017.09.003

100. Shen XM, Zheng BY, Huang XR, Wang L, Huang JD. The first silicon(IV) phthalocyanine-nucleoside conjugates with high photodynamic activity. *Dalton Trans* 2013;**42**:10398–403.
101. Bio M, Rajaputra P, Nkepang G, You Y. Far-red light activatable, multifunctional prodrug for fluorescence optical imaging and combinational treatment. *J Med Chem* 2014;**57**:3401–9.
102. Erbas-Cakmak S, Cakmak FP, Topel SD, Uyar TB, Akkaya EU. Selective photosensitization through an AND logic response: optimization of the pH and glutathione response of activatable photosensitizers. *Chem Commun (Camb)* 2015;**51**:12258–61.
103. Jiang XJ, Lau JT, Wang Q, Ng DK, Lo PC. pH- and thiol-responsive BODIPY-based photosensitizers for targeted photodynamic therapy. *Chemistry* 2016;**22**:8273–81.
104. Mitra K, Gautam S, Kondaiah P, Chakravarty AR. BODIPY-appended 2-(2-pyridyl)benzimidazole platinum(II) catecholates for mitochondria-targeted photocytotoxicity. *ChemMedChem* 2016;**11**:1956–67.
105. Fraix A, Blangetti M, Guglielmo S, Lazzarato L, Marino N, Cardile V, et al. Light-tunable generation of singlet oxygen and nitric oxide with a bichromophoric molecular hybrid: a bimodal approach to killing cancer cells. *ChemMedChem* 2016;**11**:1371–9.
106. Lincoln R, Durantini AM, Greene LE, Martínez SR, Knox R, Becerra MC, et al. meso-Acetoxymethyl BODIPY dyes for photodynamic therapy: improved photostability of singlet oxygen photosensitizers. *Photochem Photobiol Sci* 2016;**16**:178–84.
107. Ozdemir T, Bila JL, Sozmen F, Yildirim LT, Akkaya EU. Orthogonal bodipy trimers as photosensitizers for photodynamic action. *Org Lett* 2016;**18**:4821–3.

Please cite this article as: Zhang Juan, et al. An updated overview on the development of new photosensitizers for anticancer photodynamic therapy. *Acta Pharmaceutica Sinica B* (2017), http://dx.doi.org/10.1016/j.apsb.2017.09.003

ANEXO II

A xanthene derivative, free or associated to nanoparticles, as a new potential agent for anticancer photodynamic therapy

Juan Zhang[1,2,] Wellington Tavares de Sousa Júnior[1], Victor Carlos Mello da Silva[1], Mosar Correa Rodrigues[1,3], José Athayde Vasconcelos Morais[1,3], Cheng-Shi Jiang[2,*], João Paulo Figueiró Longo[3], Ricardo Bentes Azevedo[3] and Luís Alexandre Muehlmann[1,*]

[1] Faculty of Ceilandia, University of Brasília, Brasilia 72220275, Brazil;

[2] School of Biological Science and Technology, University of Jinan, Jinan 250022, China;

[3] Institute of Biological Sciences, University of Brasília, Brasilia 70910900, Brazil;

Correspondence should be addressed to Cheng-Shi Jiang; jiangchengshi-20@163.com and Luís Alexandre Muehlmann; luismuehlmann88@gmail.com

Abstract: The efficacy and safety of photodynamic therapy (PDT) have drawn much attention from clinicians and researchers in the field of anticancer treatments since the early 1900´s. Despite the numerous positive outcomes the works on PDT have brought to light over the last decades, much room remains for improvements in PDT tools, mainly on photosensitizer molecules. This works reports the first experiments evidencing the photosensitizing activity of DHX-1, a xanthene derivative-based near-infrared (NIR) probe recently described in the literature, both as a free molecule and associated to a nanostructured lipid carrier. The results show that the DHX-1 presents a broad band of light absorption within the optical window of biological tissues (600-800 nm), generates reactive oxygen species when photoactivated, and is phototoxic against murine breast adenocarcinoma 4T1 cells and murine fibroblast NIH-3T3 *in vitro*. Moreover, the association of DHX-1 to a nanostructured lipid carrier enhanced its activity against cancer cells in aqueous media and strongly reduced its phototoxicity against the normal cell line.

Keywords: photodynamic therapy; xanthene derivative; nanostructured lipid carrier; breast adenocarcinoma; nanotechnology

1. Introduction

The Photodynamic therapy (PDT) has long been pointed out as an effective and safe modality of cancer therapy [1]. Anticancer PDT is based on the focal photoactivation of photosensitizers (PS), directly on the target tissue, eliciting photochemical reactions that eventually lead to oxidative stress [2]. The main consequences of these events are the direct cytotoxicity, collapse of the tumor microvasculature, and/or activation of immune response against tumor antigens [3]. A particularly important benefit of PDT as a cancer therapy is the possibility to restrict its effects to the irradiated site, sparing the normal tissues. Although PDT has been successfully applied in the treatment of different cancers, still considerable room remains for the improvement of PS molecules and PS delivery systems. The majority of the clinically available PS molecules present poor water solubility, low absorption in near-infrared (NIR) region, inadequately long half-life, and intense accumulation into the skin [4].

Many different compounds have been proposed as new PS candidates [2], such as the xanthene derivatives. Rose Bengal, for example, is a photoactive fluorescent dye tested as a PS for antimicrobial [5] and anticancer [6] PDT. Despite the encouraging results obtained with xanthenes as PS, however, relatively few works have focused on obtaining xanthene derivatives for anticancer PDT.

During our continued project for developing new PS systems based on nanostructured formulations [7–10], the dye DHX-1 (Fig. 1), with a xanthene-indolium framework and peak of light absorption at 698 nm, reported by Yuan et al in 2012 [11], came to our attention. This compound and its analogs were described as a new class of NIR dye for biological imaging applications in living animals. So far, this DHX-1 series of compounds were described as near-infrared fluorescent probe for imaging *in vitro* or *in vivo* small molecules or enzymes, such as H_2O_2 and thiols [11–13], alkaline phosphatase [14], β-galactosidase [15], nitroreductase [16], and hNQO1 [17]. To our knowledge, the potential PS activity of this series of compounds has not been investigated. Thus, in the present study, the xanthene-indolium derivative DHX-1 was prepared and evaluated for its *in vitro* activity as PS against cancer cells, both free and incorporated into nanostructured lipid carriers.

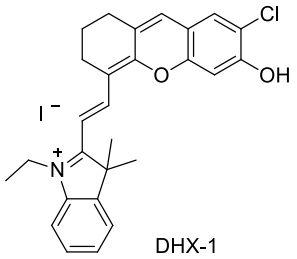

Figure 1. Structure of DHX-1.

2. Materials and Methods

Dimethyl sulfoxide (DMSO), 1,3-diphenylisobenzofuran (DPBF) and Kholiphor® HS were obtained from Sigma, USA. The Roswell Park Memorial Institute (RPMI) medium and Dulbecco's modified Eagle medium (DMEM) were obtained from Gibco, EUA. The 3-(4,5-dimethylthiazol-2yl)-2,5-diphenyltetrazolium bromide (MTT) was purchased from Invitrogen, EUA. The phosphate buffered saline (PBS) was supplied by Laborclin, Brazil. The babassu oil was obtained from Amazon Oil, Brazil. Commercially available reagents were used without further purification. Organic solvents were evaporated with reduced pressure using Büchi evaporators. Reactions were monitored by TLC using Yantai JingYou (China) GF254 silica gel plates. Silica gel column chromatography was performed on silica gel (200-300 mesh) from Qingdao Hailang (China). NMR spectra were measured on Bruker Avance III 600 MHz spectrometer. Chemical shifts were expressed in δ (ppm) and coupling constants (J) in Hz using solvent signals as internal standards ($CDCl_3$, δ_H 7.26 ppm and δ_C 77.0 ppm). ESI-MS was recorded on an Agilent 1260-6460 Triple Quard LC/MS.

*2.1 Synthesis of **1a***

The compound **1a** (Fig. 2) was prepared starting from 2,3,3-trimethyllindolenine and cyclohexanone according to the previously reported protocol [14]. ^{1}H NMR (600 MHz, $CDCl_3$) δ 8.36 (d, J = 12.0 Hz, 2H), 7.41 (d, J = 6.0 Hz, 2H), 7.40 (t, J = 6.0 Hz, 2H), 7.29 – 7.25 (m, 2H), 7.20 (d, J = 6.0 Hz, 2H), 6.21 (d, J = 12.0 Hz, 2H), 4.25 (d, J = 8.0 Hz, 4H), 2.75 (s, 4H), 1.99 (s, 2H), 1.72 (s, 12H), 1.47 (t, J = 8.0 Hz, 6H). ^{13}C NMR (600 MHz, $CDCl_3$) 171.9, 150.7, 144.5, 141.7, 141.2, 128.9, 127.4, 125.4, 122.3, 110.8, 101.0, 49.4, 40.1, 28.1, 26.8, 20.7, 12.5. ESI-MS calcd for $C_{34}H_{40}ClN_2^+$ (M^+): 511.2, Found 511.2.

2.2 Synthesis of Compound DHX-1

The synthesis of DHX-1 was completed according to the previously reported protocol [11]. A solution of 4-chloro resorcin (**1b**, Fig. 2) (67 mg, 0.46 mmol) and triethylamine (0.15 mL) in 1.5 mL DMF was stirred at room temperature under nitrogen atmosphere for 10 min. Compound **1a** (100 mg, 0.15 mmol) in DMF (1.5 mL) was added to the mixture, and the reaction mixture was heated at 75 °C for 4 h. The solution was then removed under reduced pressure. The crude product was purified by silica gel flash chromatography using CH_2Cl_2/EtOH (50:1) as eluent to give DHX-1 as a blue-green solid (25.5 mg, 12.6%). ^{1}H NMR (600 MHz, $CDCl_3$): δ 8.16 (d, J = 12.0 Hz, 2H), 7.40 (s, 1H), 7.28-7.33 (m, 3H), 7.11 (t, J = 6.0 Hz, 2H), 6.90 (d, J = 6.0 Hz, 2H), 6.80 (s, 1H), 5.70 (d, J = 12.0 Hz, 2H), 4.90 (q, J = 6.0 Hz, 2H), 2.67 (t, J = 6.0 Hz, 2H), 2.61 (t, J = 6 Hz, 2H), 1.92-1.86 (m, 2H), 1.66 (s, 6H), 1.36 (t, J = 6.0 Hz, 3H). ^{13}C NMR (600 MHz, $CDCl_3$): 167.7, 161.3, 157.2, 142.6, 140.3, 139.1, 136.1, 128.5, 127.4, 123.5, 122.4, 118.8, 115.6, 114.9, 108.8, 103.9, 95.7, 48.3, 38.7, 28.6, 28.3, 24.5, 21.2, 11.8. ESI-MS calcd for $C_{27}H_{27}ClNO_2^+$ (M^+): 432.1, Found 432.1.

2.3 Nanostructured lipid carriers preparation

Different nanostructured lipid carriers were prepared by a phase inversion temperature (PIT) method, and a final formulation was chosen based on its colloidal properties. Different proportions of babassu oil to Compritol® 888 ATO in the lipid mix, and different ratios of the surfactant Kolliphor® HS to the lipid mix were tested.

In brief, the lipid mix and the Kolliphor® HS were mixed at 60 °C, under magnetic stirring (350 RPM) for 5 minutes. Then, this mixture was diluted with water (1:10, w:v), and the coarse emulsion formed was then heated to 75 °C. The transparent emulsion obtained in this temperature was kept under magnetic stirring for 10 minutes. Next, the emulsion was left to cool to room temperature, with the nanostructured lipid carriers being formed by the solidification of lipid/surfactant droplets.

The nanostructured lipid carrier containing DHX-1 (NLC-DHX) used in the subsequent experiments was prepared by diluting DHX-1 to a concentration of 25 mg/mL in a mixture of babassu oil, Compritol® 888 ATO and Kholiphor® HS (1:1:2, w:w:w) at 60 °C, under magnetic stirring (350 RPM) for 5 minutes. Then, the preparation of NLC-DHX proceeded as described in the general protocol above. Blank

nanostructured lipid carrier (NLC) was also prepared by this same method, without DHX-1.

2.4 Evaluation of colloidal properties.

The mean particle size and polydispersity index (PDI) of NLC were evaluated at 25 °C by photon correlation spectroscopy and electrophoretic laser Doppler velocimetry (ZetaSizer Nano ZS®, Malvern Instruments, Malvern, UK) with the angle of 90°. Prior to measurement, samples were diluted with distilled water (1:10, v:v).

2.5 Spectroscopic analysis

The DHX-1 and the NLC-DHX were diluted to 40 µM DHX-1in DMSO and water, respectively. Then, 200 µL of the DHX-1 solution or NLC-DHX dispersion were placed in 96-well microplate in triplicate, and its absorption spectra was recorded in a spectrophotometer (Spectramax M2, Molecular Devices, USA) between 350 and 750 nm. Blanks consisted of pure DMSO and water.

2.6 Evaluation of ROS production

To evaluate the capacity of DHX-1 to produce singlet oxygen under irradiation, the DPBF method was used, according to Spiller et al [18]. Briefly, 200 µL-aliquots of DHX-1 in DMSO (40 µM) and NLC-DHX dispersed in water (40 µM DHX-1) were plated in 96-well plates. Then, 10 µL of a solution of DPBF in ethanol (0.22 mg/mL) were added to each aliquot. Controls consisted of DHX-1 or NLC-DHX without DPBF, and DPBF alone. Then, the microplate was irradiated with a LED (λ 660 nm, XL001WP01NRC660, Shenzhen S. O. Co, China) at cumulative energy densities and read in a spectrophotometer (Spectramax M2, Molecular Devices, USA) at 414 mm.

2.7 Biological assays

2.7.1 Cell culture

Murine breast adenocarcinoma cells (4T1) were maintained in RPMI medium supplemented with 10% (v:v) FBS and 1% (v:v) antibiotics solution (100 penicillin Units/mL and 100 µg streptomycin/mL). Murine fibroblasts (NIH-3T3) were maintained

in DMEM supplemented with 10% (v:v) FBS and 1% (v:v) antibiotic solution. Cells were kept in an incubator under a humidified atmosphere with 5% CO_2 at 37 °C.

2.7.2 In vitro treatment design

The cells were culture for 24 h at an initial concentration of 1×10^4 cells per well, washed twice with PBS, and then exposed for 15 min to 200 µL of culture medium containing different concentrations of DHX, NLC-DHX or NLC. Then, the cells were washed twice with PBS, covered with 200 µL of culture medium, and: 1) maintained in the dark, or 2) irradiated with a light emitting diode (LED, λ 660 nm) at a final energy density of 25.8 J/cm^2. The control consisted of cells that received only culture medium. Then the cells were washed with PBS, cultured for further 24 h, and their viability was measured.

2.7.3 Cell viability assay

The cells were treated as described above, then exposed to 200 µL of MTT solution (0.5 mg/mL in culture medium), as previously described [19]. Next, the MTT solution was removed, the cells were washed with PBS, and the formazan formed by viable cells was extracted with 200 µL DMSO. The absorption at λ 595 nm was then measured using a spectrophotometer (SpectramaxM2; Molecular Devices LLC). This experiment was performed in quintuplicate for each treatment, and the results were expressed as percentages relative to control.

3. Results and Discussion

3.1. Synthesis of DHX-1

This compound was prepared according to a previously reported protocol [11], as shown in Fig. 2. Briefly, treatment of synthetic **1a** [14] and commercially available 4-chlorobenzene-1,3-diol (**1b**) in DMF with in the presence of Et_3N at 75 °C for 4 h yielded DHX-1. The ^1H and ^{13}C NMR spectral data of DHX-1 were in agreement with the literature data [11]. The spectra can found be in the Supporting Information, which was attached at the end of this article.

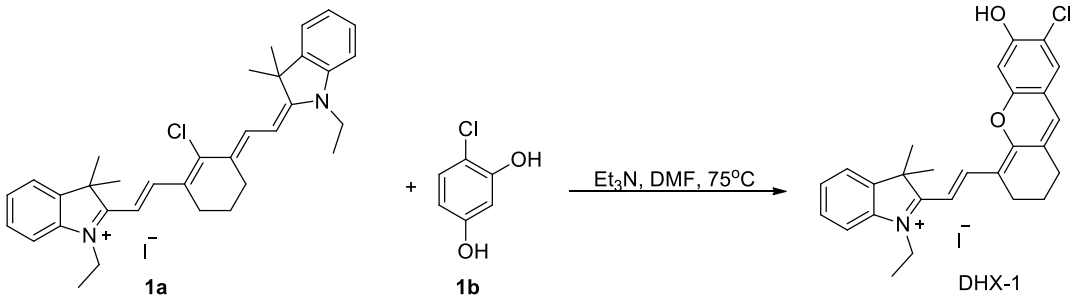

Figure 2. The synthesis of DHX-1.

3.2. Nanostructured lipid carriers

Different compositions of lipid mix (babassu oil plus Compritol® 888 ATO), and different proportions of lipid mix to Kolliphor® HS were tested. As shown in Fig. 3, these parameters affected the colloidal properties of the formulation. Particularly, the nanoparticles obtained with a lipid mix containing babassu oil below 52.5% (w:w) showed low polydispersity index (PDI) values and hydrodynamic diameters from 30 to 70 nm (Fig. 3A). Therefore, the concentration of babassu oil in the lipid mix used for the production of nanostructured lipid carrier containing DHX-1 (NLC-DHX) and NLC was set to 50% (w:w). The surfactant concentration, which was expressed as surfactant:lipids ratio (w:w), also affected the properties of the nanostructured lipid carrier. As shown in Fig. 3B, surfactant-to-lipids ratios (SLR) below 0.7 gave formulations with PDI of 0.3 or higher, showing wider size distributions than formulations produced with SLR above 0.8. Therefore, giving all these results, the final formulation of nanostructured lipid carriers (NLC) consisted of a lipid mix containing babassu oil/Compritol® 888 ATO (1:1), and a SLR of 1.0. The colloidal properties of both NLC and NLC containing DHX-1 (NLC-DHX) are shown in Table 1.

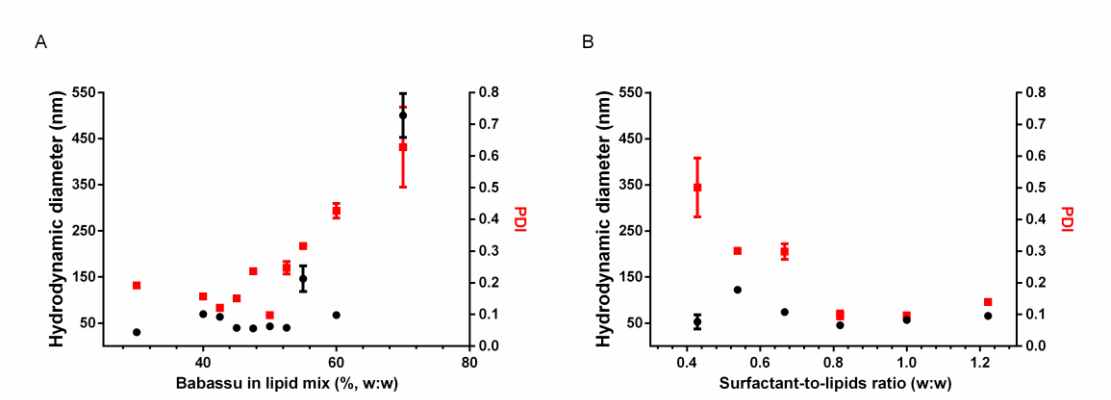

Figure 3. Influence of the concentration of babassu oil in the lipid mix (A), and of the surfactant-to-oil ratio (B), on the hydrodynamic diameter and polydispersity index (PDI) of nanostructured lipid carriers produced by phase inversion temperature.

Table 1. Colloidal characteristics of NLC and NLC-DHX.

	Hydrodynamic diameter (nm)	Polydispersity index	Zeta potential (mV)
NLC	50.0 ± 0.4	0.119 ± 0.022	-3.30 ± 0.12
NLC-DHX	92.1 ± 0.7	0.215 ± 0.030	-1.12 ± 0.09

3.3 Light absorption spectra

The DHX-1 presented a wide band of light absorption, ranging from about 550 to 700 nm, with two main peaks at 612 and 665 nm, as shown in Fig. 4. This is an important feature of DHX-1 regarding its potential application as a PS for anticancer PDT. Here it was interesting to note that the peak of maximal absorption was at 698 nm in Yuan's study [11], which was different in our result. The reason might be attributed to the different solvents used, which has a great impact on the spectroscopic test result of this group of xanthane derivatives. In Yuan's experiment, the absorption spectra was accorded in the solvent of pH 7.4 PBS/MeOH (1:1) which showed maximal peak at 698 and a shoulder peak at around 650; however in our experiment the absorption spectra were accorded in the solvent of DMSO or water, which possible make the absorption blue shift. Most of the biological tissues have an optical window, i.e., a particular range of electromagnetic wavelengths, mostly between 650 and 800 nm, that are poorly absorbed by the tissue components, such as water and hemoglobin [2]. Therefore, DHX-1 can absorb light even at deep layers of the target tissue, a feature that favors its efficacy in anticancer PDT.

Due to their hydrophobic structure, DHX-1 molecules aggregate in aqueous media, leading to quenching phenomena that significantly impair their PS activity. Thus, the DHX-1 was also tested as the NLC-DHX, a formulation consisting of DHX-1 dissolved into the lipid matrix of a nanostructured lipid carrier, as described above, a strategy that

allowed maintaining, in water, the characteristic peak of light absorption by DHX-1 (Fig. 4).

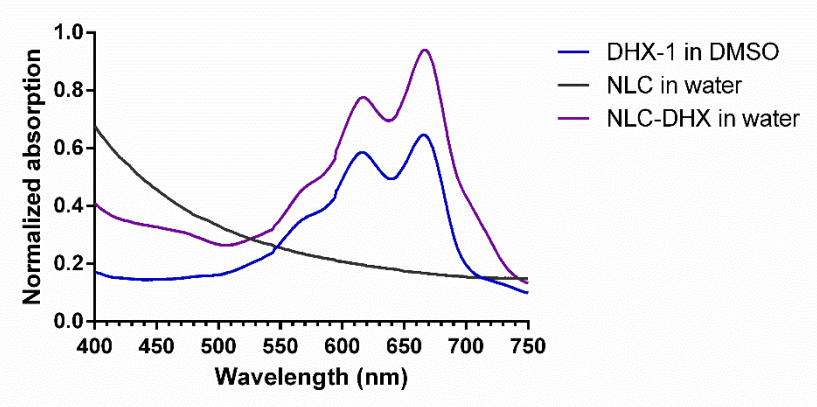

Figure 4. Absorption spectra of DHX-1 dissolved in DMSO (DHX-1 in DMSO) or in water (DHX-1 in water), nanostructured lipid carrier containing DHX-1 and dispersed in water (NLC-DHX in water), and nanostructured lipid carrier dispersed in water (NLC in water). The concentration of DHX-1 was 40 µM for DHX-1 in DMSO, DHX-1 in water and NLC-DHX in water. The amounts of nanoparticles in NLC-DHX and NLC were the same.

3.4 Photoactivated generation of ROS

In PDT, the light excites the PS to a singlet state, which may then be converted to a more stable excited triplet state [2]. The excited triplet state of the PS may be involved in type I and type II photoreactions. The type I photoreactions are based on the interaction of the excited PS with different substrates, finally leading to the production of different reactive oxygen species (ROS) [20]. The type II photoreactions consist of the conversion, mediated by the excited triplet state PS, of ground triplet state molecular oxygen ($^3O_2$) to its excited singlet state ($^1O_2$) [2]. Thus, triggering photoreactions by the photoactivation of the PS is a crucial event in PDT. As shown in Fig. 5, the irradiated DHX-1, both as the free molecule dissolved in DMSO and as the NLC-DHX dispersed in water, generated ROS in a light dose-dependent fashion. This result confirms that DHX-1 acts as a PS under irradiation. Moreover, the similar profiles of ROS generation presented by DHX-1 and NLC-DHX show that the association of this PS to the nanostructure maintains its activity in an aqueous medium. This means that NLC-DHX would be adequate for the use in PDT by parenteral routes.

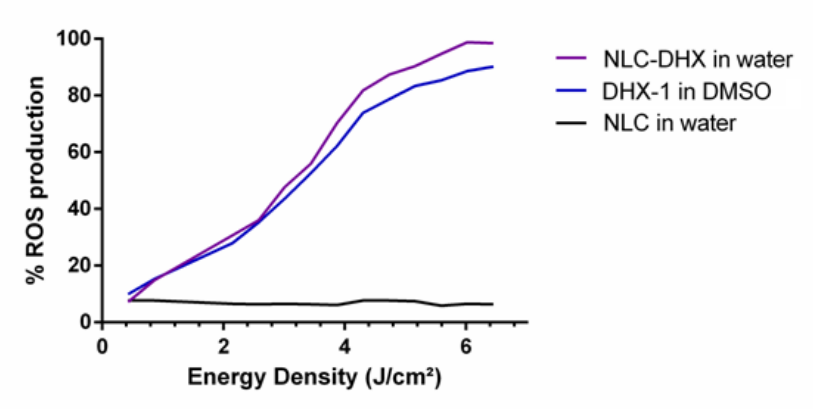

Figure 5. Photoactivated production of reactive oxygen species (ROS) by DHX-1 dissolved in DMSO (DHX-1 in DMSO), nanostructured lipid carrier containing DHX and dispersed in water (NLC-DHX in water), and nanostructured lipid carrier dispersed in water (NLC in water). The concentration of DHX-1 was 40 µM for DHX-1 in DMSO and NLC-DHX in water. The amount of nanoparticles in NLC-DHX and NLC was the same. Samples were irradiated with a light emitting diode, λ 660 nm.

3.5 Cytotoxicity in vitro

The production of ROS by the photoactivated PS in the target tissue eventually leads to oxidative stress, which can be lethal to the affected cells. As shown in Fig. 6, the compound DHX-1 presented evident, concentration-dependent phototoxicity in both 4T1 and NIH-3T3 cells *in vitro* after photoactivation. Noteworthy, the toxicity exhibited by DHX-1 in the dark against both cells was negligible, with only the highest concentration tested, 20 µM, being significantly toxic to NIH-3T3. This result indicated that DHX-1 was a good potential PS by showing cytotoxicity only under lighting condition. More significantly, on one hand, NLC-DHX at low concentrations was more phototoxic than DHX-1 to 4T1 cells, while less cytotoxic at the highest concentration tested; on the other hand, NLC-DHX was not photocytotoxic against NIH-3T3 cells even at the highest concentration. These findings suggest that this nanostructured carrier changes the interaction of DHX-1 with these cells, which may be beneficial for anticancer PDT. However, to explain the selectivity of NLC-DHX towards cancerous 4T1 over NIH 3T3, a lot of experiment are conducted with molecular biological methods.

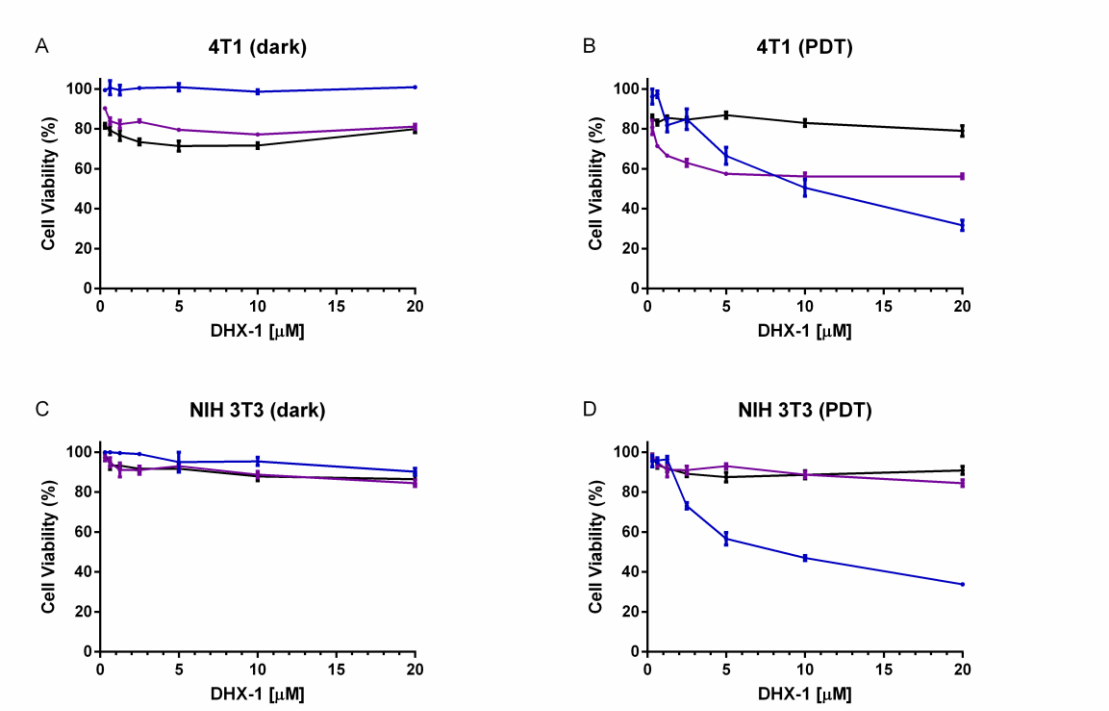

Figure 6. Viability of 4T1 and NIH-3T3 cells treated *in vitro* with DHX-1 (blue line), NLC-DHX (nanostructured lipid carrier with DHX-1; purple line) and NLC (nanostructured lipid carrier; black line), and irradiated (PDT, 25.8 J/cm^2) or not (dark). In A, $p<0.05$ for NLC-DHX vs DHX-1 at all concentrations; $p<0.05$ for NLC vs NLC-DHX only at 2.6 and 5.0 μM. In B, $p<0.05$ for NLC-DHX vs DHX-1 at all concentrations, except at 10.0 μM; $p<0.05$ for NLC vs NLC-DHX at all concentrations, except at 0.3 μM. In C, no statistically significant differences were found for NLC-DHX vs DHX-1, and for NLC vs NLC-DHX, at all concentrations; $p<0.05$ for DHX-1 0.0 vs. 20.0 μM. In D, $p<0.05$ for NLC-DHX vs DHX-1 at concentrations ≥2.6 μM; no statistically significant differences were found for NLC vs NLC-DHX.

4. Conclusions

This work shows for the first time that DHX-1, a xanthene derivative first reported by Yuan and collaborators in 2012 [11], presents PS activity *in vitro*. Moreover, the association of DHX-1 to a nanostructured lipid carrier allowed maintaining its activity in aqueous media and reduced its *in vitro* phototoxicity towards NIH-3T3 cells, the normal cell line used in this work. These results and the previously reported data on DHX-1 suggest that this xanthene derivative is a potential PS used in PDT application.

Conflicts of Interest: The authors declare that there is no conflict of interest regarding the publication of this article.

Acknowledgments: This research work was financially supported by the Brazilian Government Agencies FAP/DF and CNPq, Natural Science Foundation of China [No. 21672082], and Shandong Key Development Project [No. 2016GSF201209].

Supplementary Materials: The NMR spectra of **1a** and DHX-1 are listed in the supplementary materials.

Abbreviations

PDT	photodynamic therapy
PS	photosensitizers
NIR	near-infrared
H_2O_2	hydrogen peroxide
hNQO1	human NAD(P)H:quinone oxidoreductase 1
Et_3N	triethylamine
DMF	dimethyl formamide
NMR	Nuclear magnetic resonance
PDI	polydispersity index
NLC	nanostructured lipid carrier
SLR	surfactant-to-lipids ratios
ROS	reactive oxygen species
$^3O_2$	triplet state oxygen
$^1O_2$	singlet state oxygen
DMSO	dimethyl sulfoxide
DPBF	1,3-diphenylisobenzofuran
MTT	3-(4,5-dimethylthiazol-2yl)-2,5-diphenyltetrazolium bromide
LC/MS	liquid chromatography-mass spectrometry

PIT phase inversion temperature

References

1. J.C. Kennedy, R.H. Pottier, and D.C Pross, “Photodynamic therapy with endogenous protoporphyrin. IX: Basic principles and present clinical experience,” *Journal of Photochemistry and Photobiology B: Biology,* vol. 6, pp. 143–148, 1990.
2. J. Zhang, J.P. C.S. Jiang, Figueiró Longo, R.B. Azevedo, H. Zhang, and L.A. Muehlmann, “An updated overview on the development of new photosensitizers for anticancer photodynamic therapy,”*Acta Pharmaceutica Sinica B*, vol. 8, pp 137–146, 2018.
3. T.J. Dougherty, C.J. Gomer, B.W. Henderson, G. Jori, D. Kessel, M. Korbelik, J. Moan, and Q. Peng, “Photodynamic therapy,” *Journal of the National Cancer Institute,* vol. 90, pp. 889–905, 1998.
4. S. Yano, S. Hirohara, M. Obata, Y. Hagiya, S. Ogura, A. Ikeda, H. Kataoka, M. Tanaka, and T. Joh, “Current states and future views in photodynamic therapy,” *Journal of Photochemistry and Photobiology C: Photochemsitry Reviews*, vol. 12, pp. 46–67, 2011.
5. A. Costa, V.M. Rasteiro, C.A. Pereira, R.D. Rossoni, J.C. Junqueira, and A.D. Jorge, “The effects of rose bengal- and erythrosine-mediated photodynamic therapy on *Candida albicans,*”. *Mycoses*, vol. 55, pp. 56–63, 2012.
6. E. Panzarini, V. Inguscio, G.M. Fimia, and L. Dini, “Rose bengal acetate photodynamic therapy (RBAc-PDT) induces exposure and release of damage-associated molecular patterns (DAMPs) in human HeLa cells,” *PLoS One*, vol. 9, e105778, 2014.
7. L.A. Muehlmann, M.C. Rodrigues, J.P. Longo, M.P. Garcia, K.R. Py-Daniel, A.B. Veloso, P.E. de Souza, S.W. da Silva, and R.B. Azevedo, “Aluminium-phthalocyanine chloride nanoemulsions for anticancer photodynamic therapy: Development and in vitro activity against monolayers and spheroids of human mammary adenocarcinoma MCF-7 cells,” *Journal of Nanobiotechnology,* vol. 13, pp.36, 2015.
8. L.A. Muehlmann, B.C. Ma, J.P. Longo, Mde F. Almeida Santos, and R.B. Azevedo, “Aluminum-phthalocyanine chloride associated to poly(methyl vinyl ether-co-maleic anhydride) nanoparticles as a new third-generation photosensitizer for

anticancer photodynamic therapy," *International Journal of Nanomedicine*, vol. 9, pp. 1199–1213, 2014.

9. M.C. Rodrigues, L.A. Muehlmann, J.P. Longo, R.C. Silva, I.B. Graebner, I.A. Degterev, C.M. Lucci, R.B. Azevedo, and M.P. Garcia, "Photodynamic Therapy Based on Arrabidaea chica (Crajiru) Extract Nanoemulsion: In vitro Activity against Monolayers and Spheroids of Human Mammary Adenocarcinoma MCF-7 Cells," *Journal of Nanomedicine & Nanotechnology*, vol. 6, pp. 1000286, 2015.
10. V. Monge-Fuentes, L.A. Muehlmann, J.P. Longo, J.R. Silva, M.L. Fascineli, P. de Souza, F. Faria, I.A. Degterev, A. Rodriguez, F.P. Carneiro, C.M. P. Escobar, R.F. Amorim, and R.B. Azevedo, "Photodynamic therapy mediated by acai oil (Euterpe oleracea Martius) in nanoemulsion: A potential treatment for melanoma," *Journal of Photochemistry and Photobiology B: Biology*, vol. 166, pp. 301–310, 2017.
11. L. Yuan, W. Lin, S. Zhao, W. Gao, B. Chen, L. He, and S. Zhu, "A unique approach to development of near-infrared fluorescent sensors for in vivo imaging," *Journal of American Chemical Society*, vol. 134, pp. 13510–13523, 2012.
12. F. Xu, H. Li, Q. Yao, J. Fan, J. Wang, and X. Peng, "A NIR fluorescent probe: imaging endogenous hydrogen peroxide during an autophagy process induced by rapamycin," *Journal of Materials Chemistry B*, vol. 4, pp. 7363–7367, 2016.
13. Y. Tang, X. Kong, Z.R. Liu, A. Xu, and W. Lin, "Lysosome-targeted turn-on fluorescent probe for endogenous formaldehyde in living cells," *Analytic Chemistry*, vol. 88, pp. 9359–9363, 2016.
14. Y. Tan, L. Zhang, K.H. Man, R. Peltier, G. Chen, H. Zhang, L. Zhou, F. Wang, D. Ho, S.Q Yao, Y. Hu, and H. Sun, "Reaction-based off–on near-infrared fluorescent probe for imaging alkaline phosphatase activity in living cells and mice," *ACS Applied Materials & Interfaces*, vol. 9, pp. 6796–6803, 2017.
15. J. Zhang, C. Li, C. Dutta, M. Fang, S. Zhang, A. Tiwari, T. Werner, F.T. Luo, H. Liu, "A novel near-infrared fluorescent probe for sensitive detection of β-galactosidase in living cells,". *Analytica Chimica Acta*, vol. 968, pp. 97–104, 2017.
16. D. Yang, H.Y. Tian, T.N. Zang, M. Li, Y. Zhou, and J.F Zhang, "Hypoxia imaging in cells and tumor tissues using a highly selective fluorescent nitroreductase probe," *Scientific Reports,* vol. 7, pp. 9174, 2017.

17. C. Zhang, B.-B. Zhai, T. Peng, Z. Zhong, L. Xu, Q.-Z. Zhang, L.-Y. Li, L. Yi, and Z. Xi, “Design and synthesis of near-infrared fluorescence-enhancement probes for the cancer-specific enzyme hNQO1,” *Dyes Pigments,* vol. 143, pp.245–251, 2017.
18. W. Spillerm, H. Kliesch, D. Wöhrle, S. Hackbarth, B. Röder, and G. Schnurpfeil, “Singlet Oxygen Quantum Yields of Different Photosensitizers in Polar Solvents and Micellar Solutions,” *Journal of Porphyrins and Phthalocyanines*, vol. 02, pp. 145, 1998.
19. T. Mosmann, “Rapid colorimetric assay for cellular growth and survival: Application to proliferation and cytotoxicity assays,” *Journal of Immunological Methods*, vol. 65, pp. 55–63, 1983.
20. H. Ding, H. Yu, Y. Dong, R. Tian, G. Huang, D.A. Boothman, B.D. Sumer, and J. Gao, “Photoactivation switch from type II to type I reactions by electron-rich micelles for improved photodynamic therapy of cancer cells under hypoxia,” *Journal of Controlled Release*, vol.156, pp. 276–280, 2011.

Supporting Information

Table of Contents

Figure S1. ^{1}H spectrum of **1a**

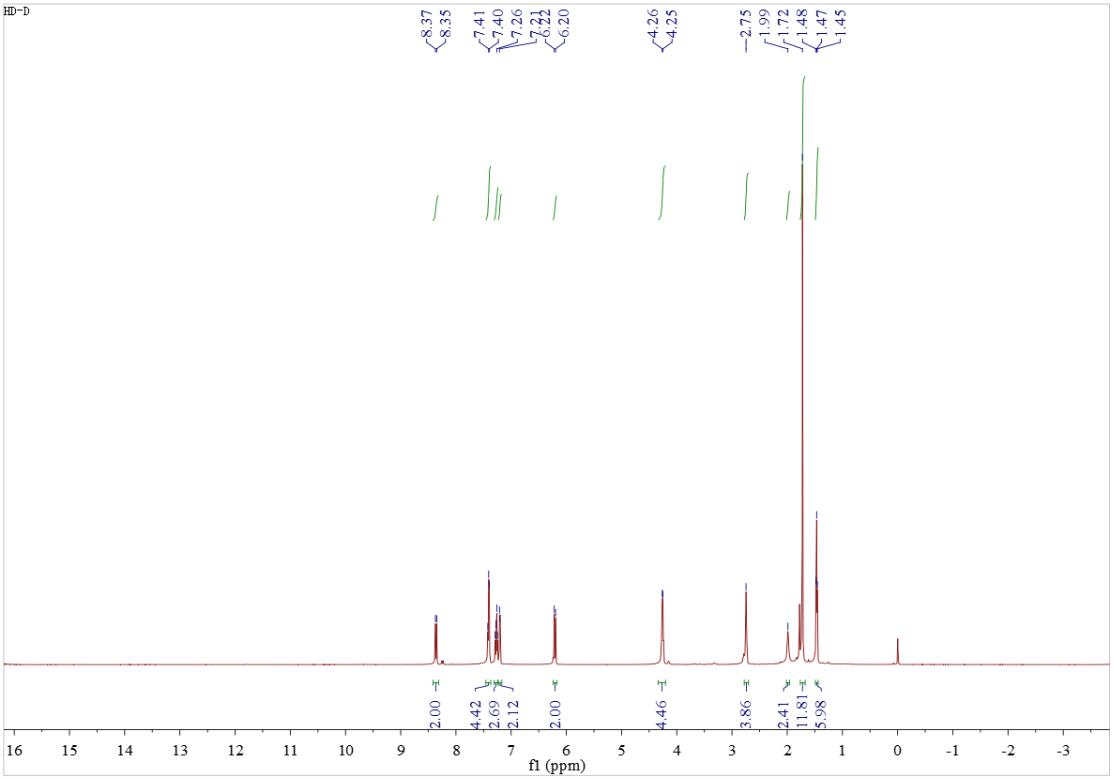

Figure S2. ^{13}C spectrum of **1a**

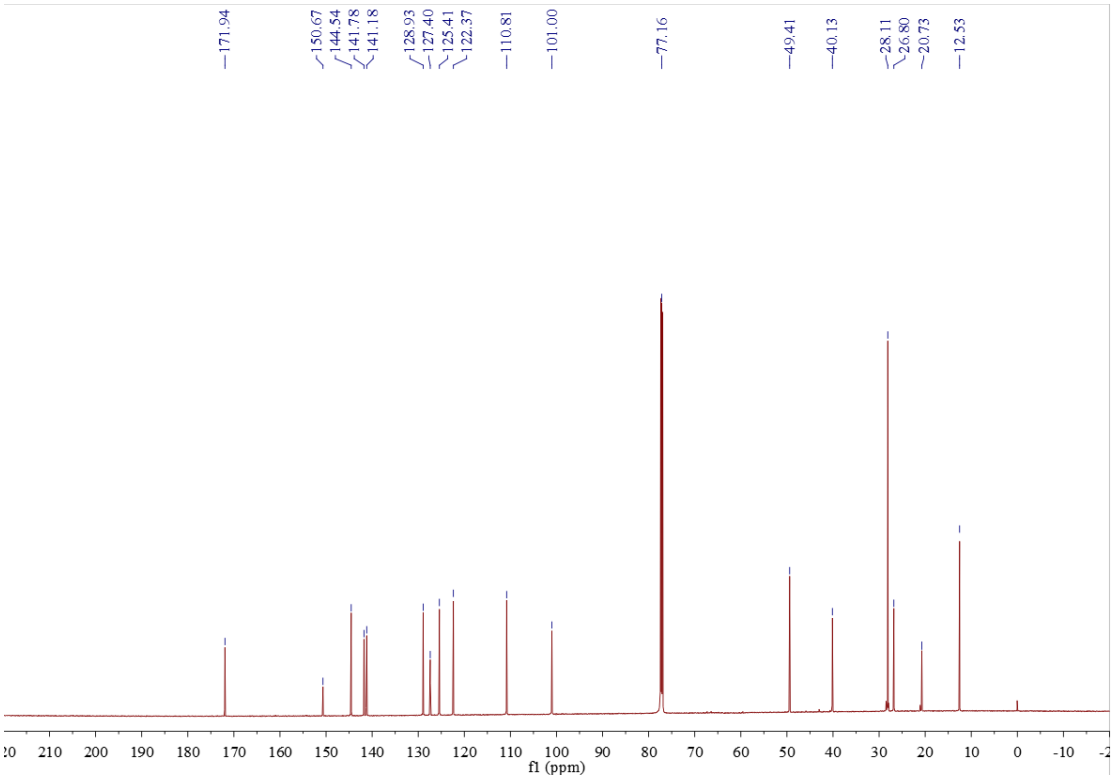

Figure S3. MS spectrum of **1a**

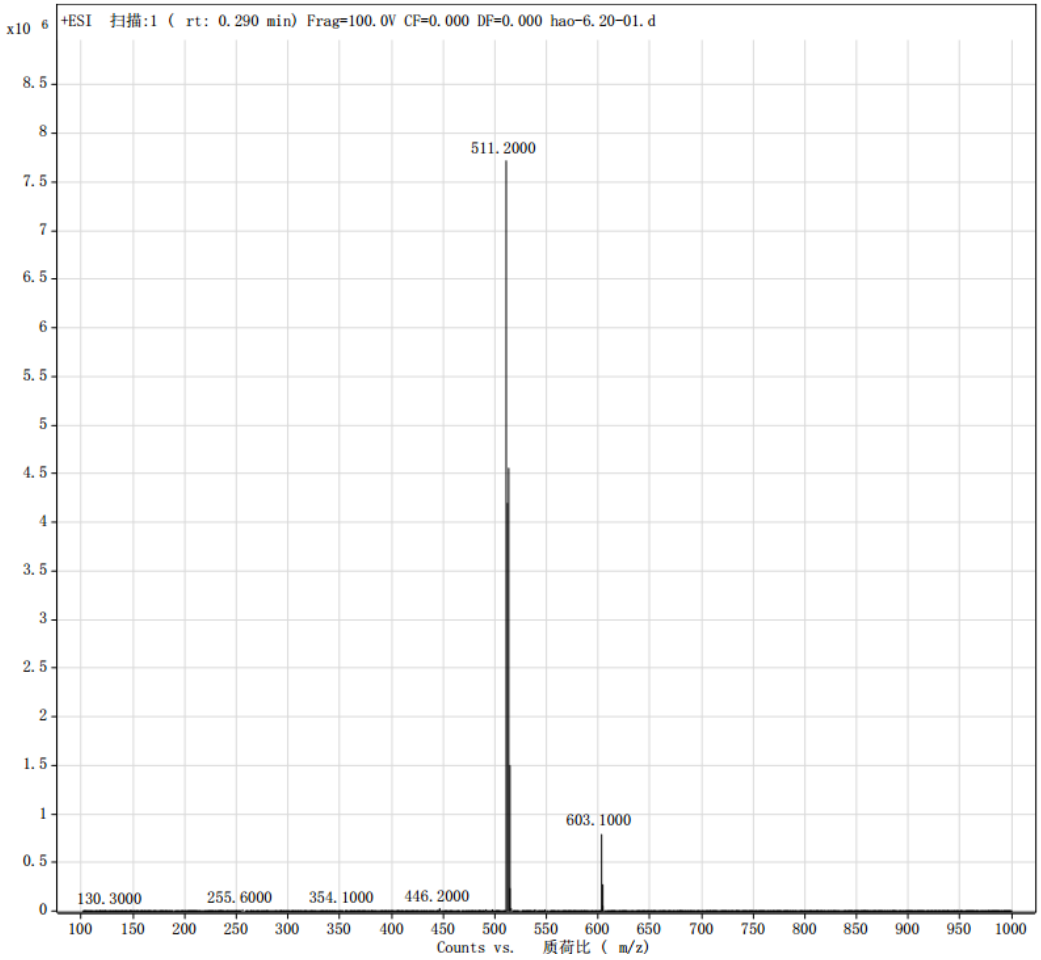

Figure S4. ^{1}H spectrum of DHX-1

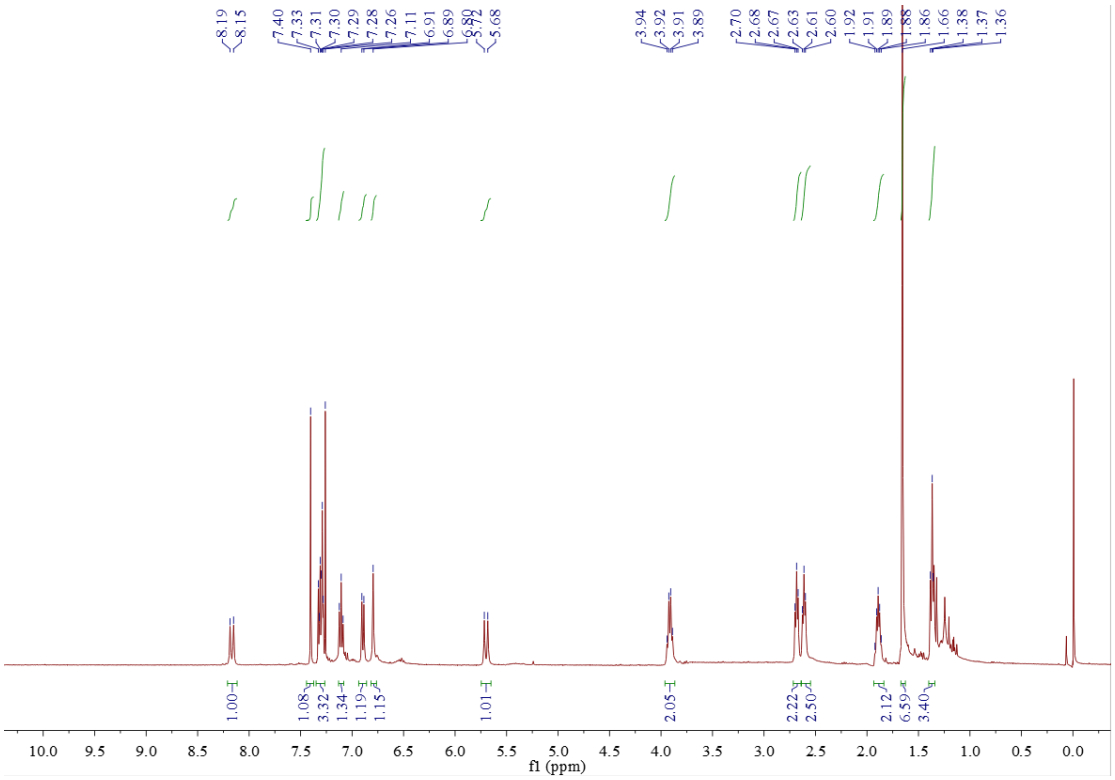

Figure S5. 13C spectrum of DHX-1

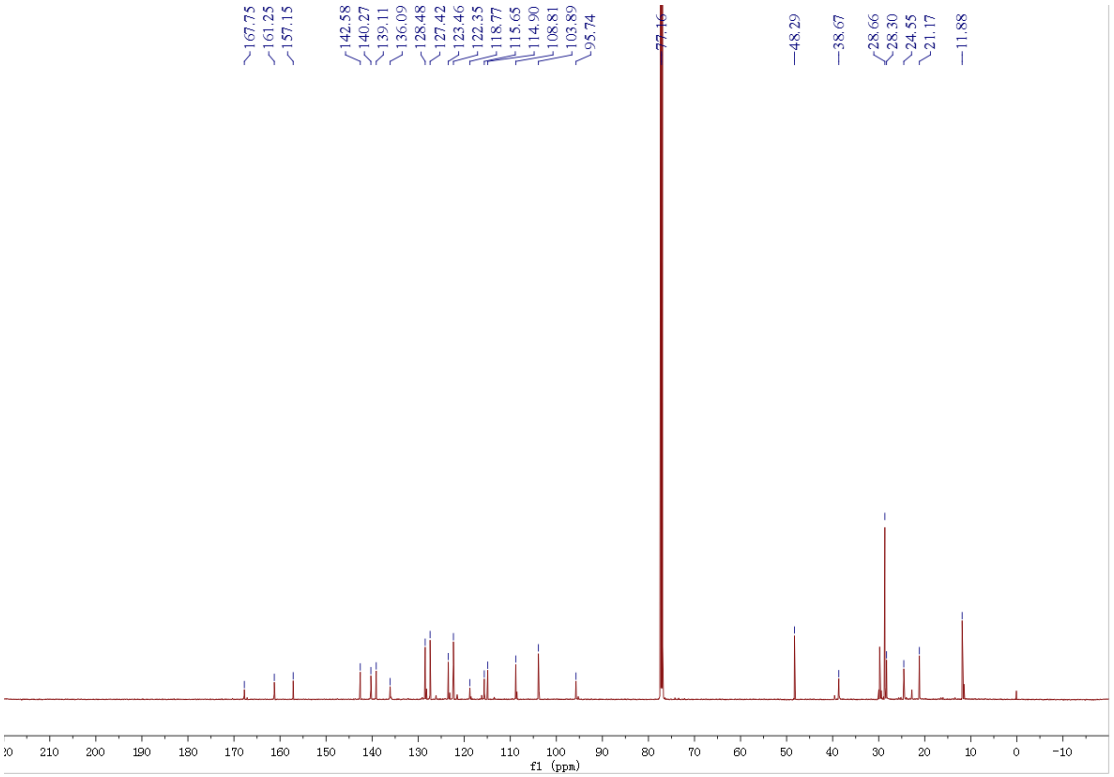

Figure S6. MS spectrum of DHX-1

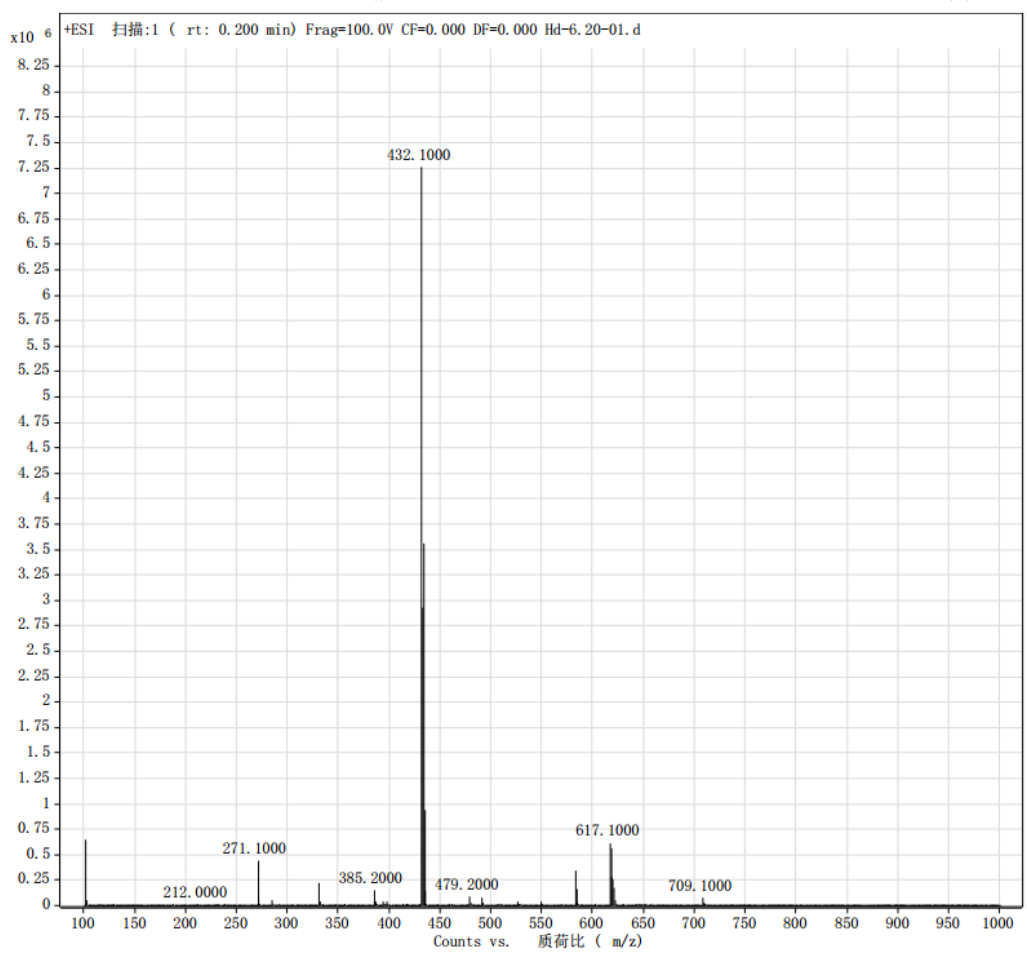

ANEXO III

Synthesis and evaluation of new potential benzo[*a*]phenoxazinium photosensitizers for anticancer photodynamic therapy

Juan Zhang[1,2,] Wellington Tavares de Sousa Júnior[1], Victor Carlos Mello da Silva[1], Mosar Correa Rodrigues[1,3], José Athayde Vasconcelos Morais[1,3], Cheng-Shi Jiang[2,*], Hua Zhang[2,*], João Paulo Figueiró Longo[3], Ricardo Bentes Azevedo[3] and Luís Alexandre Muehlmann[1,*]

[1] Faculty of Ceilandia, University of Brasília, Brasilia 72220275, Brazil;

[2] School of Biological Science and Technology, University of Jinan, Jinan 250022, China;

[3] Institute of Biological Sciences, University of Brasília, Brasilia 70910900, Brazil;

Correspondence should be addressed to Cheng-Shi Jiang, jiangchengshi-20@163.com; Hua Zhang, and Luís Alexandre Muehlmann; luisalex@unb.br

Abstract: In the present work, five benzo[*a*]phenoxazinium derivatives were prepared and evaluated *in vitro* as for their photodynamic activities against two cell lines, normal murine fibroblasts cell NIH-3T3 and murine breast adenocarcinoma cell 4T1. Most of these compounds are water soluble and red light absorbers, showing low fluorescence quantum yield. Of these compounds, **PS4** exhibited a higher quantum yield for ROS generation. The assays with cells *in vitro* showed that **PS1** and **PS4** were not significantly toxic in the dark, but robustly reduced the viability of the tested cells under photoactivation. Interestingly, **PS5** was particularly selective to 4T1 cells, being strongly phototoxic against these cells and nearly non-phototoxic to NIH3T3. The results described in this report suggest that these new benzo[*a*]phenoxazinium derivatives are potential candidates to photosensitizers for anticancer photodynamic therapy.

Keywords: Benzo[*a*]phenoxazinium chloride; Photosensitizer; Anticancer; red light; Photodynamic therapy

Introduction

Photodynamic therapy (PDT) is a minimally invasive protocol used for anticancer therapy.[1] PDT is based on the focal photoactivation of photosensitizers (PSs), which can directly act on the target tissues and then elicit photochemical reactions that eventually lead to oxidative stress.[2] The main consequences of these events include direct cytotoxicity, collapse of the tumor microvasculature, and/or activation of immune response against tumor antigens.[3] A particularly important benefit of PDT as a cancer therapy is the possibility to restrict its effects to the irradiated site, sparing the normal tissues. Although PDT has been successfully applied in the treatment of skin, gynecological, gastrointestinal, and some head and neck cancers, only a few PSs (e.g. porfimer sodium, temoporfin, aminolevulinic acid and photofrin) have been put into the market.[4,5] Up to now, most current work focus on the improvement of porphhyrin or chlorin-type PS molecules and synthesis of new type of PSs with high water solubility, strong absorption in near-infrared (NIR) region, and long half-life.[2,6]

During our continued project for developing new generation of PS[7,8,9,10], the benzo[*a*]phenoxazinium dyes come to our attention due to their good photostability, high molar absorption, long-wavelength absorption, and relative low fluorescence quantum yield.[11,12,13] Literature survey indicated that benzo[*a*]phenoxazinium derivatives exhibited antifungal[12,14], antimalarial activity,[15] and also functioned as PSs in antimicrobial PDT.[16,17] However, to our knowledge, the potential anticancer PDT of benzo[*a*]phenoxazinium dyes has been little-investigated.[18] In this context, the main objective of the present work was to design and synthesize several new benzo[*a*]phenoxazinium chlorides **PS1**-**PS5** (Fig. 1) and investigate their potential anticancer photodynamic activity.

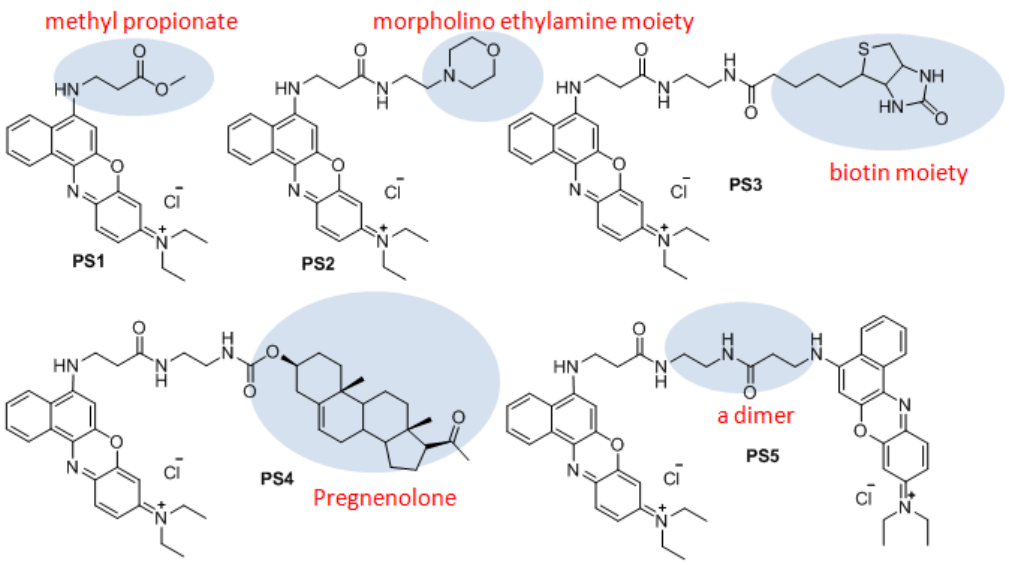

Figure 1. Structures of new benzo[*a*]phenoxazinium chlorides **PS1** to **PS5**.

1. Experimental

2.1. Materials and instruments

Dimethyl sulfoxide (DMSO), 1,3-diphenylisobenzofuran (DPBF) and Kholiphor® HS were obtained from Sigma, USA. The Roswell Park Memorial Institute (RPMI) medium and Dulbecco's modified Eagle medium (DMEM) were obtained from Gibco, EUA. The 3-(4,5-dimethylthiazol-2yl)-2,5-diphenyltetrazolium bromide (MTT) was purchased from Invitrogen, EUA. The phosphate buffered saline (PBS) was supplied by Laborclin, Brazil. Commercially available reagents were used without further purification. Organic solvents were evaporated with reduced pressure using Büchi evaporators. Reactions were monitored by TLC using Yantai JingYou (China) GF254 silica gel plates. Silica gel column chromatography was performed on silica gel (200-300 mesh) from Qingdao Hailang (China). NMR spectra were measured on Bruker Avance III 600 MHz spectrometer. Chemical shifts were expressed in δ (ppm) and coupling constants (J) in Hz using solvent signals as internal standards ($CDCl_3$, δ_H 7.26 ppm and δ_C 77.2 ppm; CD_3OD, δ_H 3.31 ppm and δ_C 49.0 ppm; d_6-acetone, δ_H 2.05 ppm and δ_C 29.8 ppm). ESI-MS was recorded on an Agilent 1260-6460 Triple Quard LC/MS, and HR-ESI-MS data were acquired on an Agilent Q-TOF 6520.

*1.2. Synthesis of **PS1***

Synthesis of compound **2**: The mixture of naphthalen-1-amine **1** (2.00 g, 14.0mmol), 3-bromopropanoic acid (2.14 g, 14.4 mmol) and Et_3N (1.60 g, 14.4 mmol) in 10 ml EtOH was refluxed overnight. The solution was then removed under reduced pressure. The crude product was purified by silica gel flash chromatography using CH_2Cl_2/MeOH (10:1) as eluent to give compound **2** as a white solid (1.0g, 26%). ^{1}H NMR (600 MHz, CD_3OD): 7.95 (d, *J* = 7.9 Hz, 1H), 7.73 (d, *J* = 7.8 Hz, 1H), 7.41-7.37 (m, 2H), 7.29 (dd, *J* = 7.6, 8.1 Hz, 1H), 7.17 (d, *J* = 8.1 Hz, 1H), 6.63 (d, *J* = 7.6 Hz, 1H), 3.56 (t, *J* = 6.8 Hz, 2H), 2.74 (t, J = 6.8 Hz, 2H). ^{13}C NMR (150 MHz, CD_3OD): 176.3, 144.8, 135.9, 129.3, 127.6, 126.6, 125.4, 125.3, 121.7, 118.2, 105.2, 40.8, 34.4. ESI-MS m/z $[M+H]^+$ 216.2.

Synthesis of compound **4**: The soltion of 3-diethylaminophenol **3** (3.3 g) in mixture of 7 mL of concentrated HCl and 7 ml of water was cooled to 0^{o}C, and then a solution ofsodium nitrite (1.38 g) in 10 ml water was added dropwise to the above mixture. The reaction was stirred at 0-5 ^{o}C for 3.5 hour to give a brown slurry. The slurry was filtrate and washed with 6 ml of 4M aqueous HCl. The filter was to give compound **4** as a brown solid (3.0g, 26%). This compound was used in the next step without further purification. ESI-MS m/z $[M+H]^+$ 195.2.

Synthesis of compound **PS1**: To a cold solution (ice bath) of **4** (160mg, 0.6 mmol) in 10 ml MeOH was added **2**(100mg, 0.5 mmol) and 5 drop of concentrated HCl. The mixture was refluxed for 4 h. The solution was evaporated and purified by silica gel flash chromatography using CH_2Cl_2/MeOH (10:1) as eluent to give **PS1** as a blue solid (45 mg, 24%). ^{1}H NMR (600 MHz, CD_3OD): 8.83-8.80 (m, 1H), 8.29 (d, *J* = 8.0 Hz, 1H), 7.88 (dd, *J* = 7.2, 8.0 Hz, 1H), 7.81 (dd, *J* = 5.0, 9.3 Hz, 1H), 7.77 (dd, *J* = 7.2, 8.2 Hz, 1H), 7.28 (d, *J* = 9.3 Hz, 1H), 6.96 (s, 1H), 6.89 (s, 1H), 3.99 (t, *J* = 6.7 Hz, 2H), 3.75 (s, 3H), 3.71 (q, *J* = 7.2 Hz, 4H), 2.96 (t, *J* = 6.7 Hz, 2H), 1.35 (t, *J* = 7.2 Hz, 6H). ^{13}C NMR (150 MHz, CD_3OD): 173.2, 159.1, 155.9, 153.1, 149.9, 134.7, 134.2, 132.9, 132.6, 132.1, 130.8, 125.2, 124.7, 123.8, 117.0, 97.0, 94.4, 52.5, 47.1, 41.4, 33.6, 13.0. ESI-MS *m/z* $[M]^+$ 404.3.HR-ESIMS: $[M]^+$ calcd for $C_{24}H_{26}N_3O_3^+$ 404.1969, found 404.1967.

*1.3. Synthesis of **PS2***

Synthesis of compound **5**: The compound **2** (100 mg, 0.5 mmol) was solved in 10 mL CH_2Cl_2, and then 2-morpholinoethanamine (120mg, 0.9 mmol), HATU (200 mg, 0.5 mmol) and 0.2ml $iPrNEt_2$ was added. The mixture was stirred overnight, and then concentrated. The residue was purified by silica gel chromatography with petroleum ether/acetone (1:1) as eluent to give compound **5** as a white solid (128 mg, 84%). ^{1}H NMR (600 MHz, $CDCl_3$):*δ* 7.83 (d, *J* = 8.0 Hz, 1H), 7.78 (d, *J* = 9.2 Hz, 1H), 7.45-7.41 (m, 2H), 7.35 (dd, *J* = 7.5, 8.2 Hz, 1H), 7.25 (d, *J* = 8.2 Hz, 1H), 6.54 (d, *J* = 7.5 Hz, 1H), 6.27 (brs, 1H), 5.07 (brs, 1H), 3.64 (t, *J* = 6.0 Hz, 2H), 3.50 (brs, 4H), 3.32 (t, *J* = 6.0 Hz, 2H), 2.64 (d, *J* = 6.0 Hz, 2H), 2.38 (t, *J* = 6.0 Hz, 2H), 2.29 (brs, 4H). ^{13}C NMR (150 MHz, $CDCl_3$):*δ* 171.8, 142.9, 134.4, 128.6, 126.5, 125.8, 124.8, 123.7, 120.0, 117.7, 104.4, 66.7, 56.8, 53.2, 40.3, 35.5, 35.3. ESI-MS *m/z*: 328.3 $[M+H]^+$.

Synthesis of compound **PS2**: To a cold solution of compound **4** (50mg, 0.2 mmol) in 5 ml EtOH was added compound **5** (60 mg, 0.2 mmol) and 5 drop of concentrated HCl. The mixture was refluxed for 4 h. The solution was evaporated and purified by silica gel flash chromatography using CH_2Cl_2/MeOH (10:1) as eluent to give compound **PS2** as a blue solid (54 mg, 55%). ^{1}H NMR (600 MHz, CD_3OD): *δ* 8.72 (s, 1H), 8.39 (s, 1H), 7.84 (s, 1H), 7.75 (s, 2H), 7.25 (s, 1H), 6.85 (s, 1H), 4.04-3.96 (m, 6H), 3.70-3.66 (m, 8H), 3.34 (s, 2H), 3.18 (s, 2H), 2.91 (s, 2H), 1.35 (s, 6H). ^{13}C NMR (150 MHz, CD_3OD): 174.1, 158.9, 155.8, 152.9, 149.7, 134.5, 134.2, 132.9, 132.3, 131.9, 130.8, 125.4, 124.5, 124.2, 117.0, 96.9, 94.6, 64.8, 58.1, 53.4, 41.8, 35.1, 34.7, 13.0. ESI-MS m/z $[M]^+$ 502.2.HR-ESIMS: $[M]^+$ calcd for $C_{29}H_{36}N_5O_3^+$ 502.2813, found 502.2812; $[M+H]^{2+}$ calcd for $C_{29}H_{37}N_5O_3^{2+}$ 251.6442, found 251.6445.

*1.4. Synthesis of **PS3***

Synthesis of compound **6**: The compound **2** (100 mg, 0.5 mmol) was solved in 10 mL CH_2Cl_2, and then *tert*-butyl (2-aminoethyl)carbamate (149 mg, 1.0 mmol), HATU (200 mg, 0.5 mmol) and 0.2ml $iPrNEt_2$ was added. The mixture was stirred overnight, and then concentrated. The residue was purified by silica gel chromatography with

CH_2Cl_2/MeOH (10:1) as eluent to give compound **6** as a white solid (160 mg, 96%). ^{1}H NMR (600 MHz, $CDCl_3$):δ 7.91-7.89 (m, 1H), 7.79-7.77 (m, 1H), 7.45-7.41 (m, 2H), 7.46-7.43 (m, 1H), 7.34 (dd, *J* = 7.6, 8.0 Hz, 1H), 7.27 (d, *J* = 7.0 Hz, 1H), 6.6 (d, *J* = 7.6 Hz, 1H), 6.48 (brs, 1H), 4.85 (brs, 1H), 3.61 (t, *J* = 6.0 Hz, 2H), 3.37-3.34 (m, 2H), 3.26-3.24 (m, 2H), 2.63 (t, *J* = 6.0 Hz, 2H), 1.41 (s, 9H). ^{13}C NMR (150 MHz, $CDCl_3$):δ 172.6, 157.2, 142.9, 134.5, 128.7, 126.6, 126.0, 125.1, 124.0, 120.3, 118.2, 105.0, 80.0, 41.1, 40.8, 40.3, 35.2, 28.4. ESI-MS *m/z*: 358.0 $[M+H]^+$.

Synthesis of compound **7**: To a solution (ice bath) of **6** (120 mg, 0.34 mmol) in 5 ml CH_2Cl_2 was added 100 □L trifluoroacetic acid under 0^{o}C. The mixture was stirred overnight, and then concentrated to give a residue, which was used in the next step without further purification. The obtained residue was solved in 5 mL CH_3CN, and then 172 mg Biotin-NHS, 0.2ml Et_3N was added. The mixture was stirred overnight, and then concentrated. The residue was purified by silica gel chromatography with CH_2Cl_2/MeOH (10:1) as eluent to give compound **7** as a white solid (85 mg, 52%). ^{1}H NMR (600 MHz, DMSO-d_6):δ 8.08 (d, *J* = 8.3 Hz, 1H), 7.99 (brs, 1H), 7.81 (brs, 1H), 7.75 (d, *J* = 8.3 Hz, 1H), 7.43 (ddd, *J* = 1.0, 6.7, 8.4 Hz, 1H), 7.39 (ddd, *J* =1.4, 6.8, 9.0 Hz, 1H), 7.29 (dd, *J* = 7.8, 7.9 Hz, 1H), 7.11 (d, *J* = 8.2 Hz, 1H), 6.54 (d, *J* = 8.6 Hz, 1H), 6.42 (s, 1H), 6.35 (s, 1H), 6.19 (dd, *J* = 5.4, 5.5 Hz, 1H), 4.28-4.26 (m, 1H), 4.11-4.09 (m, 1H), 3.44-3.41 (m, 1H), 3.31 (m, 5H), 2.78 (dd, *J* = 5.1, 12.5 Hz, 1H), 2.56(d, *J* = 12.5 Hz, 1H), 2.04 (t, *J* = 1.1 Hz, 1H), 1.61-1.57 (m, 1H), 1.53-1.43 (m, 3H), 1.32-1.23 (m, 2H), 1.17 (t, *J* = 7.3 Hz, 1H).^{13}C NMR (150 MHz, DMSO-d_6): δ 172.4, 171.1, 162.7, 143.8, 134.0, 127.9, 126.8, 125.6, 124.0, 123.0, 121.4, 115.6, 102.9, 61.0, 59.2, 55.4, 45.7, 40.1, 38.5, 38.3, 35.3, 34.8, 28.2, 28.0, 25.2. ESI-MS *m/z*: 484.3 $[M+H]^+$.

Synthesis of compound **PS3**: To a cold solution of **4** (50mg, 0.2 mmol) in 5 ml EtOH was added **7** (60 mg, 1.2 mmol) and 5 drop of concentrated HCl. The mixture was refluxed for 4 h. The solution was evaporated and purified by silica gel flash chromatography using CH_2Cl_2/MeOH (10:1) as eluent to give **PS3** as a blue solid (53 mg, 62%). ^{1}H NMR (600 MHz, CD_3OD): δ 8.89-8.83 (m, 1H), 8.37 (d, *J* = 7.5 Hz, 1H), 7.89-7.79 (m, 2H), 7.75-7.55 (m, 2H), 7.29 (d, *J* = 9.0 Hz, 1H), 7.01 (s, 1H), 6.91 (s, 1H), 4.46 (s, 1H), 4.28 (s, 1H), 4.01 (s, 1H), 3.72-3.71 (m, 4H), 3.56 (s, 1H), 3.15(s, 1H), 2.89-

2.74 (m, 2H), 2.66 (s, 1H), 2.15 (s, 1H), 1.67-1.51 (m, 4H), 1.35 (t, *J* = 7.0 Hz, 1H), 1.17-1.14 (m, 2H). ^{13}C NMR (150 MHz, CD_3OD): ⍰⍰176.4, 173.2, 159.1, 155.8, 153.2, 149.8, 134.7, 134.3, 132.9, 132.6, 132.1, 130.9, 125.5, 124.7, 124.0, 121.7, 117.0, 97.0, 94.5, 63.3, 61.6, 56.9, 47.1, 42.0, 41.0, 40.4, 39.9, 36.7, 35.5, 29.7, 29.4, 26.7, 13.0.ESI-MS m/z $[M]^+$ 658.2.HR-ESIMS: $[M]^+$ calcd for $C_{35}H_{44}N_7O_4S^+$ 658.3170, found 658.3171.

*1.5. Synthesis of **PS4***

Synthesis of compound **9**: To a solution of compound 8 (300mg, 0.6 mmol) in 10 ml CH_2Cl_2 was added 300⍰L trifluoroacetic acid under 0^{o}C. The mixture was stirred overnight, and then concentrated to give a residue, which was used in the next step without further purification. The above residue was solved in 10 mL CH_2Cl_2, and then compound **2** (128 mg, 0.6 mmol), HATU (248mg, 1.1 equiv) and 0.2ml $iPrNEt_2$ was added. The mixture was stirred overnight, and then concentrated. The residue was purified by silica gel chromatography with petroleum ether/acetone (1:1) as eluent to give compound **9** as a white solid (205 mg, 57%). ^{1}H NMR (600 MHz, $CDCl_3$): δ 7.87 (d, *J* = 7.5 Hz, 1H), 7.78 (m, 2H), 7.46-7.42 (m, 2H), 7.34 (dd, *J* = 7.9, 7.8 Hz, 1H), 7.25 (d, *J* = 8.2 Hz, 1H), 6.62 (d, *J* = 7.5 Hz, 1H), 5.34 (s, 1H), 5.15 (s, 1H), 4.95 (s, 1H), 3.62-3.60 (m, 2H), 3.36 (d, *J* = 5.4 Hz, 1H), 2.62 (dd, *J* = 6.1, 6.1 Hz, 1H), 2.53 (dd, *J* = 9.1, 8.8 Hz, 1H), 2.20-2.14 (m, 3H), 2.12 (s, 3H), 2.05-1.96 (m, 2H), 1.83-1.82 (m, 2H), 1.68-1.43 (m, 9H), 1.25-1.21 (m, 1H), 1.15-1.09 (m, 1H), 0.98 (s, 3H), 0.62 (s, 3H). ^{13}C NMR (150 MHz, $CDCl_3$): δ 209.8, 172.7, 157.3, 143.6, 139.8, 134.5, 128.7, 126.6, 126.0, 125.0, 123.9, 122.4, 120.3, 117.9, 104.6, 74.8, 63.8, 57.0, 50.0, 44.1, 40.9, 40.7, 40.5, 38.9, 38.6, 37.1, 36.7, 35.4, 31.9, 31.9, 31.7, 28.2, 24.6, 23.0, 21.1, 19.4, 13.4. ESI-MS *m/z*: $[M+H]^+$600.1.

Synthesis of compound **PS4**: To a cold solution (ice bath) of compound **4** (30 mg, 0.13 mmol) in 5 ml EtOH was added compound **9** (50 mg, 0.08 mmol) and 5 drop of concentrated HCl. The mixture was refluxed for 4 h. The solution was evaporated and purified by silica gel flash chromatography using CH_2Cl_2/MeOH (10:1) as eluent to give compound **PS4** as a blue solid (45 mg).^{1}H NMR (600 MHz, CD_3OD): δ 8.82 (d, *J* = 11 Hz, 1H), 8.31 (dd, *J* = 8.3, 8.4 Hz, 1H), 7.88 (dd, *J* = 7.4, 7.6 Hz, 1H), 7.82 (d, *J* = 9.2 Hz, 1H), 7.79 (dd, *J* = 7.3, 7.6 Hz, 1H), 7.28 (d, *J* = 8.7 Hz, 1H), 6.99 (s, 1H), 6.89 (s, 1H), 5.02 (s,

1H), 4.23 (m, 1H), 3.99-3.97 (m, 2H), 3.72-3.69 (m, 4H), 2.79-2.77 (m, 2H), 2.55 (dd, *J* = 6.7, 7.0 Hz, 1H), 2.15-2.08 (m, 5H), 1.98 (d, *J* = 8.2 Hz, 1H), 1.73-1.60 (m, 6H), 1.83-1.82 (m, 2H), 1.38 (d, *J* = 6.7 Hz, 1H), 1.35 (t, *J* = 7.2 Hz, 1H), 0.82 (s, 3H), 0.52 (s, 3H). ^{13}C NMR (150 MHz, CD_3OD): *δ* 212.1, 173.4, 159.0, 158.9, 155.7, 153.0, 149.7, 141.1, 141.1, 134.2, 132.9, 132.6, 130.9, 125.6, 125.5, 124.1, 124.0, 123.0, 116.8, 97.1, 94.7, 75.3, 64.6, 57.9, 51.2, 47.1, 44.9, 41.1, 39.7, 38.0, 37.5, 36.1, 35.6, 35.5, 33.0, 32.9, 32.6, 31.7, 29.1, 25.4, 23.7, 22.0, 19.6, 13.5, 13.0. ESI-MS *m/z*: $[M]^+$ 774.4. HR-ESIMS: $[M]^+$ calcd for $C_{47}H_{60}N_5O_5^+$ 774.4589, found 774.4595.

*1.6. Synthesis of **PS5***

Synthesis of compound **10**: To a solution (ice bath) of compound **6** (170mg, 0.5 mmol) in 5 ml CH_2Cl_2 was added 500 □L trifluoroacetic acid under 0°C. The mixture was stirred overnight, and then concentrated to give a residue, which was used in the next step without further purification. The above residue was solved in 5 mL CH_2Cl_2, and then compound **2** (102 mg, 0.5 mmol), HATU (200 mg, 0.5 mmol) and 0.2 ml $iPrNEt_2$ was added. The mixture was stirred overnight, and then concentrated. The residue was purified by silica gel chromatography with CH_2Cl_2/MeOH (20:1) as eluent to give compound **10** as a white solid (185 mg, 87%). ^{1}H NMR (600 MHz, d_6-acetone): *δ* 8.40 (d, *J* = 8.4 Hz, 1H), 7.76 (d, *J* = 8.4 Hz, 1H), 7.41-7.38 (m, 3H), 7.29 (dd, *J* = 7.9, 7.9 Hz, 1H), 7.15 (d, *J* = 8.2 Hz, 1H), 6.59 (d, *J* = 7.4 Hz, 1H), 5.84 (s, 1H), 3.52 (t, *J* = 6.4 Hz, 2H), 3.30 (t, *J* = 2.6 Hz, 2H), 2.57 (d, *J* = 6.4 Hz, 2H). ^{13}C NMR (150 MHz, d_6-acetone): *δ* 172.9, 144.9, 135.5, 129.1, 127.6, 126.4, 125.1, 124.6, 121.7, 117.2, 104.4, 41.1, 40.1, 35.7. ESI-MS *m/z*: $[M+H]^+$ 455.1.

Synthesis of compound **PS5**: To a cold solution of compound **4** (125mg, 0.5 mmol) in 5 ml EtOH was added compound **10** (100 mg, 0.2 mmol) and 5 drop of concentrated HCl. The mixture was refluxed for 4 h. The solution was evaporated and purified by silica gel flash chromatography using CH_2Cl_2/MeOH (10:1) as eluent to give compound **PS5** as a purple solid (80 mg, 45%). ^{1}H NMR (600 MHz, CD_3OD): *δ* 8.29 (d, *J* = 7.9 Hz, 1H), 8.26 (d, *J* = 8.0 Hz, 1H), 7.65 (dd, *J* = 7.3, 7.6 Hz, 1H), 7.57 (dd, *J* = 7.3, 9.3 Hz, 1H), 7.47 (d, *J* = 9.3 Hz, 1H), 7.11 (d, *J* = 9.2 Hz, 1H), 6.61 (s, 1H), 6.58 (s, 1H), 3.74 (s, 2H),

3.64 (q, *J* = 7.1 Hz, 4H), 3.40 (s, 2H), 2.81 (s, 2H), 1.34 (t, *J* = 7.1 Hz, 6H). ^{13}C NMR (150 MHz, CD_3OD): *δ* 173.5, 158.4, 155.6, 152.2, 149.1, 134.0, 133.9, 132.8, 131.9, 131.5, 130.7, 125.1, 124.2, 124.2, 116.9, 96.9, 94.4, 47.2, 42.2, 40.3, 35.1, 13.1. ESI-MS *m/z* $[M]^{2+}$ 402.3.HR-ESIMS: $[M]^{2+}$ calcd for $C_{48}H_{52}N_8O_4^{2+}$ 402.2050, found 402.2049.

1.7. General spectroscopic measurements

Absorption spectra were recorded in a Shimadzu UV-2600spectrophotometer (Shimadzu, Japan). Fluorescence measurements were performed using anAgilent Cary Eclipse (Varian, USA). Fluorescence spectra were corrected for the instrumental response of the system.All solutions were prepared using Milli-Q grade water. The fluorescence quantum yields (ϕ) were determined according to the method (Eq. (1)) below.

$$\phi_u = \phi_s \times (F_u / F_s) \times (A_s / A_u) \times (\eta_u / \eta_s)^2 \qquad (1)$$

Where ϕ is fluorescence quantum yield; F is integrated area under the corrected emission spectra; η is the refractive index of the solution; A is the absorbance at the excitation wavelength; the subscripts u and s refer to the unknown and the standard, respectively. We chose fluorescein in water as reference, $\phi_s = 0.98$.[19]

1.8. ROS detection

To evaluate the capacity of the compounds to produce singlet oxygen, the DPBF method was used. Briefly, 200 µL-aliquots of compounds in DMSO (40 µM) were plated in 96-well plates. Then, 10 µL of a solution of DPBF in ethanol (0.22 mg/mL) were added to each aliquot. Controls consisted of each compound without DPBF, and DPBF alone. Then, the microplate was irradiated every 10 seconds using 660 nm LED (Light Emitting Diode, XL001WP01NRC660, Shenzhen S. O. Co, CHI). The optical density of the DPBF solution at 414 nm was used as an index of ROS production, as the DPBF is degraded by ROS and its light absorption at this wavelength is thus decreased.

1.9. Cell viability assay

The viability of 4T1 and NIH-3T3 cells were measured by MTT assay. Briefly, 4T1 e

NIH-3T3, $1x10^4$ cells per well, were treated with different concentrations of the compounds for 30 minutes, in RPMI and DMEM, respectively, and then washed twice with PBS. After, the microplates were: 1) maintained in the dark, or 2) irradiated with a light emitting diode (LED, λ 660 nm) at a final energy density of 25.8 J/cm^2. The control consisted of cells that received only culture medium. Next, the cells were washed with PBS, cultured for further 24 h, and then the culture medium was replaced by a 0.5 mg/mL MTT solution in culture medium. The cells were then incubated for 2.5 h at 37 ^oC in a 5% CO_2, humid atmosphere. The MTT solution was then discarded, the formazan produced by the viable cells was extracted with 200 µL DMSO, and the optical density was read at λ 595 nm with a microplate spectrophotometer. This experiment was performed in triplicate for each treatment, and the results were expressed as percentages relative to control.

1.10. Statistical analysis

Data were analyzed by one-way ANOVA, with Sidak's post-test (α = 0.05). Analyzes were performed with GraphPad Prism® 6.0 software.

2. Results and discussion

3.1 Design and Synthesis

The ligand-mediated targeting strategy in PDT has been explored to increase the efficacy and reduce adverse effects of PSs.2 In the present work, five benzo[*a*]phenoxazinium chlorides possessing different functional fragments at 5-amino positionwere prepared: **PS1** was a simple previously reportedbenzo[*a*]phenoxazinium derivative with methyl propionate;[13] **PS2** possesses a morpholinoethylamine moiety, a ligand for targeting lysosomal;[20] **PS3** was equipped with a biotinmoiety, which serves as a well-known tumor-targeting molecule[21]and frequently used for delivery of PS to cancer tissues; **PS4** was a conjugate of benzo[*a*]phenoxazinium and pregnenolone. Pregnenolone, animportant naturally

occurring endogenous steroid, is known as a precursor to most of hormones, and several groups of pregnenolone derivatives were reported to have anticancer activity;[22,23] **PS5** was synthesized as a dimer to determine superimposed effect of benzo[*a*]phenoxaziniumcore on anticancer PDT efficacy.

The synthetic route for target compounds **PS1**-**PS5** is depicted in Schemes 1-5, respectively. Briefly, compound **2** was synthesized by alkylation of 1-naphthylamine (**1**) with 3-bromopropanoic acid, and nitroso derivative **4** was prepared from the nitration reaction of 3-(diethylamino)phenol (**3**). Then reaction of compounds **2** and **4** (in refluxingmethanol) produced target compound **PS1**. The coupling reaction of **2**with 2-morpholinoethanamine, *tert*-butyl (2-aminoethyl)carbamatev*tert*-butyl (2-aminoethyl)carbamate, and pregnenolone derivative **8** yielded intermediates **5**, **6** and **9**, respectively. Deprotection of *N*-Boc in **6** followed by coupling with Biotin-NHS gave compound **7** or followed by reaction with **2** produced **10**. Starting from intermediates **5**, **7**, **9**, **10** and using compound **4** once again, the target benzo[*a*]phenoxaziniums **PS2** to **PS5** were finally obtained in the last step using a similar synthetic protocol as that of **PS1**.

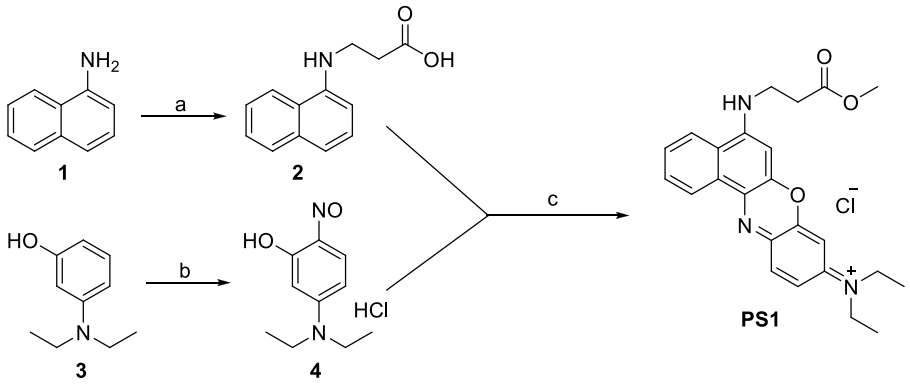

Scheme 1. The synthesis of **PS1**. Reagents and conditions: (a) 3-bromopropanoic acid, Et_3N, MeOH, reflux, overnight; (b) Cocn. HCl, sodium nitrite, H_2O, 0-5 ^oC, 3.5 h; (c) Cocn. HCl, MeOH, reflux, 4 h.

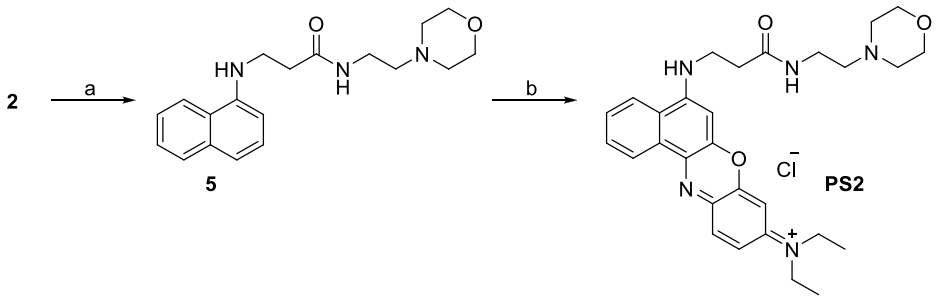

Scheme 2. The synthesis of **PS2**. Reagents and conditions: (a) 2-morpholinoethanamine, HATU, $iPrNEt_2$, CH_2Cl_2; (b) compound **4**, Cocn. HCl, EtOH, reflux, 4 h.

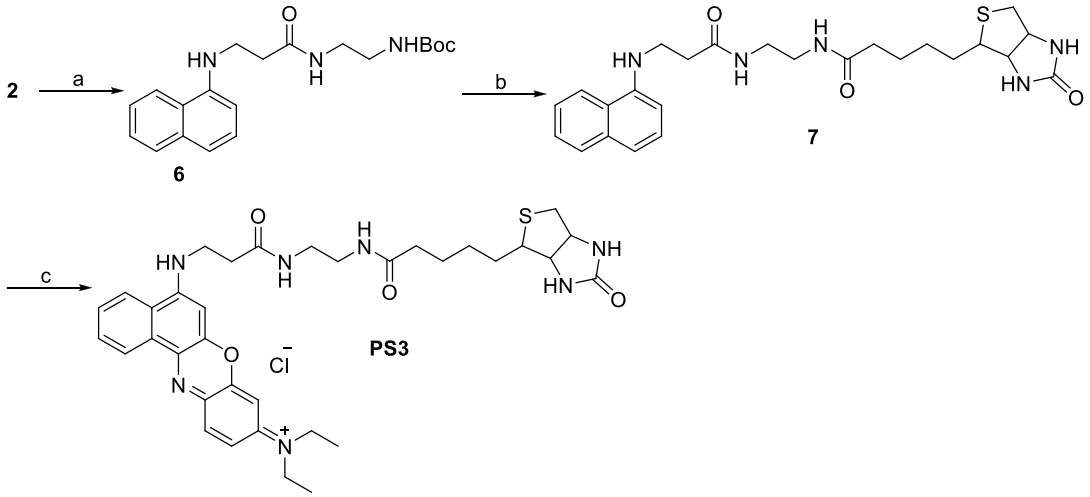

Scheme 3. The synthesis of **PS3.** Reagents and conditions: (a) *tert*-butyl (2-aminoethyl)carbamate, HATU, $iPrNEt_2$, CH_2Cl_2; (b) i. trifluoroacetic acid, CH_2Cl_2, 0^oC, overnight; ii. Biotin-NHS, Et_3N, CH_3CN, r.t., overnight; (c) compounds **4**, EtOH, 5 drop of Cocn. HCl, reflux, 4 h.

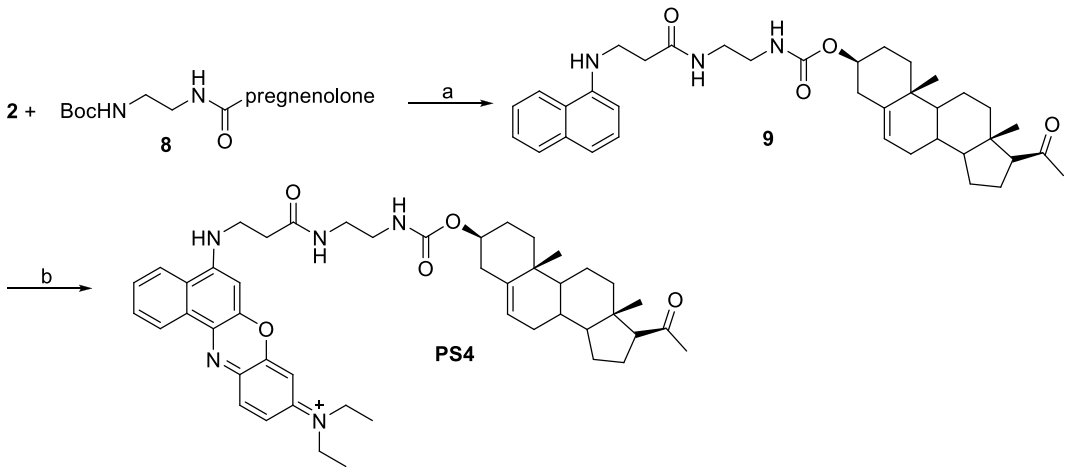

Scheme 4. The synthesis of **PS4**. Reagents and conditions: (a) i. trifluoroacetic acid,

CH_2Cl_2, 0°C, overnight; ii. **2**, HATU, iPrNEt$_2$, CH_2Cl_2, overnight.

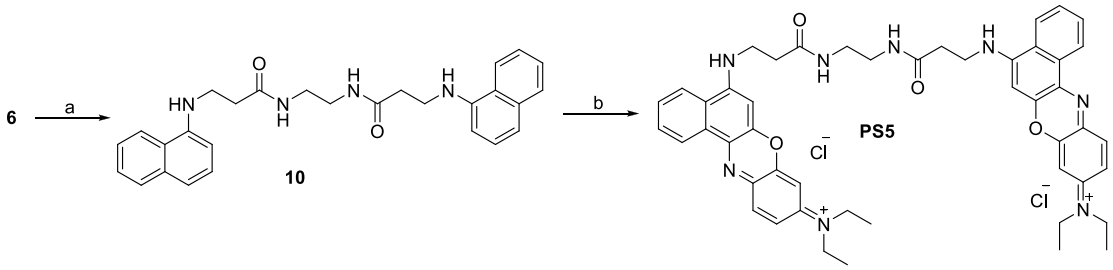

Scheme 5. The synthesis of **PS5**. Reagents and conditions: (a) i. trifluoroacetic acid, CH_2Cl_2, 0°C, overnight; ii compound **2**, HATU, iPrNEt$_2$, CH_2Cl_2, overnight; (b) compounds **4**, EtOH, 5 drop of Cocn. HCl, reflux, 4 h.

3.2 Absorption and emission studies

UV-Vis absorption and emission spectra of 5 × 10^{-6} M **PS1** to **PS5** in water were measured to investigate their optical properties (Table 1 and Fig. 1). In water, the absorption maxima (λ_{max}) for compounds **PS1** to **PS4** located at about 650 nm with the molar extinction coefficients (ε) between 22600 and 51800 $M^{-1}cm^{-1}$, which can be ascribed to the π-π* transition of the large π systems of the benzo[*a*]phenoxazinium core. **PS5** showed a shoulder peak at 649 nm (ε = 35600 $M^{-1}cm^{-1}$) from the benzo[*a*]phenoxazinium fluorophore. Meanwhile, **PS5** also showed a main absorption at 604 with a higher ε of 65000 $M^{-1}cm^{-1}$, which was probably resulted by the π-π interaction of the two intramolecular benzo[*a*]phenoxazinium fluorophores as a result of the flexibility of the amide linker.[24]

Under the excitation at 600 nm, **PS1** to **PS5** exhibited near-infrared emissions at about 681 nm with the Stokes shifts of about 35 nm. In addition, the relative fluorescence quantum yields (φ) were measured using fluorescein in water as a standard (ϕ_s = 0.98).[19] These compounds all showed low fluorescence quantum yield (0.025-0.116) which consists with that of previously reported benzo[*a*]phenoxazinium chlorides,[12,13] indicating they might not tend to decay back to the ground state by emitting fluorescence after excitation, and could potentially act as desirable candidates for photodynamic therapy.

Table 1

Absorption and emission data of benzo[*a*]phenoxazinium chlorides **PS1** to **PS5**

Compounds	λ_{abs}[a]	ε[b]	λ_{em}[a]	⍰λ[a]	ϕ_u
PS1	648	47400	681	33	0.075
PS2	649	35400	682	33	0.077
PS3	650	51800	684	34	0.082
PS4	651	22600	686	35	0.116
PS5	649 (604)	35600 (65000)	686	37	0.025

[a]nm

[b]$M^{-1}cm^{-1}$

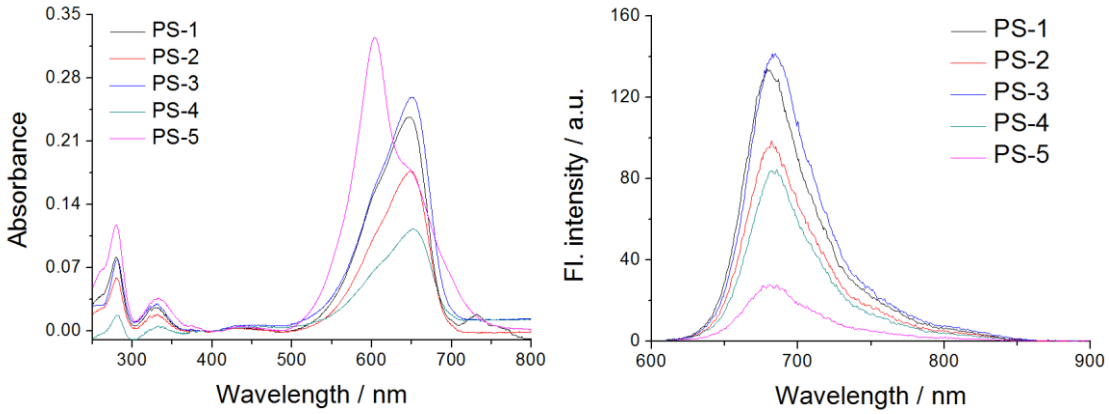

Figure 2. Absorption (A) and fluorescence (B) spectra of **PS1**-**PS5** in water.

3.3. ROS production

The reactive oxygen species (ROS) generated in photoreaction is the key factor for PDT as it can induce cytotoxicity via damage to the biomolecules including proteins, nucleic acids and lipids. Therefore, compounds PS1 to PS5 were evaluated for their effects on the production of ROS by DPBF method. The figure 3 shows the results of ROS production by the compounds irradiated with different energy densities. All the PS molecules produced ROS in an energy-dependent fashion. Remarkably, the

photoactivated production of ROS was more intense with **PS4**, suggesting that this compound has a higher quantum yield for ROS generation. The **PS3**, on the contrary, showed a lower production of ROS. Based on these obsevation, it was clearly that the different attached ligands had a great impact on their ROS production, and the effect factors could mainly be the physicochemical property of the ligands. Given these results, it is possible to suggest that all of the PS molecules described in this study are potential candidates for anticancer PDT.

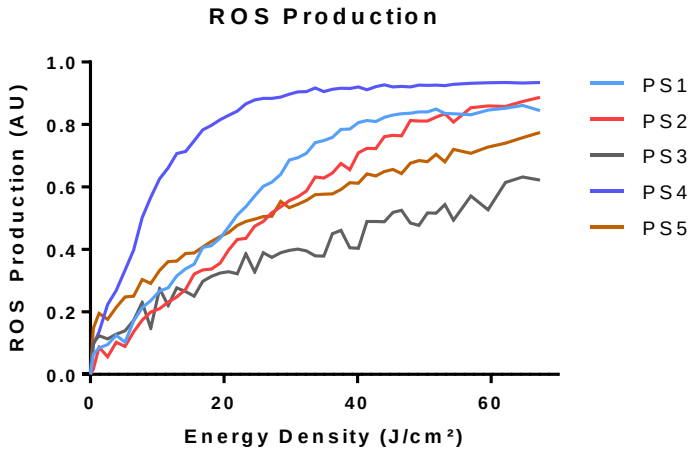

Figure 3. Photoactivated production of reactive oxygen species (ROS) by the candidate photosensitizers (PS1 to PS5) expressed as arbitrary units (AU).

3.4. Photodynamic activity against cells in vitro

Finally, photodynamic activities of **PS1** to **PS5** against two cell lines, including murine breast adenocarcinoma cell 4T1 and normal murine fibroblast cell NIH-3T3, were tested by irradiated (PDT) with 25.8 J/cm^2 of light (λ 660 nm) or not (dark) in MTT bioassay. As shown in Fig. 4, all the tested compounds did not display significant toxicity towards both NIH-3T3 and 4T1 cells in the dark with inhibition ratio less than 50% within the concentration of 2.5 to 40 μM. The absence of toxicity in the dark is a requirement for a desirable PS, as it avoids that non-irradiated tissues become affected during a PDT protocol. Regarding the photodynamic activity, it is remarkable that both **PS1** and **PS4** robustly reduced the viability of 4T1 and NIH3T3 cells in a concentration-dependent manner ($p<0.05$) when they were photoactivated. However, both compounds lack selectivity toward cancerous 4T1 compared with NIH-3T3, which

might to due to the attached ligands, methyl propionate and pregnenolone, are lipophilic groups making the compounds pass the cell member more easily. So both compounds can easily go inside of cell and works as PS in PDT condition. Compound **PS3** presented no evident photodynamic activity against 4T1 cells. Interesting results were also obtained with **PS5**, which showed a significant antiproliferative activity against 4T1 cells but no activity against NIH-3T3 in PDT experiment, indicating that this compound might have a better selectivity towards the cancerous cells tested in this study. It was well-known that the surface of cancer cells are negetive charged, while the compound **PS5** is more charged by positive charge, which means that this compound could be more tent to interact with cancerous cells. This was speculated to be the reason why **PS5** dispyled selectivity toward cancerous 4T1 cells. Of course, more experiment should be conducted to check this speculation and confirm its clear action mechansim.

In our opinion, the compounds **PS1**, **PS4** and **PS5** are more interesting and worth more further work to study their activity and PDT application. Alought PS1 and PS4 lack selectivity towards cancerous cells, this drawback could be avolided by applying nanotechnoligy and limiting the light illumination to the patholigical tissues. With regards to **PS5**, some further structural modification works are need to make its activity more potent. For example, we can change the length of diamine linkage to make it longer or shorter to find the most optimal distance between two benzo[a]phenoxazinium fragment. Of course, execpt cancer cell models the activity of these compounds can be tested in other pharmacological model, such as antifugal or antibacterial models.

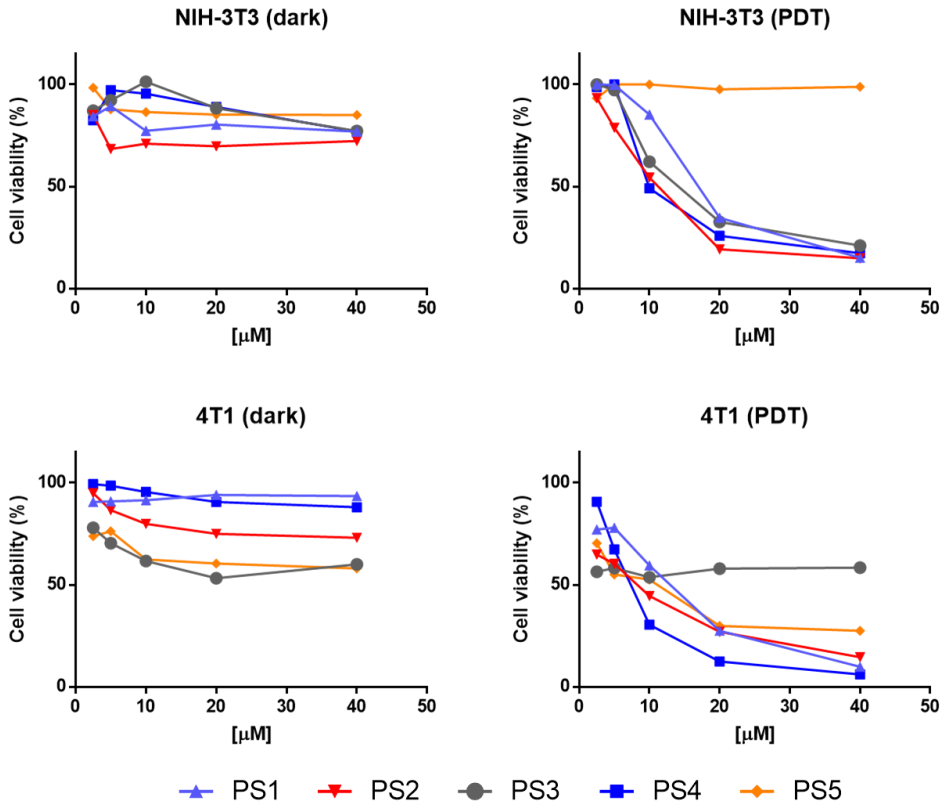

Figure 4. Viability of 4T1 and NIH-3T3 cells treated with different concentrations of compounds **PS1** to **PS5** in dark or PDT condition.

4. Conclusions

Four benzo[*a*]phenoxazinium chlorides **PS1-PS4** bearing different functional groups in amino side chain and one dimmer **PS5** were prepared. The investigation on optical properties of **PS1** to **PS5** in water indicated that they are red light absorbers, and exhibited emissions at about 681 nm with the Stokes shifts of about 35 nm after excited at 600 nm. Meanwhile, they showed low fluorescence quantum yield (0.025-0.116), indicating their great potential in undergoing intersystem crossing to form a relatively long-lived triplet state. The ROS production study revealed that all these benzo[*a*]phenoxaziniums produced ROS in an energy-dependent fashion with **PS4** having a higher ROS quantum yield. Finally, the anticancer photodynamic therapy (PDT) activities of this series of benzo[*a*]phenoxaziniums were evaluated for their anticancer PDT activity for the first time. The bioassay results indicated that **PS1** and **PS4** showed significantly anticancer PDT activity against normal murine fibroblasts cell NIH-3T3 and

caner cell 4T1 but have no activity in the dark condition, and **PS5** showed intriguing anticancer PDT activity by selectively targeting 4T1 cells. Together with the optical properties and photodynamic bioassay results, this series of benzo[a]phenoxazinium derivatives can be highlighted as new anticancer PS.

Disclosure statement

The authors declare no conflicts of interest.

Acknowledgements

This research work was financially supported by the Natural Science Foundation of China [No. 21672082], Shandong Key Development Project [No. 2016GSF201209], the Young Taishan Scholars Program [No. tsqn20161037], Shandong Natural Science Foundation for Distinguished Young Scholars [No. JQ201721], Shandong Talents Team Cultivation Plan of University Preponderant Discipline [No. 10027], and the Brazilian Government Agencies FAP/DF and CNPq.

Appendix A. Supplementary data

Supplementary data related to this article can be found at xxx.

References

1 J.C. Kennedy, R.H. Pottier, and D.C Pross, “Photodynamic therapy with endogenous protoporphyrin. IX: Basic principles and present clinical experience,”*Journal of Photochemistry and Photobiology B: Biology,* vol. 6, pp. 143–148, 1990.

2 J. Zhang, J.P. C.S. Jiang, Figueiró Longo, R.B. Azevedo, H. Zhang, and L.A. Muehlmann, “An updated overview on the development of new photosensitizers for anticancer photodynamic therapy,” *Acta Pharmaceutica Sinica B*, vol. 8, pp. 137–146, 2018.

3 T.J. Dougherty, C.J. Gomer, B.W. Henderson, G. Jori, D. Kessel, M. Korbelik, J. Moan, and Q. Peng, “Photodynamic therapy,” *Journal of the National Cancer Institute,* vol. 90, pp. 889–905, 1998.

4 S.H. Lim, C. Thivierge, P. Nowak-Sliwinska, J. Han, H. van den Bergh, G. Wagnières, K. Burgess and H.B. Lee, “In vitro and in vivo photocytotoxicity of boron dipyrromethene derivatives for photodynamic therapy,” *Journal of Medicinal Chemistry*, vol. 53, pp. 2865–2874, 2010.

5 Z. Meng, B. Yu, G. Han, M. Liu, B. Shan, G. Dong, Z. Miao, N. Jia, Z. Tan, B. Li, W. Zhang, H. Zhu, C. Sheng and J. Yao, “Chlorin p6-Based Water-Soluble Amino Acid Derivatives as Potent Photosensitizers for Photodynamic Therapy,” *Journal of Medicinal Chemistry*, vol. 59, pp. 4999-5010, 2016.

6 S. Yano, S. Hirohara, M. Obata, Y. Hagiya, S. Ogura, A. Ikeda, H. Kataoka, M. Tanaka, and T. Joh, “Current states and future views in photodynamic therapy,” *Journal of Photochemistry and Photobiology C: Photochemsitry Reviews*, vol. 12, pp. 46–67, 2011.

7 L.A. Muehlmann, M.C. Rodrigues, J.P. Longo, M.P. Garcia, K.R. Py-Daniel, A.B. Veloso, P.E. de Souza, S.W. da Silva, and R.B. Azevedo, “Aluminium-phthalocyanine chloride nanoemulsions for anticancer photodynamic therapy: Development and in vitro activity against monolayers and spheroids of human mammary adenocarcinoma MCF-7 cells,” *Journal of Nanobiotechnology,* vol. 13, pp.36, 2015.

8 L.A. Muehlmann, B.C. Ma, J.P. Longo, Mde F. Almeida Santos, and R.B. Azevedo, “Aluminum-phthalocyanine chloride associated to poly(methyl vinyl ether-co-maleic anhydride) nanoparticles as a new third-generation photosensitizer for anticancer photodynamic therapy,” *International Journal of Nanomedicine*, vol. 9, pp. 1199–1213, 2014.

9 M.C. Rodrigues, L.A. Muehlmann, J.P. Longo, R.C. Silva, I.B. Graebner, I.A. Degterev, C.M. Lucci, R.B. Azevedo, and M.P. Garcia, “Photodynamic Therapy Based on Arrabidaeachica (Crajiru) Extract Nanoemulsion: In vitro Activity against Monolayers and Spheroids of Human Mammary Adenocarcinoma MCF-7 Cells,” *Journal of Nanomedicine& Nanotechnology*, vol. 6, pp. 1000286, 2015.

10 V. Monge-Fuentes, L.A. Muehlmann, J.P. Longo, J.R. Silva, M.L. Fascineli, P. de Souza, F. Faria, I.A. Degterev, A. Rodriguez, F.P. Carneiro, C.M. Lucci, P. Escobar, R.F. Amorim, and R.B.Azevedo, “Photodynamic therapy mediated by acai oil (Euterpe oleraceaMartius) in nanoemulsion: A potential treatment for melanoma,” *Journal of Photochemistry and Photobiology B: Biology*, vol. 166, pp. 301–310, 2017.

11 L. Yuan, W. Lin, K. Zheng, L. He, and W. Huang, “Far-red to near infrared analyte-responsive fluorescent probes based on organic fluorophore platforms for fluorescence imaging,” *Chemical Society Reviews*, vol. 42, pp. 622–661, 2013.

12 P.S.M. Inês, B. Leitão, B. Rama Raju, S. Naik, P.J.G. Coutinho, M. João Sousa, and M.S.T. Gonçalves, “Synthesis and photophysical studies of new benzo[a]phenoxazinium chlorides as potential antifungal agents,” *Tetrahedron Letters*, vol. 57, pp. 3936–3941, 2016.

13 V.H.J. Frade, M.S.T. Goncalves, P.J.G. Coutinho, and J.C.V.P. Moura, “Synthesis and spectral properties of long-wavelength flurescent dyes, ” *Journal of Photochemistry and Photobiology A: Chemistry*, vol. 185, pp. 220–230, 2007.

14 V.H.J. Frade, M.J. Sousa, J.C.V.P. Moura, and M.S.T. Gonçalves, “Synthesis of naphtho[2,3-*a*]phenoxazinium chlorides: Structure–activity relationships of these heterocycles and benzo[*a*]phenoxazinium chlorides as new antimicrobials,” *Bioorganic & Medicinal Chemistry*, vol. 16, pp. 3274–3282, 2008.

15 Y. Mizukawa, J.F. Ge, A. BakarMd, I. Itoh, C. Scheurer, S. Wittlin, R. Brun, H. Matsuoka, and M. Ihara, “Novel synthetic route for antimalarial benzo[a]phenoxazine derivative SSJ-183 and two active metabolites,” *Bioorganic & Medicinal Chemistry*, vol. 22, pp. 3749–3752, 2014.

16 M. Lopes, C.T. Alves, B. Rama Raju, M.S. Gonçalves, P.J. Coutinho, M. Henriques, I. Belo I, “Application of benzo[*a*]phenoxazinium chlorides in antimicrobial photodynamic therapy of Candida albicans biofilms,” *Journal of Photochemistry and Photobiology B: Biology*, vol. 141, pp. 93–99, 2014.

17 J.W. Foley, X. Song, T.N. Demidova, F. Jalil, and M.R. Hamblin, “Synthesis and properties of benzo[*a*]phenoxaziniumchalcogen analogues as novel broad-spectrum antimicrobial photosensitizers,” *Journal of Medicinal Chemistry*, vol. 49, pp. 5291–5299, 2006.

18 L. Cincotta, J.W. Foley, and A.H. Cincotta, “Novel red absorbing benzo[a]phenoxazinium and benzo[*a*]phenothiazinium photosensitizers: in vitro evaluation,” *Photochemistry and Photobiology*, vol. 46, pp. 751–758, 1987.

19 J. Fan, H. Dong, M. Hu, J. Wan, H. Zhang, H. Zhu, W. Sun, and X. Peng, “Fluorescence imaging lysosomal changes during cell division and apoptosis observed using Nile Blue based near-infrared emission,” *Chemical Communications*, vol. 50, pp 882–884, 2014.

20 Y. Tang, D. Lee, J. Wang, G. Li, J. Yu, W. Lin, and J. Yoon, “Development of fluorescent probes based on protection-deprotection of the key functional groups for biological imaging,” *Chemical Society Reviews*, vol. 44, pp. 5003–5015, 2015.

21 S. Chen, X. Zhao, J. Chen, J. Chen, L. Kuznetsova, S.S. Wong, and I Ojima, “Mechanism-based tumor-targeting drug delivery system. Validation of efficient vitamin receptor-mediated endocytosis and drug release,” *Bioconjugate Chemistry*, Vol. 21, pp. 979–987, 2010.

22 J.L. Song, J. Zhang, C.L. Liu, C. Liu, K.K. Zhu, F.F. Yang, X.G. Liu, J.P. Figueiró Longo, L. Alexandre Muehlmann, R.B. Azevedo, Y.Y. Zhang, Y.W. Guo, C.S. Jiang, and H. Zhang, “Design and synthesis of pregnenolone/2-cyanoacryloyl conjugates with dual NF-κB inhibitory and anti-proliferative activities,” *Bioorganic & Medicinal Chemistry Letters*, vol. 27, pp. 4682–4686, 2017.

23 M. Iqbal Choudhary, M. ShahabAlam, Atta-Ur-Rahman, S. Yousuf, Y.C. Wu, A.S. Lin, and F. Shaheen, “Pregnenolone derivatives as potential anticancer agents,” *Steroids*, vol. 76, pp. 1554–1559, 2011.

24 H. Takafusa, K. Kikuchi, Y. Urano, S. Sakamoto,K. Yamaguchi, and T. Nagano, “Design and Synthesis of an Enzyme-Cleavable Sensor Molecule for Phosphodiesterase Activity Based on Fluorescence Resonance Energy Transfer,” *Journal of the American Chemical Society*, vol. 124, pp. 1653–1657, 2002.

Supporting Information

Figure 1. 1H spectrum of **PS-1**

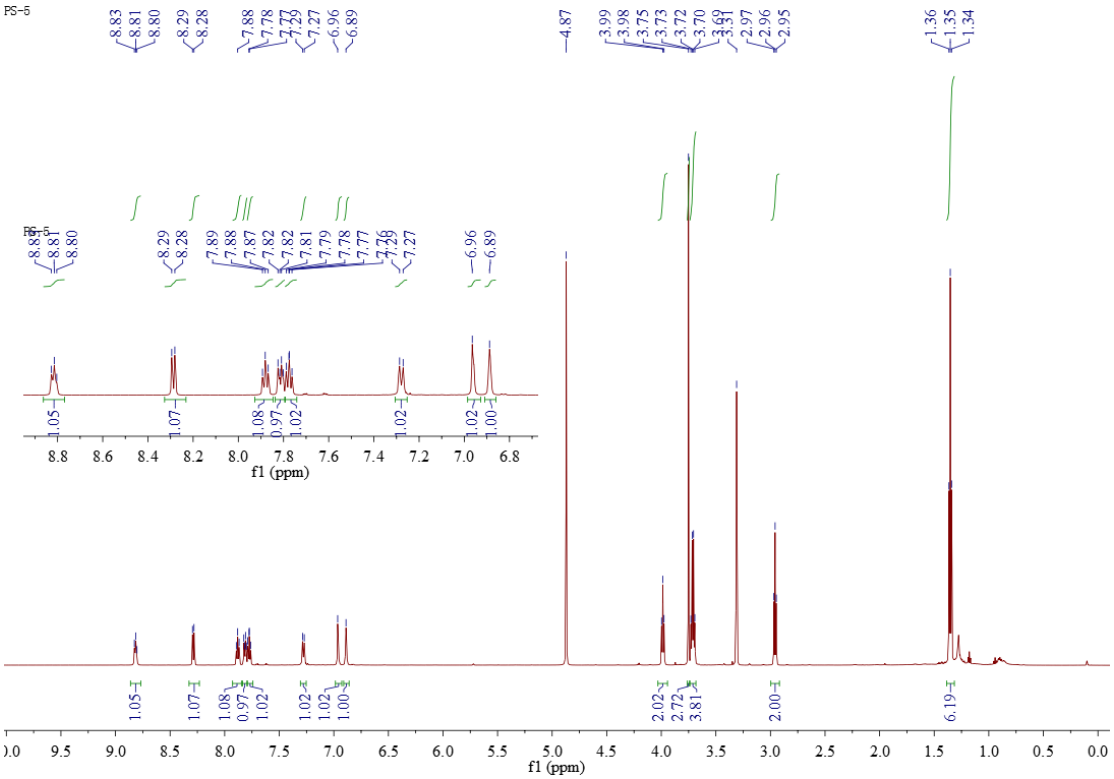

Figure 2. ^{13}C spectrum of **PS-1**

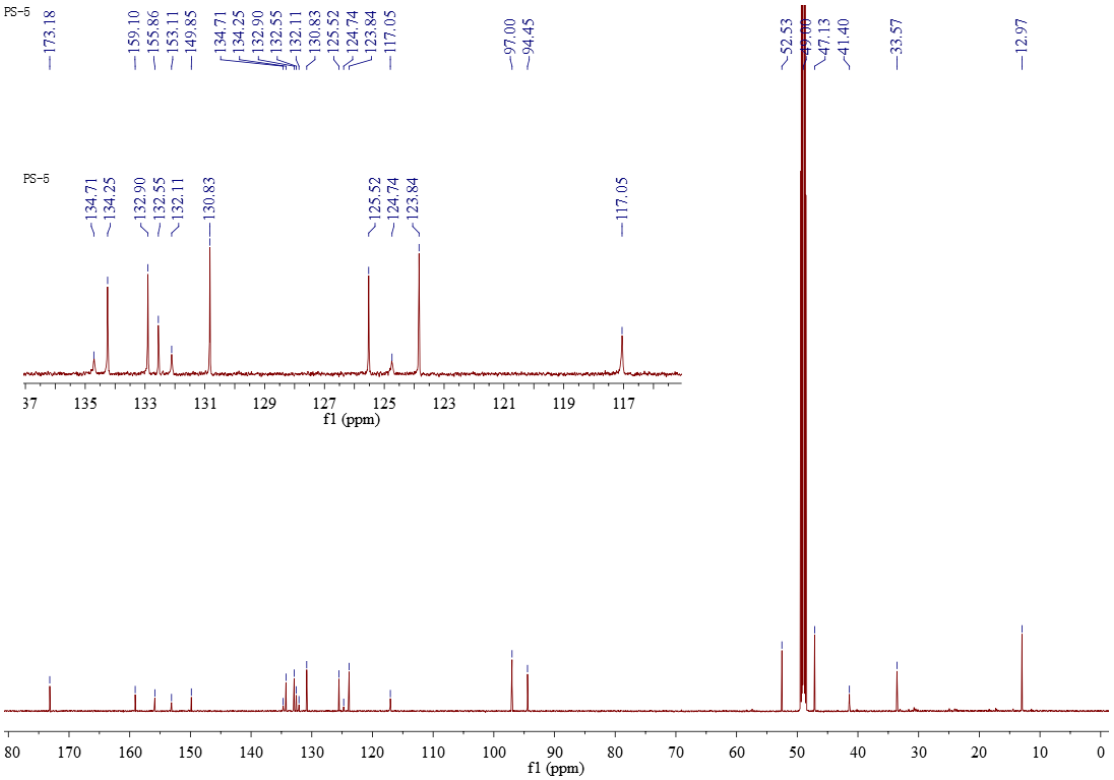

Figure 3. LR-MS spectrum of **PS-1**

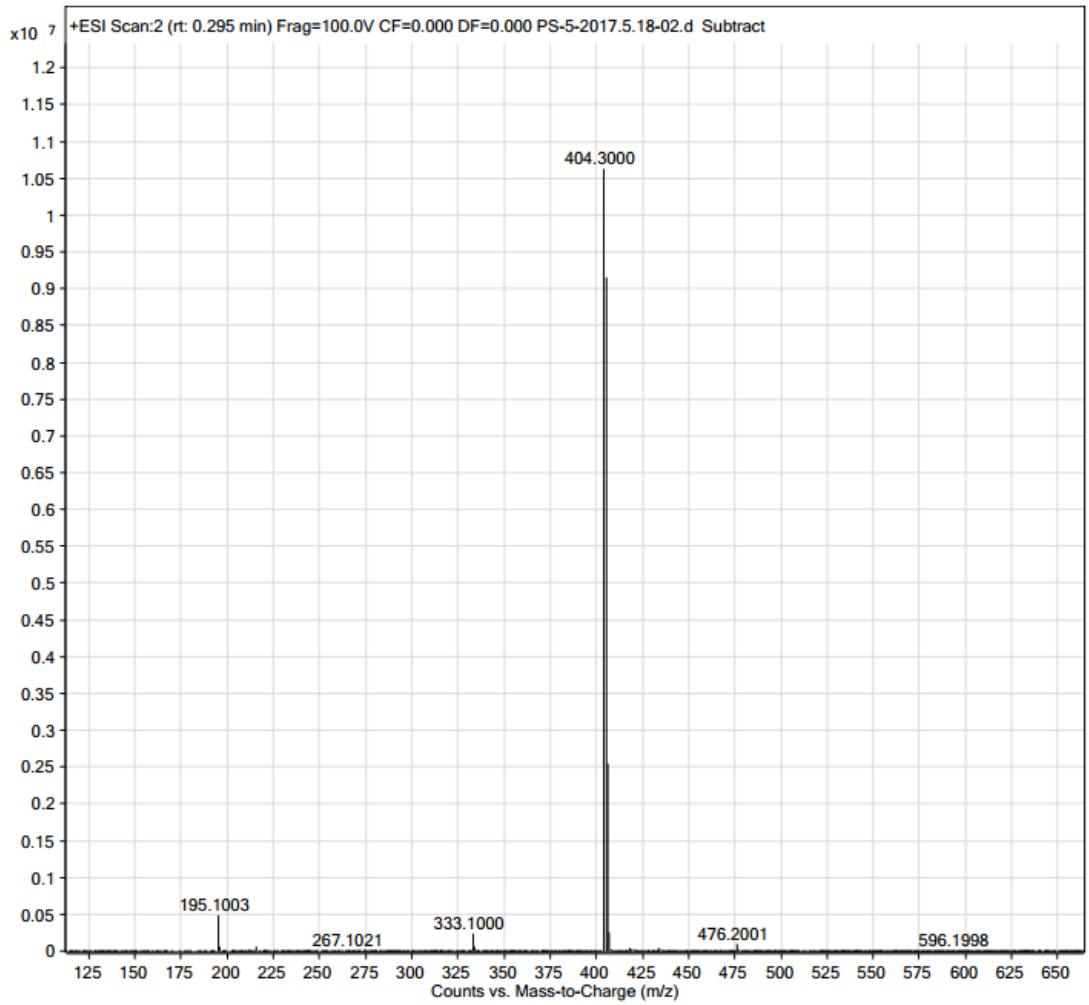

Figure 4. HR-MS spectrum of **PS-1**

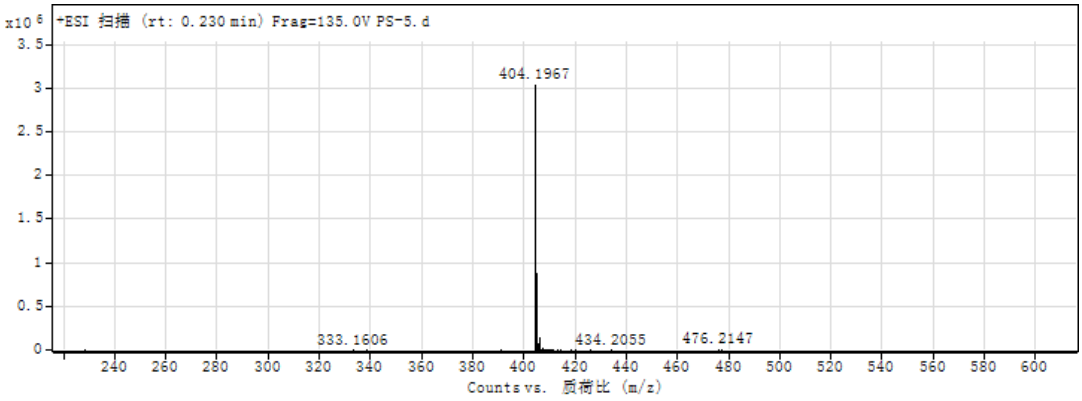

Figure 5. ^{1}H spectrum of **PS-2**

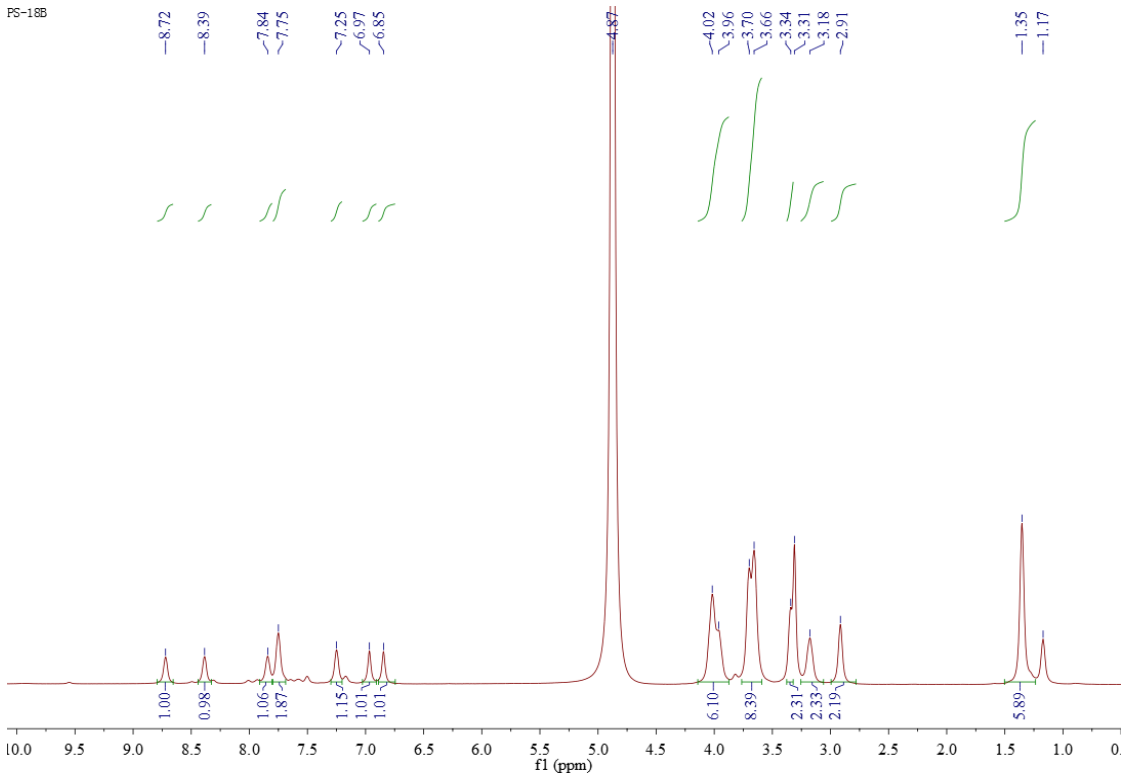

Figure 6. ^{13}C spectrum of **PS-2**

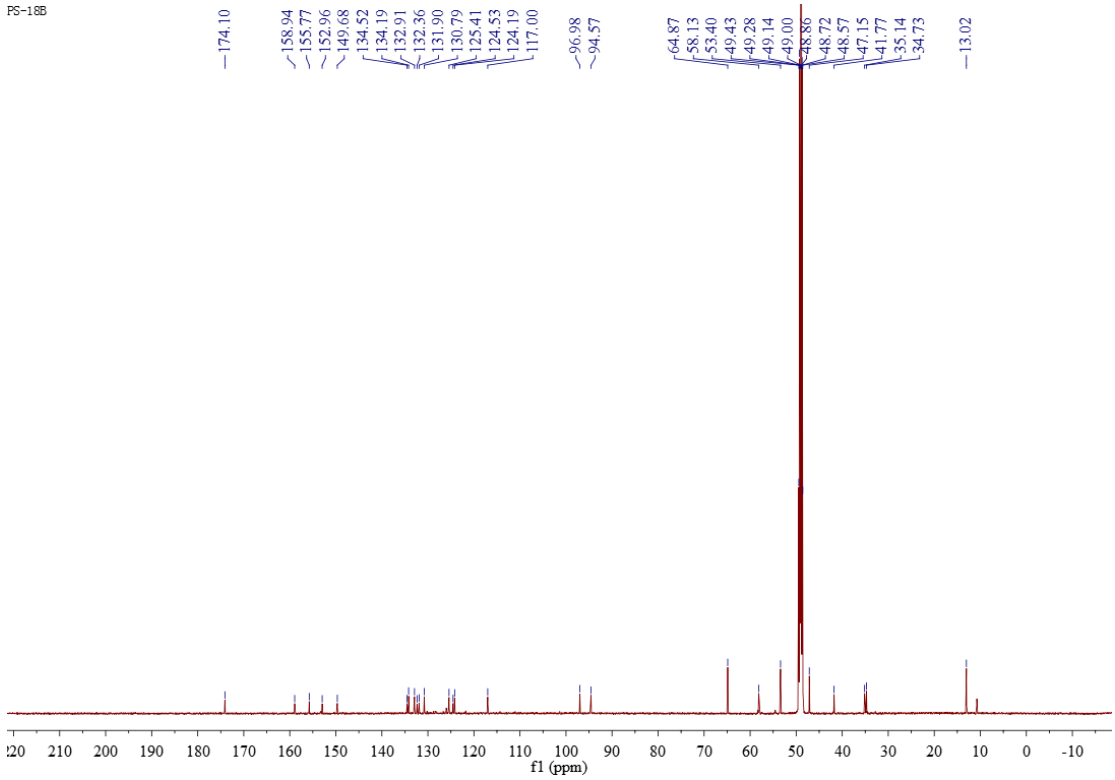

Figure 7. LR-MS spectrum of **PS-2**

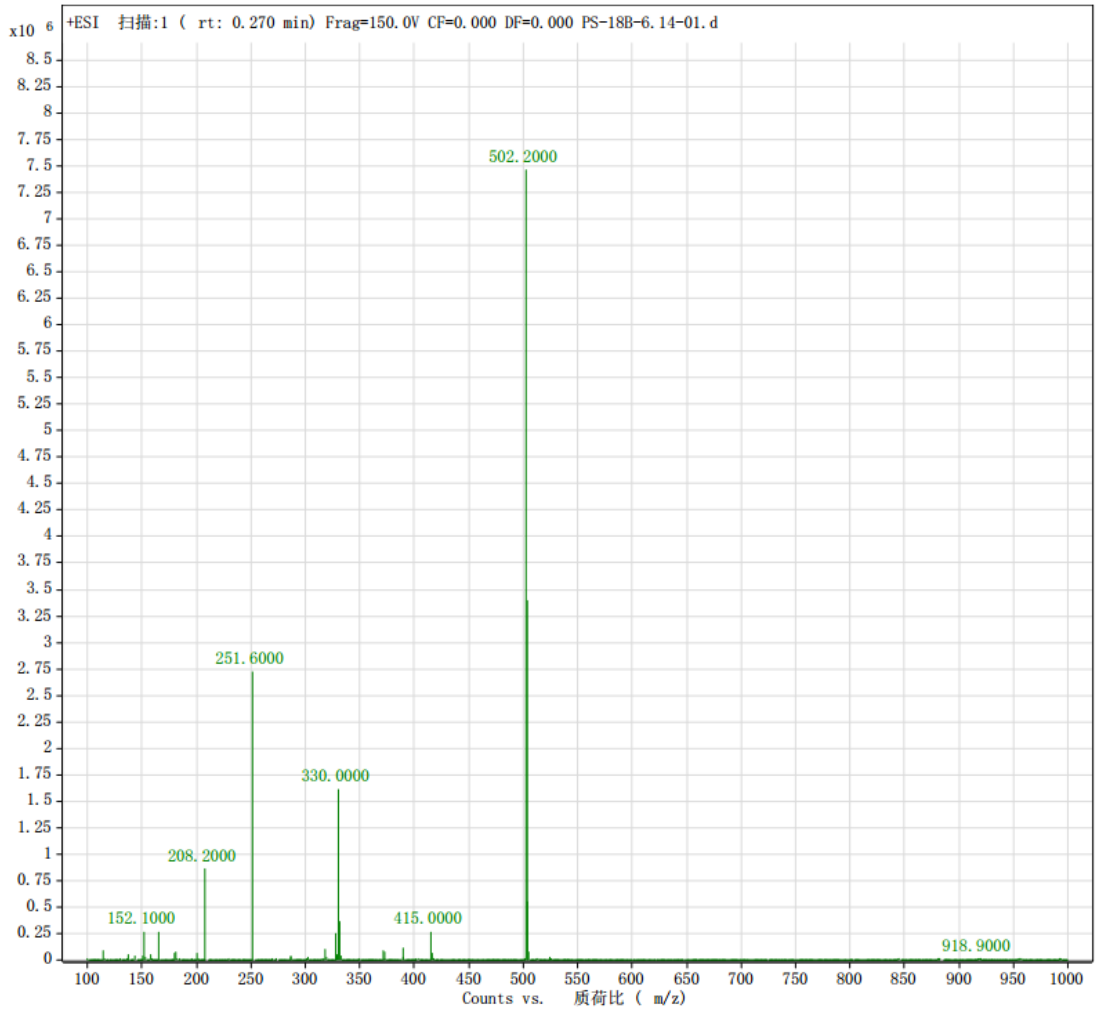

Figure 8. HR-MS spectrum of **PS-2**

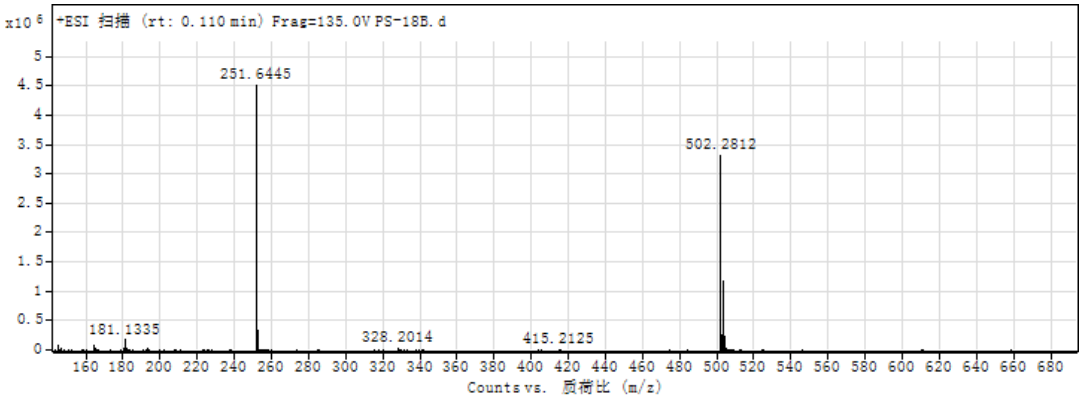

Figure 9. ^{1}H spectrum of **PS-3**

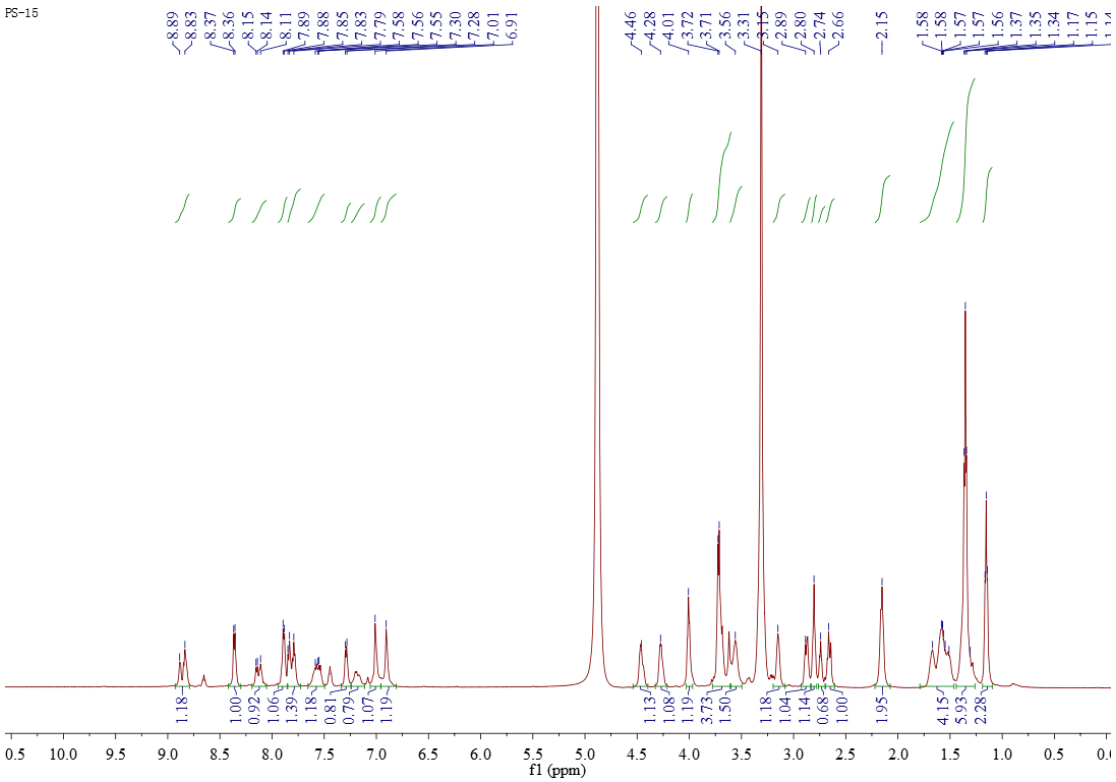

Figure 10. ^{13}C spectrum of **PS-3**

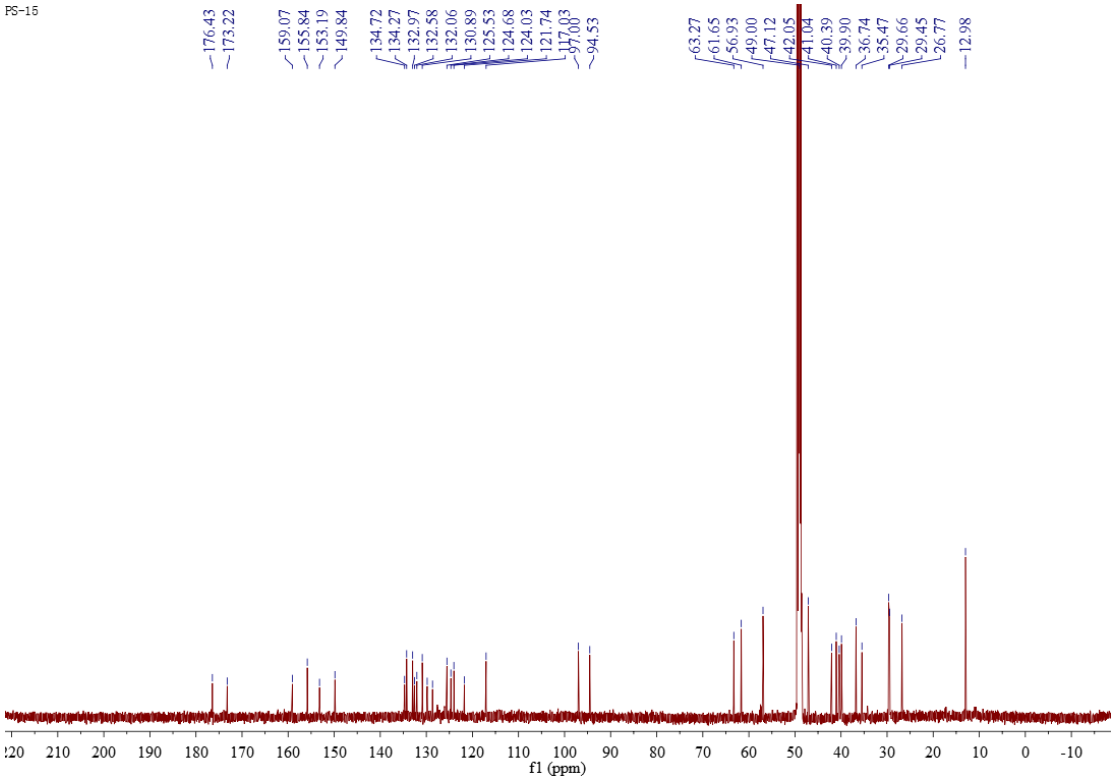

Figure 11. LR-MS spectrum of **PS-3**

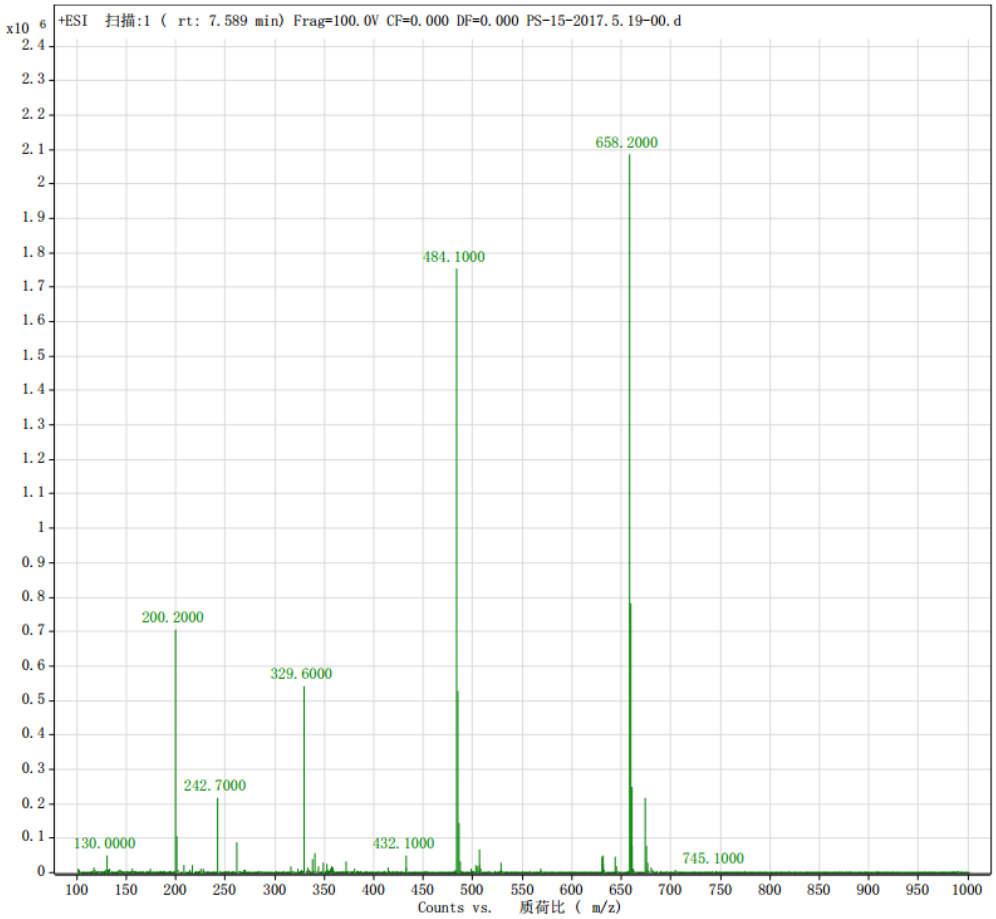

Figure 12. HR-MS spectrum of **PS-3**

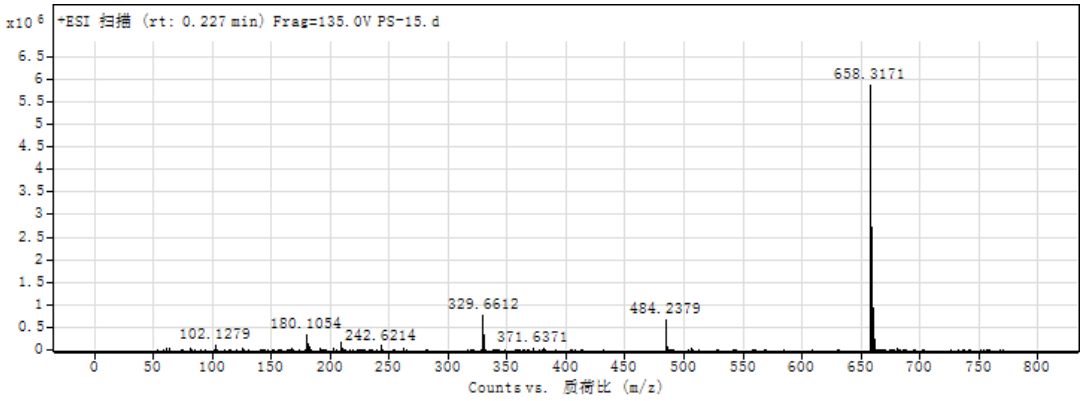

Figure 13. ^{1}H spectrum of **PS-4**

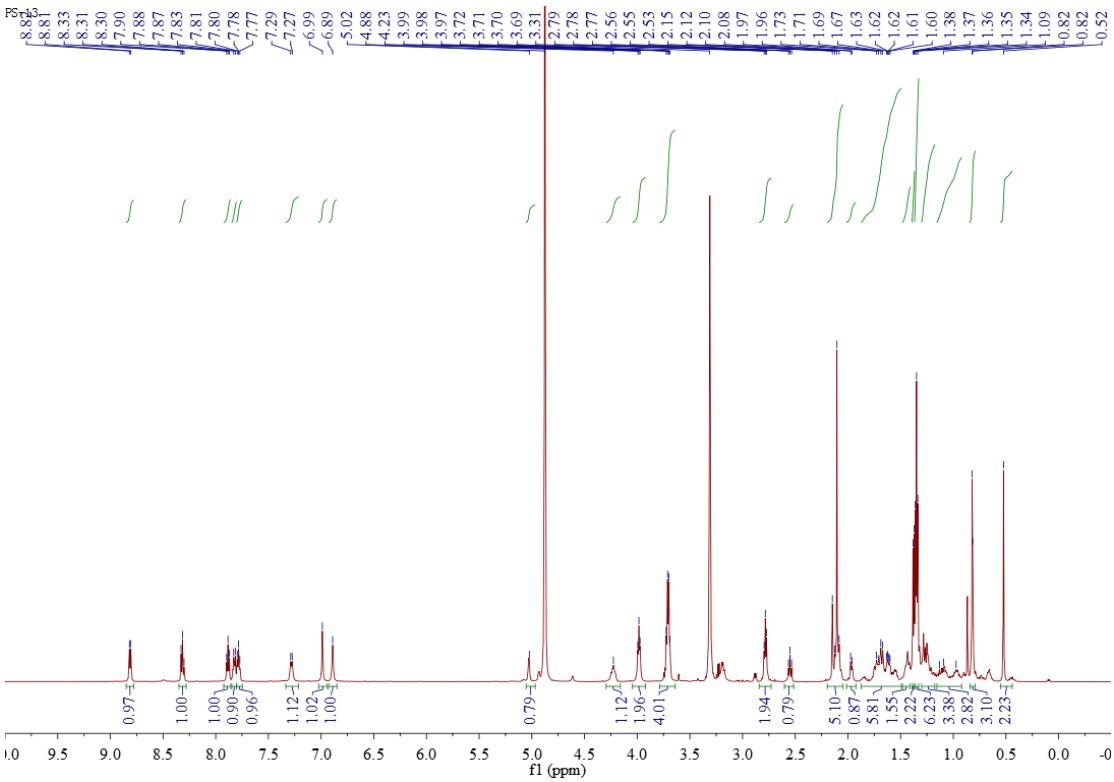

Figure 14. ^{13}C spectrum of **PS-4**

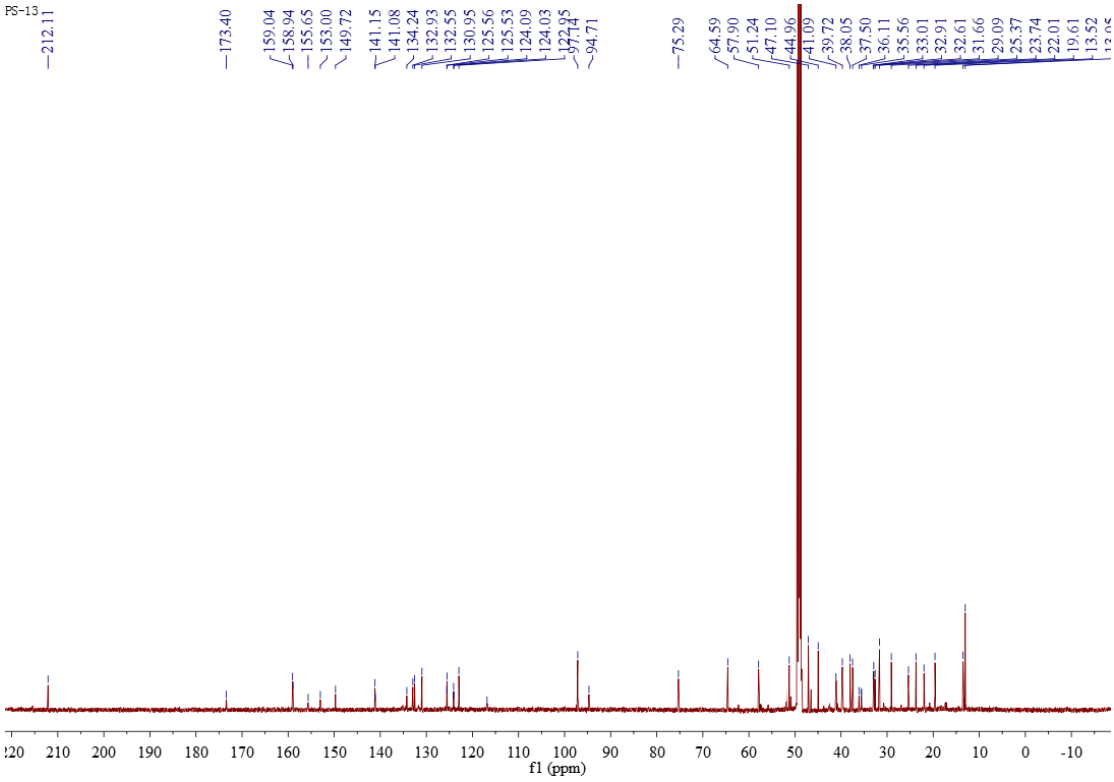

Figure 15. LR-MS spectrum of **PS-4**

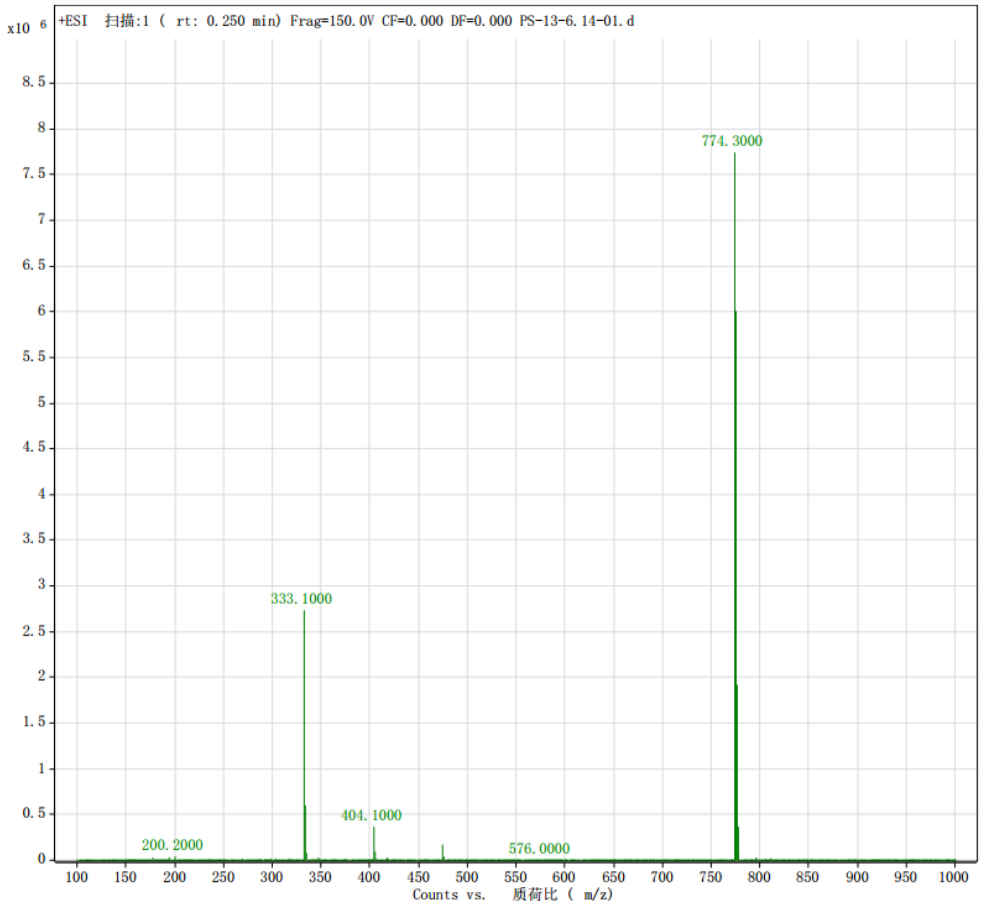

Figure 16. HR-MS spectrum of **PS-4**

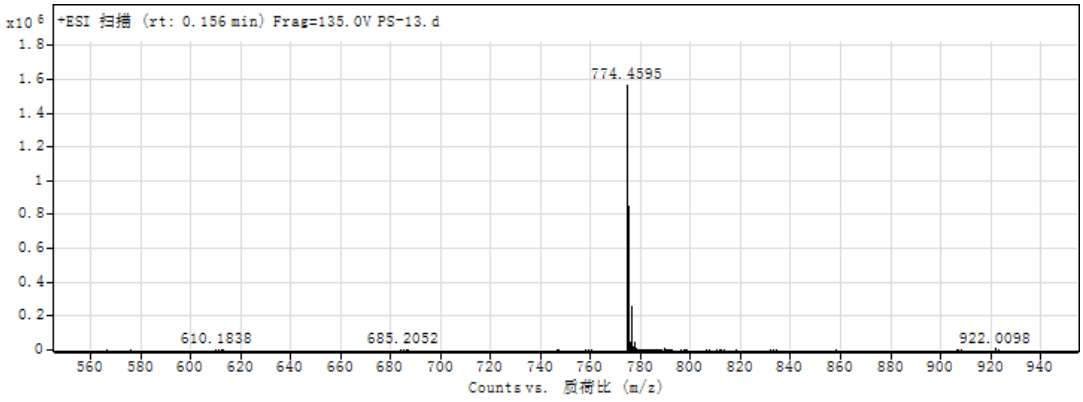

Figure 17. ^{1}H spectrum of **PS-5**

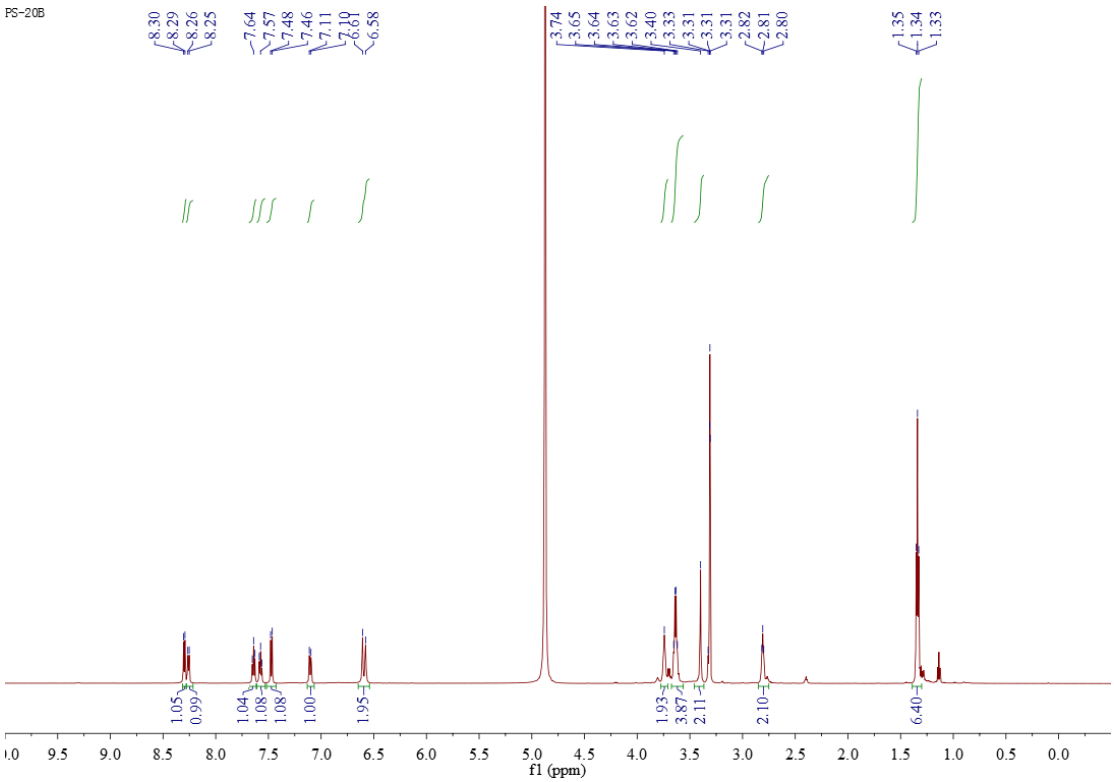

Figure 18. ^{13}C spectrum of **PS-5**

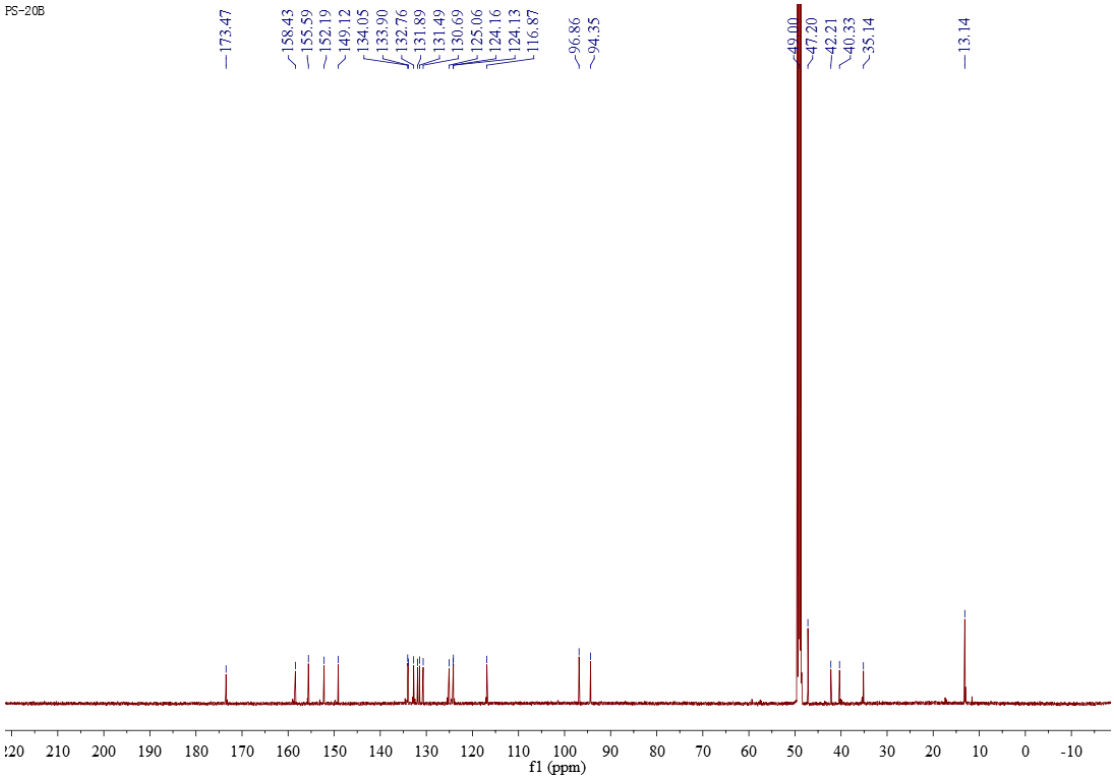

Figure 19. LR-MS spectrum of **PS-5**

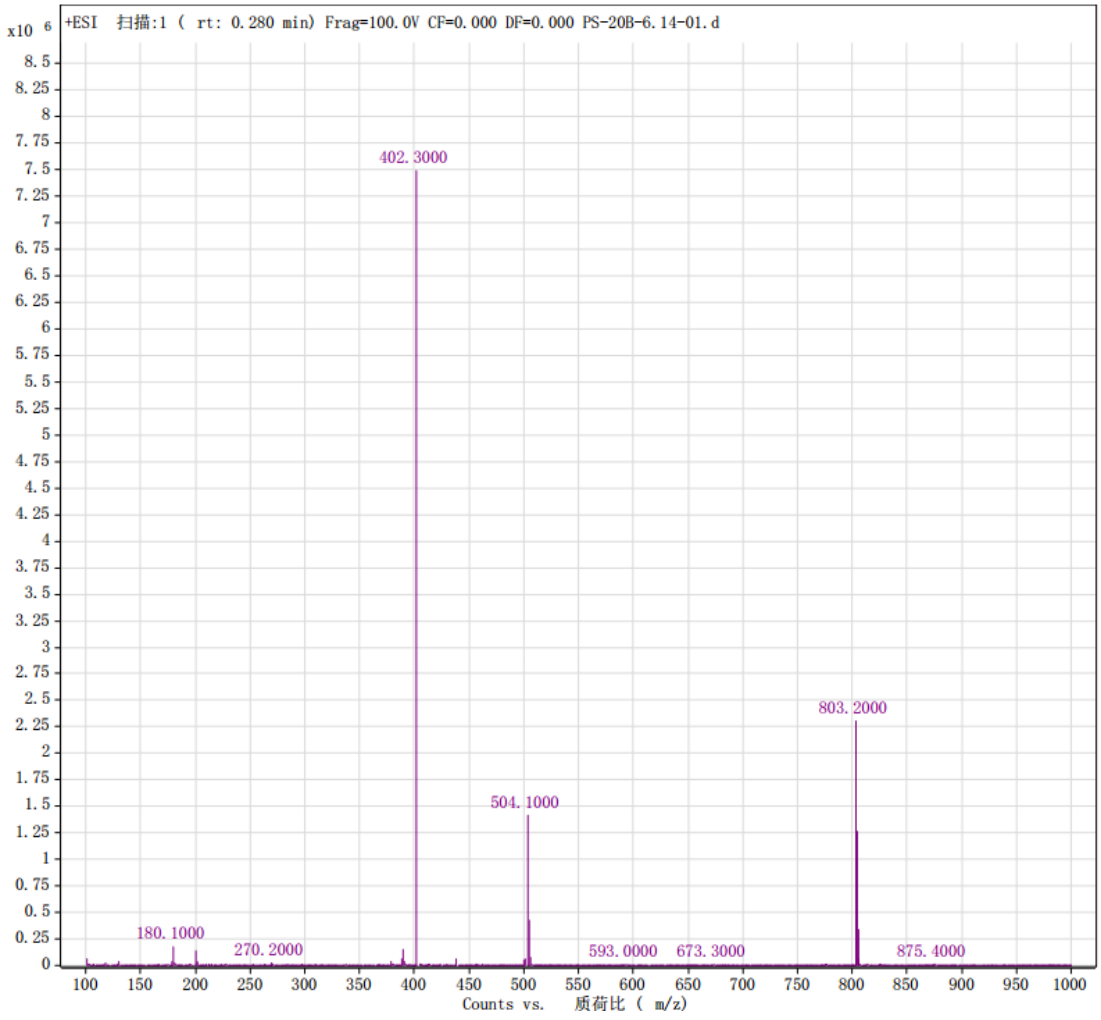

Figure 20. HR-MS spectrum of **PS-5**

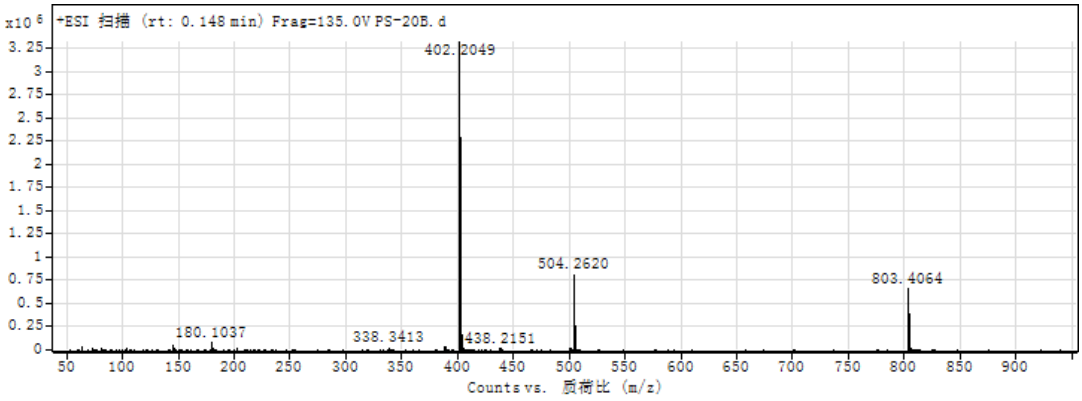

CONCLUSÃO

Neste trabalho foram apresentados três artigos: 1) uma revisão que expôs a importância do desenvolvimento de novos fotossensibilizantes, bem como discutiu as estratégias utilizadas atualmente para atingir este objetivo; 2) um artigo de pesquisa, que descreveu a síntese, a caracterização e os testes *in vitro* de eficácia fotodinâmica do composto DHX-1 livre e incorporado a um carreador lipídico nanoestruturado; 3) um artigo de pesquisa que descreveu a síntese de cinco compostos derivados de benzo[a]fenoxazínio (PS1 ao PS5) que apresentaram atividade fotodinâmica contra células de adenocarcinoma mamário murino 4T1 *in vitro*. Os resultados destes estudos gerou moléculas com grande potencial para serem utilizadas como fotossensibilizantes para terapia fotodinâmica anticâncer.